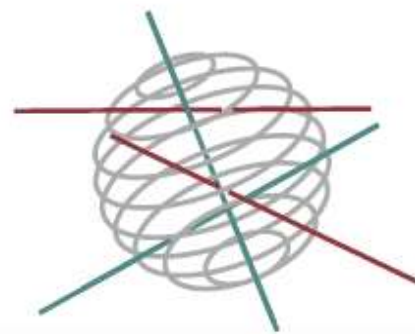


SSD

SCIENCE FOR A SUSTAINABLE DEVELOPMENT



MODELLING ATMOSPHERIC COMPOSITION AND CLIMATE FOR THE BELGIAN TERRITORY

MACCBET

Nicole van Lipzig, Sajjad Saeed, Matthias Demuzere, Hendrik Wouters, Koen De Ridder, Dirk Lauwaet, Jean-Pascal van Ypersele de Strihou, Philippe Marbaix, Kwinten van Weverberg, Cecille Villanueva-Birriel, Laurent Delobbe, Maryna Lukach.



ENERGY



TRANSPORT AND MOBILITY



AGRO-FOOD



HEALTH AND ENVIRONMENT



CLIMATE



BIODIVERSITY



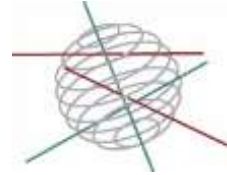
ATMOSPHERE AND TERRESTRIAL AND MARINE ECOSYSTEMS



TRANSVERSAL ACTIONS



**SCIENCE FOR A SUSTAINABLE DEVELOPMENT
(SSD)**



Climate

FINAL REPORT

**MODELLING ATMOSPHERIC COMPOSITION AND CLIMATE FOR
THE BELGIAN TERRITORY**

MACCBET

SD/CS/04A

Promotors

Nicole van Lipzig, KU Leuven, Afdeling Geografie, Celestijnenlaan 200E,
bus 2409, 3001 Heverlee

Koen De Ridder, Vlaamse Instelling voor Technologisch Onderzoek N.V.
(VITO)

Jean-Pascal van Ypersele de Strihou, Université Catholique de Louvain
(UCL)

Laurent Delobbe, Koninklijk Meteorologisch Instituut van België
(KMI)

Authors

Nicole van Lipzig, Sajjad Saeed, Matthias Demuzere, Hendrik Wouters,
Koen De Ridder, Dirk Lauwaet, Jean-Pascal van Ypersele de Strihou,
Philippe Marbaix, Kwinten van Weverberg, Cecille Villanueva-Birriel,
Laurent Delobbe, Maryna Lukach



Published in 2017 by the Belgian Science Policy
Avenue Louise 231
Louizalaan 231
B-1050 Brussels
Belgium
Tel: +32 (0)2 238 34 11 – Fax: +32 (0)2 230 59 12
<http://www.belspo.be>

Contact person: Martine Vanderstraeten
+32 (0)2 238 36 10

Neither the Belgian Science Policy nor any person acting on behalf of the Belgian Science Policy is responsible for the use which might be made of the following information. The authors are responsible for the content.

No part of this publication may be reproduced, stored in a retrieval system, or transmitted in any form or by any means, electronic, mechanical, photocopying, recording, or otherwise, without indicating the reference:

N. van Lipzig, S. Saeed, M. Demuzere, H. Wouters, K. De Ridder, D. Lauwaet, J.-P. van Ypersele de Strihou, Ph. Marbaix, K. van Weverberg, C. Villanueva-Birriel, L. Delobbe, M. Lukach, **Modelling atmospheric composition and climate for the Belgian territory (MACCBET)**. Final Report. Brussels: Belgian Science Policy 2017 – 88 p. (Research Programme Science for a Sustainable Development)

Table of Contents

ACRONYMS, ABBREVIATIONS AND UNITS	5
EXECUTIVE SUMMARY	7
1. INTRODUCTION	11
1.1. Context.....	11
1.2. Objectives.....	11
1.3. Major deviations from the original project planning	13
2. METHODOLOGY AND RESULTS.....	15
Section 1 : Surface Precipitation (deliverables: D1.1, D1.2, D1.3, D1.4).....	15
Section 2: Hail and Graupel in COSMO-CLM (deliverables: D2.1, D2.2, D2.3, D2.4, D2.5).....	21
Section 3: Impact of contrails in COSMO-CLM (deliverables D3.1, D3.2)	28
Section 4: Urban climate modelling (deliverables D4.1-D4.4 and D5.1-D5.3).....	31
Section 5: High resolution climate simulations over Belgium (D6.1; D6.2; D6.3)	47
Section 6: Air quality modelling (deliverables D7.1, D7.2, D7.3)	56
3. POLICY SUPPORT	67
4. DISSEMINATION AND VALORISATION	69
5. PUBLICATIONS.....	73
6. ACKNOWLEDGEMENTS	81
7. REFERENCES	83

ACRONYMS, ABBREVIATIONS AND UNITS

<u>Name</u>	<u>Abbreviations</u>
Anthropogenic Heat Emission	AHE
Air quality modelling in Urban Regions using an Optimal Resolution Approach	AURORA
Basel UrBan Boundary Layer Experiment	BUBBLE
Belgian Science Policy Office	BELSPO
COSMO model in Climate Mode	COSMO-CLM
Community Land Model	ClandM
Cloud optical thickness	COT
Cloud top pressure	CTP
Circumglobal wave train	CGT
Coupled Model Intercomparison Project	CMIP5
Canopy and Aerosol Particle Interactions in TOulouse Urban Layer	CAPITOUL
Convection Permitting climate Simulation	CPS
Downward shortwave radiation	DSR
European Centre for Medium-Range Weather Forecast	ECMWF
Empirical Orthogonal Function	EOF
Global Climate Model	GCM
Heat Wave Day	HWD
Heat Wave Degree Day	HWDD
High air traffic density area simulation	AV Simulation
Integrated Forecasting System	IFS
Katholieke Universiteit Leuven	KUL
Koninklijk Lyceum van Antwerpen	KLA
Mono Nitrogen Oxides	NOx
Mean Apparent Vertical Profile of Reflectivity	MAVPR
Normalized Difference Vegetation Index	NDVI
Outgoing shortwave radiation	OSR
Outgoing longwave radiation	OLR
Pseudo Constant Altitude Plan Position Indicator	PCAPPI
Quantitative Precipitation Estimation	QPE
Reference Simulation	REF
Royal Meteorological Institute Belgium	RMI
Regional Climate Model	RCM
Satellite Application Facility on Climate Monitoring	CM SAF
Simulations without contrail parameterization	NOAV Simulation
Soil-Vegetation-Atmosphere-Transfer	SVAT
Standard Simulation	STD
TERRA Model With urban parameterization	TERRA_URB
Université Catholique de Louvain	UCL
Urban Boundary Layer Climate Model	UrbClim
Urban heat island	UHI
Urban Frabric	UF
Van LeeMputten	VLM
Vlaamse Instelling voor Technologisch Onderzoek	VITO
Working group	WG
1-moment microphysical schemes	1M scheme

2-moment microphysical schemes	2M scheme
Representative Concentration Pathway	RCP
Top of the atmosphere	TOA
Coupled Model Intercomparison Project Phase5	CMIP5

EXECUTIVE SUMMARY

The aim of the project is to establish projections of future climate and air quality for Belgium, at an unprecedented spatial resolution, using the latest insights and parameterizations of processes affecting regional climate and atmospheric composition. The project is largely based on the “COSMO model in Climate Mode” (COSMO-CLM), a state-of-the-art regional climate model. The project consisted of three phases, the development phase, the implementation phase and the analysis phase where climate and air quality information was interpreted and communicated to stakeholders.

The project succeeds in all three phases. During the **development phase**, the regional climate model COSMO-CLM was developed in several ways. All these improvements were important for the high-resolution climate model simulations in a later phase. The major model developments are listed below. More details can be found in section 2 and references to scientific publications within this section.

1. The two-moment microphysics scheme of Seifert and Beheng (2006), was successfully implemented in the COSMO-CLM model. The effect that this implementation has on the modelled surface precipitation was found to be small. The breakup threshold was determined to be a key parameter in the microphysics scheme and improvements of extreme precipitation might be established with a better constraint of this parameter.
2. Graupel and hail were implemented in the two-moment microphysics scheme by Seifert and Beheng (2006). The sensitivity of surface precipitation amounts to having hail included or not was found to be limited.
3. An urban parameterization was developed and implemented in COSMO-CLM. This parameterization is based on improved surface-layer transfer coefficients which can deal with very small thermal roughness lengths typical for urban surfaces.
4. A model for downscaling of atmospheric fields over cities, called Urban Boundary Layer Climate Model (UrbClim), was finalized. The model was evaluated for the cities of Ghent and Toulouse.

During the **implementation phase**, climate and air quality simulations were performed for Belgium at a spatial resolution of 3 km, yielding an unprecedented level of detail in regional climate simulations for Belgium. The advantage of this 3km spatial resolution is that COSMO-CLM can explicitly simulate deep convection, rather than having to use a sub-grid convection parameterization. Such a downscaling is therefore called a Convection Permitting climate Simulation (CPS). In addition, a processing of radar data was performed to obtain climatological information on precipitation and hail.

During the **analysis phase**, the data interpretation took place. The major breakthroughs are listed below

1. CPSs were performed for a retrospective 10 year period. The daily precipitation cycle remarkably improved in these model simulations. Major other improvements were the representation of extreme precipitation events and the spatial variability of precipitation. In addition, it was found that the CPS model intensifies the increase in precipitation extremes due to increased greenhouse-gasses, compared to the forcing non-CPSs.

2. High-resolution urban climate simulations over Belgium have been performed with COSMO-CLM and newly developed urban parameterization. Sensitivity experiments demonstrate that the existence of the urban fabric (presence of streets and buildings), the anthropogenic heat emission (combustion and other heat release into the atmosphere) as well as their synergic forcings determine urban heat island intensities at the scale of the cities, and need to be taken into account in climate-mitigation and climate-adaptation scenarios.
3. Urban climate largely affects air quality. In particular, high ozone concentrations during ozone peaks are prolonged in the evening and night in cities due to an enhanced vertical turbulent transport of pollutants in the urban boundary layer: The prolonged ozone concentrations are explained by the enhanced vertical transport of high ozone concentrations from aloft towards to surface above cities. This is despite the higher emissions that would lead to more ozone destruction in the evening. The enhanced vertical transport results from the urban heating which destabilized the boundary layer.
4. The radar observations for precipitation and hail events were improved. The algorithms analyse together the vertical profiles of reflectivity and the temperature profiles to estimate occurrence and severity of hail. According to this dataset, the hail season for the territory in and around Belgium starts in April and lasts for 6 months until October with 6.6 times higher probability to have hail in July, than in September. The daily maximum occurs between 15:00 and 18:00 UTC.

MACCBET was also very successful in leverage of scientific results to stakeholders. Apart from the 16 peer-reviewed publications directly coming out of this project, and another 4 under review, the **major valorisations** results are:

1. The MACCBET climate, air quality and urban model runs were the basis of a recently published climate assessment of Flanders (MIRA klimaatrapport 2015). This was an extremely important leverage of the MACCBET work towards policy and society in general.
2. Spatial and climatological heat-stress indicators have been developed for future heat-stress assessments in Belgium, taking into account both climate change scenarios and the effect urban expansion. The latter are based on projections of urbanization towards 2060 by VITO spatial model (Engelen et al. 2011). The results are included in the MIRA klimaatrapport 2015.
3. MACCBET results have found their way into city policy in Antwerp, Ghent, and Brussels. For example, in Antwerp, information was used to enforce certain heat-alleviating measures in the Building Code, including obligations to establish green roofs, green parking space, and green (i.e., permeable) gardens. A heat warning system is currently established in Antwerp's Ecohuis.
4. MACCBET is one of the pillars for a new BELSPO project (CORDEX-BE), which is currently ongoing. Moreover, MACCBET has facilitated involvement in the European FP7 projects for example VITO's involvement in NACLIM and RAMSES, which both consider urban climate and adaptation in various cities (Berlin, Almada, Barcelona, Bilbao, London, Skopje, New York, Rio de Janeiro, Hyderabad, ...). In this way, MACCBET contributed to the development of new policy in (at least some of) those cities.
5. MACCBET work, together with similar activities in other institutes around the world, laid the basis for a change in research focus on convection permitting simulations to provide climate information to users. For example, the recent call for CORDEX

'Flagship Pilot Studies (FPS)' calls for a coordinated effort in CPSs.

6. Two high-level symposia (mid-term and end symposium) were held that had an important function in bringing together the climate research community and the stakeholders in need of climate information.

Within the MACCBET partners, **strong synergies** were formed between the four research teams, but also more widely within the Belgian climate modelling community. Examples for this are: (1) A collaborative basis for urban climate research (KU Leuven, VITO), reflected in 5 peer-reviewed urban climate publications with different research teams of MACCBET involved. (2) Strong common expertise in evaluation of the climate models (KU Leuven, UCL and RMI). This is extremely important to evaluate and subsequently reduce systematic model errors in the climate models. (3) The regional climate modellers of MACCBET joined forces with the modellers from RMI and Université de Liège and were successful in securing funding to continue climate modelling and climate impact studies in Belgium.

1. INTRODUCTION

1.1. Context

Today, Belgium's climate projections for the future are mainly based on Global and Regional Climate Models with spatial resolutions of tens of kilometres. There are currently no regional climate runs for Belgium at kilometre scale resolution. To obtain climate projections at this scale, the COSMO-CLM model (also referred to as CCLM) has been employed. It is a non-hydrostatic limited-area atmospheric prediction system suitable for regional numerical weather prediction and regional climate modelling (< 3 km spatial resolution) (Steppeler et al., 2003). Cloud microphysics, radiation, moist convection, turbulent diffusion and parameterization of surface fluxes and soil processes are the sub-components included in the model. This state-of-the-art model resolves the relevant equations describing those processes.

Although a spatial resolution of 2.8 km is unprecedented for Belgium, it is still insufficient for the simulation of urban climate, especially for the medium-sized cities in Belgium. Even though the COSMO-CLM's non-hydrostatic framework permits using resolutions of the order of one kilometre or higher, the model has undergone little or no testing at this scale. More importantly, 1-km (or higher) resolution simulations are prohibitively expensive with respect to computation time, considering the 10-year periods to be simulated. For an in-depth understanding of the Urban Heat Island (UHI) phenomenon and an evaluation of the impact of climate change on the UHI intensity, the computationally cheap model UrbClim was developed and applied.

In recent years, the Belgian Federal Public Service for Health, Food Chain Safety and Environment has increasingly employed results from modelling in support to policy preparation, among other things to evaluate the effect of emission reduction measures on meeting the targets of the European Air Quality Directives. However, most of the models currently in use, while fast and relatively convenient to implement on a computer, are no longer state-of-the-art instruments. Through the cooperation of the different research groups, each with their own expertise, the most advanced tools available today will be used to simulate air quality, climate and cloud feedback. In this way, reliable and quantitative climate prognoses can be provided for climate impact studies, emission strategies and adaptation policies. The latter is expected to be fairly straightforward, as some members of the consortium already have been enjoying a long and fruitful relation with the Belgian Federal Public Service for Health, Food Chain Safety and Environment.

1.2. Objectives

The main objective of the proposed research is to establish projections of future climate and air quality for Belgium, at an unprecedented spatial resolution, and using the latest insights and parameterizations of processes affecting regional climate and atmospheric composition. The project was largely based on the "COSMO model in Climate Mode" (COSMO-CLM), a state-of-the-art regional climate model. The main outcomes from the project are:

- (1) an improved regional climate modelling capacity;
- (2) high-resolution (3-km) present and future climate and air quality climatology over Belgium;
- (3) enhanced insight in the impacts of climate change on air quality and the urban heat island, and in the radiative forcing effect of contrails;

(4) Improved representation of land use changes under future climate conditions

A detailed list with deliverables with their timing (according to attachment 1 of the contract SO/CS/04A signed half 2012) is given in Table 1.

Table 1: List of deliverables and their dissemination. The four columns give the number, description of the deliverable, the responsible partner, and the submission date counted from 1 January 2011, respectively.

No.	Description	Partner	Subm date
D1.1	Implementation of the 2-moment scheme	UCL	16m
D1.2	Comparison with the 1-moment scheme	UCL	24m
D1.3	Validation of humidity and radiation field in the COSMO-CLM model	UCL	31m
D1.4	Offline coupling between the AURORA and the COSMO-CLM models	UCL	52m
D2.1	Implementation of hail and graupel hydrometeors	UCL	30m
D2.2	Development of an evaluation dataset and tools	RMI	34m
D2.3	Testing the new parameterizations based on sensitivity studies	UCL	40m
D2.4	Verification of the present-day frequency and intensity of hails storms	RMI	46m
D2.5	Present-day and future hail event simulations	KUL	46m
D3.1	Implementation of a revised contrail parameterisation in the COSMO-CLM model	UCL	28m
D3.2	Assessment of the impact of contrails on relevant climatic indicators	UCL	40m
D4.1	<i>Coupling COSMO-CLM – cIm4.0</i>	KUL	16m
D4.2	Evaluation of COSMO-CLM-clm4.0 for the present-day	KUL	22m
D4.3	Long term coarse resolution simulation COSMO-CLM-clm4.0	KUL	28m
D4.4	Assess the effect of dynamic vegetation on climate	KUL	46m
D5.1	Urban downscaling	VITO	16m
D5.2	Reference simulations	VITO	28m
D5.3	Impact of climate change on the urban heat island	VITO	46m
D6.1	Prepare EC-EARTH data as boundary conditions for COSMO-CLM	KUL	16m
D6.2	Transient climate run for Europe for 2000-2069 (25 km)	KUL	28m
D6.3	High resolution climate runs for Belgium for 10 year sub-periods	KUL	40m
D7.1	Emissions modelling	VITO	28m
D7.2	Reference air quality simulations	VITO	40m
D7.3	Impact of climate change on air quality	VITO	52m

To stress the synergy between the partners, the MACCBET final report is subdivided into 7 sections. Section 1: Surface precipitation (RMI, UCL, KU Leuven), Section 2: Hail representation and evaluation (RMI, UCL), Section 3: Contrails in the COSMO-CLM model (UCL), Section 4: Modelling urban regions on local and regional scale (VITO, KU Leuven). Section 5: Multi-decadal

high resolution climate simulations over Belgium (KU Leuven). Section 6: Air quality modelling and simulation (VITO) and Section 7: Technical tasks (VITO, KU Leuven).

1.3. Major deviations from the original project planning

There were also some deviations from the original project planning.

1. Due to technical complexity, the task D4.1 (Table 1) has been severely delayed and in order not to jeopardize the task later in the MACCBET project, an alternative approach was used to take land-use change into account. We use an alternative direct urban parameterization (Wouters et al., 2012) in the standard soil module of COSMO-CLM. Due to the above modification D4.2 (Table 1) is replaced with the “Evaluation of COSMO-CLM with urban parameterization for the present-day”. The original objective of D4.3 and D4.4 (Table 1) was to assess the effect of dynamic vegetation on climate. In Europe, the vegetation is mainly anthropogenically controlled and the influence of the vegetation dynamics on the future climate over Europe is expected to be of less importance. Therefore, it was agreed with project partners and the BELSPO that the new objective of D4.3 and D4.4 was formulated to investigate the role of land use change on future climate in the Belgian region. Land use and land cover change and variability modify the surface fluxes of heat and water vapour which in turn affects the atmospheric boundary layer with important consequences on meteorological conditions like the energy available for thunderstorms (Roger A.P Sr., 2005). Moreover, Feddema et al. (2005) noticed significantly different IPCC SRES climate simulations when including, besides the atmospheric forcing, also future land cover and land use changes. Within the new work package, different land use change scenarios for Europe and Belgium were identified and integrations were performed for the future. As urbanization is the major land use change in Europe, and this takes place at small spatial scale, we performed climate simulations at a high resolution (2.8km) instead of the coarser (~25km) simulations that were originally planned. The reference climate simulations were performed for the period (2000-2009). Due to computational constraints for the simulations on very high resolution, a snapshot of 10 years (2060-2069) was performed rather than the transient runs that were originally proposed.
2. Due to changes in Deliverable 4, transient integrations became obsolete. Large-scale dynamics in RCM is to a large extent determined by the dynamics in the GCM. A wave train analyses has been applied to examine the large scale circulation and its influence on the regional climate over Europe.

2. METHODOLOGY AND RESULTS

The MACCBET final report is subdivided into 7 sections. Each section consists of different deliverables (Table 1) and describes the results as per scientific questions addressed during the project. Section 1 gives details about surface precipitation. Section 2 gives a brief description of work on the hail representation and evaluation. Section 3 gives details about the simulations of contrails in the COSMO-CLM model. Work on the urban parameterization development and urban climate simulation is given in Section 4. Multi-decadal high resolution climate simulations over Belgium are presented in Section 5. Section 6 describes the Air quality modelling and simulation performed during the project. Section 7 gives an overview of the technical tasks completed during the project.

Section 1 : Surface Precipitation (deliverables: D1.1, D1.2, D1.3, D1.4)

Precipitation display large spatial and temporal variability and its realistic simulation is important for impact studies and assessment. In order to determine the added value of a more computational expensive and complex scheme on the simulation of precipitation and hail events, the Seifert and Beheng (2006) 2-moment (2M) scheme has been implemented into COSMO-CLM. A comparison was performed using the same microphysical scheme but emulating a 1-moment (1M) scheme by diagnosing the number concentration. This was specifically designed to ensure comparability of 1M vs. 2M versions of the scheme, avoiding other differences that may occur if two completely different schemes were used. For this purpose, a composite of 20 real-case convective simulations in Belgium during 2002-2010 were carried out. Additional experiments were performed to test specific representations of the rain microphysics within the scheme. Based on 20 real-case simulations, the 1M version of the scheme is more similar to the 2M simulations when compared to other idealized studies of this nature. For example, all schemes tend to underestimate the area of light rainfall rates, but 1M and 2M_{BASE} overestimate moderate rainfall rates. One of the advantages of using 2M schemes is the implicit representation of size sorting within the cloud. Despite of some improvements observed when using a 2M scheme with gamma distribution and a high value for the equilibrium diameter, many uncertainties still remain on the representation of certain microphysical processes such as drop breakup, important for the raindrop representation within models. ***Detailed results of this study are published in a peer reviewed journal (please see Van Weverberg et al. 2014).*** A detail of the main important questions addressed in this section are given below:

1.1. Does simulating intense precipitation with COSMO-CLM improve when using a 2M scheme?

The Seifert and Beheng (2006) 2M scheme was implemented into COSMO-CLM. Originally this scheme only contained 5 hydrometeor species (cloud water, rain, ice, snow, graupel). However, Blahak (2011) recently included an additional category, separating low and high dense rimed particles into graupel and hail, respectively. The benefits of the added hail category are discussed below. In order to determine the added value of a more computational expensive and complex scheme, a comparison was performed using the same microphysical scheme but emulating a 1M scheme by diagnosing the number concentration (this was specifically designed to ensure comparability of 1M vs. 2M versions of the scheme, avoiding other differences that may occur if two completely different schemes were used).

For this study, a composite of 20 real-case convective simulations in Belgium during 2002-2010 were carried out. Since the aim was to emphasize on precipitation representation, the focus of this study was on the representation of rain within the scheme. The comparison was not only done on the effects that the number of prognostic variables within the scheme (1M vs. 2M) has on the simulated precipitation, but also how the functional form of the hydrometeor size distribution (negative exponential vs. gamma) affects the results.

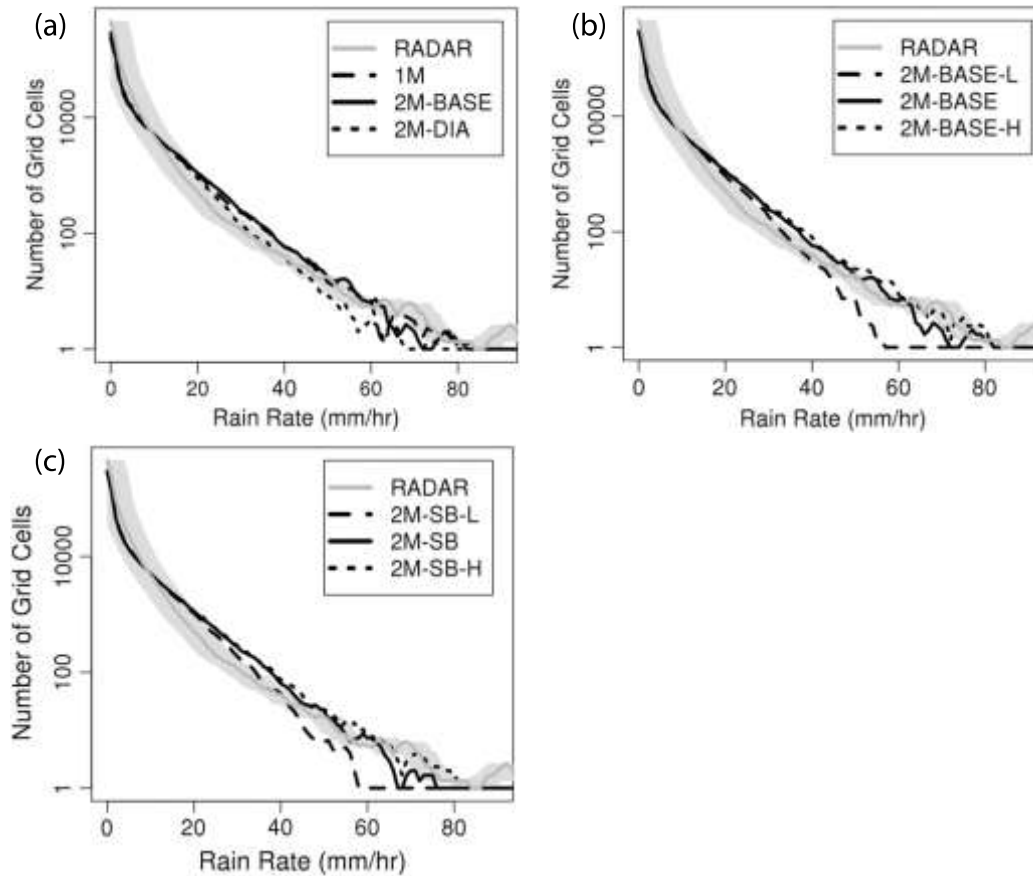


Figure 1.2 Histograms of hourly rain accumulations summed over all 20 cases and the entire analysis domain. The grey line denotes the observed distribution; the dashed, solid, and dotted lines represent different microphysical parameters changed to test its effects on the overall precipitation. (a) detailed comparison of the number of prognostic variables and shape of size distribution when using a 1-moment (1M), 2-moment exponential ($2M_{BASE}$) and 2-moment gamma ($2M_{DIA}$) simulations. (b) and (c) compare the 2-moment exponential version but using different breakup functions (BASE vs. SB) and how the equilibrium diameter affects the results (standard vs. -L and -H).

Additionally, other experiments were done testing specific representations of the rain microphysics within the scheme. One was comparing two different raindrop breakup functions; Verlinde and Cotton (1993; BASE) and Seifert and Beheng (2006; SB). The impact of varying the equilibrium diameter between three numbers was also investigated. The equilibrium diameter was changed from 450 μm (L) to 1300 μm (H) from its standard value of 900 μm .

The model simulations were compared with observed hourly and 24-hour accumulations of surface precipitation for all 20 cases obtained from three C-band weather radars in Belgium and Northern France, operated by the Royal Meteorological Institute of Belgium, the Belgian Air Traffic Control Belgocontrol and Météo France, and from a dense network of rain gauges, operated by the hydrological service of the Walloon region. Figure 1.2 shows the number of

grid points within the domain that contain a certain rainfall rate for all 20 simulated cases examining the effects of the number of prognostic variables, the functional form of the size distribution, breakup function and equilibrium diameter and evaluated against radar observations. Table 1.1 presents a summary of all simulated experiments against observations in terms of daily (24-hour) accumulated surface precipitation, the 99th percentile of the daily accumulated surface precipitation, the total rain cover (defined as the domain fraction covered by $> 1 \text{ mm day}^{-1}$), the light rain cover (defined as the domain fraction covered by $1\text{--}5 \text{ mm day}^{-1}$) and the intense precipitation cover (defined as the domain fraction covered by more than 50 mm day^{-1}).

What is surprising from this study, based on real-case simulations, is the fact that the 1M version of the scheme is more similar to the 2M simulations (Figure 1.2a) when compared to other idealized studies of this nature. For example, all schemes tend to underestimate the area of light rainfall rates, but 1M and $2M_{BASE}$ overestimate moderate rainfall rates. One of the advantages of using 2-moment schemes is the implicit representation of size sorting within the cloud. It has been found in previous studies that excessive size sorting is present in 2-moment schemes with exponential distributions causing an increase in the fallout rate of hydrometeors subsequently reaching the surface at a much faster pace (Milbrandt and Yau 2005). Notwithstanding, in this study large rainfall rates are fairly similar between 1M and $2M_{BASE}$ regardless of the excessive size sorting in the $2M_{BASE}$ just mentioned. This is because collisional drop breakup is counteracting this effect evident when looking at the impacts that the value of the equilibrium diameter has (Figure 1.2b and 1.2c) on the rainfall rates.

A low equilibrium diameter decreases both the number of grid points containing large rain rates (Figure 1.2b and 1.2c) and the area of accumulated rain (Table 1.1) magnifying the dry bias present in these simulations. Smaller equilibrium diameters increase and decrease the evaporation rate and fall velocity, respectively, affecting the intensity of precipitation at the surface and the total accumulated rain. Surprisingly, the breakup function has little effect when compared to the equilibrium diameter. In contrast, changing the functional form of the size distribution to a gamma function with diagnosed shape parameter ($2M_{DIA}$) alleviates the excessive size sorting occurring in the $2M_{BASE}$ simulations demonstrated in the improved agreement between observations and the model in the moderate rainfall rate regime (Figure 1.2a). Despite of some improvements observed when using a 2-moment scheme with gamma distribution and a high value for the equilibrium diameter, many uncertainties still remain on the representation of certain microphysical processes such as drop breakup, important for the raindrop representation within models. These results are published in a peer reviewed journal. ***For more information about the discussion of these results, please see Van Weverberg et al. (2014).***

Table 1.1 Case- and domain-averaged daily precipitation characteristics for all experiments. Provided are the daily (24-hour) accumulated surface precipitation (SP), the 99th percentile of the daily accumulated surface precipitation (99%), the total rain cover, the light rain cover and the intense precipitation cover.

	SP	99%	Total Rain Cover	Light Rain Cover	Heavy Rain Cover
	(mm)	(mm)	(%)	(%)	(%)
<i>Observed</i>	8.1	49.6	80.4	27.9	0.5
<i>1M</i>	6.4	58.9	52.3	20.5	1.3
2M-BASE	7.5	63.0	58.2	22.1	1.7
<i>2M-BASE-L</i>	7.0	51.7	59.7	23.7	1.0
<i>2M-BASE-H</i>	7.6	64.9	58.1	22.2	1.7
<i>2M-SB</i>	7.5	63.5	58.6	22.7	1.7
<i>2M-SB-L</i>	7.2	55.5	58.9	23.0	1.4
<i>2M-SB-H</i>	7.5	65.3	58.3	22.4	1.6
<i>2M-DIA</i>	6.9	52.4 ⁺	57.3	22.0	1.1
<i>2M-DIA-H</i>	7.3	61.0	56.4	22.1	1.6

1.2. How well does the COSMO-CLM model simulate large-scale atmospheric conditions and radiation fields?

In this task, an 11-year (2000-2010) simulation with COSMO-CLM model at convection-permitting resolutions (2.8 km; C3 from now on) for the Belgian area was evaluated against different observational datasets during the summer months (June, July, August) of the year with similar model configurations as in part 1.2. The aim was to identify the added value of these higher resolution runs within the framework of different environmental parameters including temperature, humidity and radiation fields.

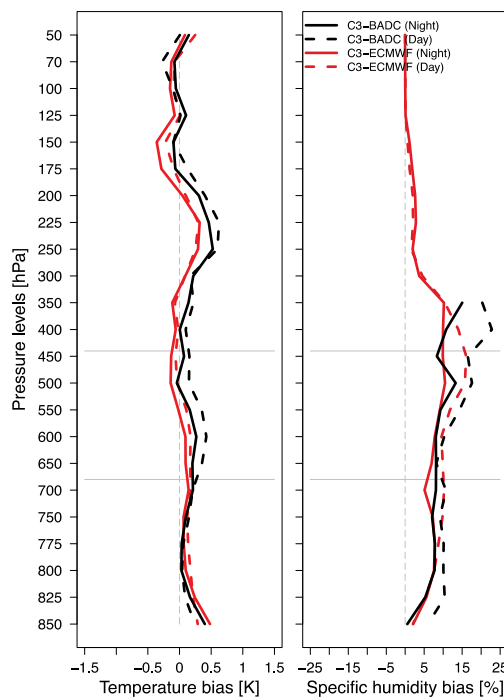


Figure 1.3 Averaged summer bias for temperature (left) and specific humidity (right) for radio soundings available during the period 2000-2010 for Uccle (WMO ID: 06447). Black and red colours refer to C3 simulations (2.8 km resolution) minus BADC and C3 minus ECMWF respectively while night and day are indicated by respectively full and dashed lines. The dashed light-grey line indicates the perfect model line. Levels below 850 hPa and above 300 hPa (for humidity only) are excluded from the analysis.

Observational vertical radiosonde profiles for Uccle were retrieved from the British Atmospheric Data Centre (BADC). For comparison, also the vertical profiles for temperature, specific humidity and wind speed have been retrieved from the grid cell covering Uccle in the European Centre for Medium-Range Weather Forecast (ECMWF) Era Interim 0.75 x 0.75 re-analysis product (Dee et al., 2011). Figure 1.3 shows model performance with respect to vertical temperature and humidity compared to BADC and ECMWF vertical profiles both during the day and at night. Regarding temperature, the model performs well above the 850 hPa level with differences between both BADC and ECMWF not exceeding 1 K. In terms of atmospheric humidity, a wet bias exists, increasing with height between the 850-300 hPa levels, but this bias is no larger than the instruments uncertainties used for the attainment of the observational dataset. From this analysis it can be concluded that any discrepancies present in the representation of precipitation, clouds and other features are not attributed to large-scale dynamics.

Satellite retrievals of cloud properties provided by EUMETSAT Satellite Application Facility on Climate Monitoring (CM SAF) were used to evaluate COSMO-CLM high-resolution simulations (Stengel et al. 2014). Cloud optical thickness (COT) and cloud top pressure (CTP) were used for the evaluation against the COSMO-CLM simulated COT. Figure 1.4 shows contour frequency by altitude diagrams (CFADs) of COT by both satellite retrievals and COSMO-CLM. High clouds with CTP < 300 hPa occur about 25 % as frequent in COSMO-CLM compared to CMSAF. Whereas thin and thick low clouds with CTP > 40 hPa occur almost twice in COSMO-CLM than CMSAF. Overall, COSMO-CLM simulations show a slight underestimation of total cloud cover. This difference in cloud features can have an impact on the radiation budget of the model especially on the Top-Of-the-Atmosphere (TOP) outgoing radiative fluxes.

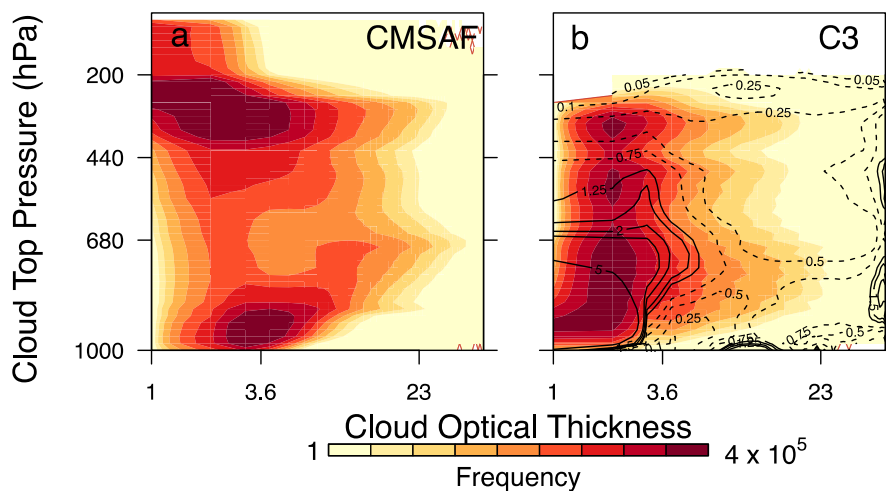


Figure 1.4. 2D-histograms of the absolute frequency of occurrence of clouds as retrieved by the CMSAF (a) and as simulated in C3 (b) for Summer (JJA) 2004-2010. Clouds are binned by COT and CTP. The contours on panel (b) denote the relative bias between the absolute frequencies in C3 and the CMSAF. Solid (dashed) lines denote a positive (negative) bias in the simulations. Only daytime hours (zenith angle <math><65^\circ</math>) are included.

These biases at the Top Of the Atmosphere (TOA) are quantified in Figure 1.5 where outgoing shortwave and longwave radiation (OSR and OLR, respectively) are compared between CMSAF and COSMO-CLM in terms of COT. Although the general trend of increasing OSR with COT is observed in COSMO-CLM, OSR is still overestimated indicating highly reflective clouds, especially in the zone of low and intermediately thick clouds. Regarding longwave radiative fluxes, COSMO-CLM captures well the decreasing trend of OLR with decreasing CTP, however it slightly underestimates it for all clouds, especially for higher

clouds. Note the overestimation of OSR partly counteracts the underestimated of cloud cover especially at high COP (Figure 1.4) resulting in a slightly seasonal-averaged positive bias compared to CMSAF observations. Likewise, the underestimation of OLR partly offsets the frequent simulated low cloud cover within the domain resulting in seasonal-averaged TOA OLR similar to those observed.

In summary, COSMO-CLM showed improvements in precipitation representation at convection-permitting resolutions, especially convective precipitation and the daily cycle of different cloud modes (not shown). However, it underestimated total cloud cover by almost 20%. Surprisingly this aspect did not affect greatly TOA radiation fluxes particularly because of compensating effects (i.e. high reflective clouds). Although this study demonstrated the great capacity of convection-permitting scale models, specifically COSMO-CLM, to study climate change, it is crucial to address such deficiencies in future studies. **Full details about the COSMO-CLM evaluation can be found in the paper (Brisson et al. 2015).**

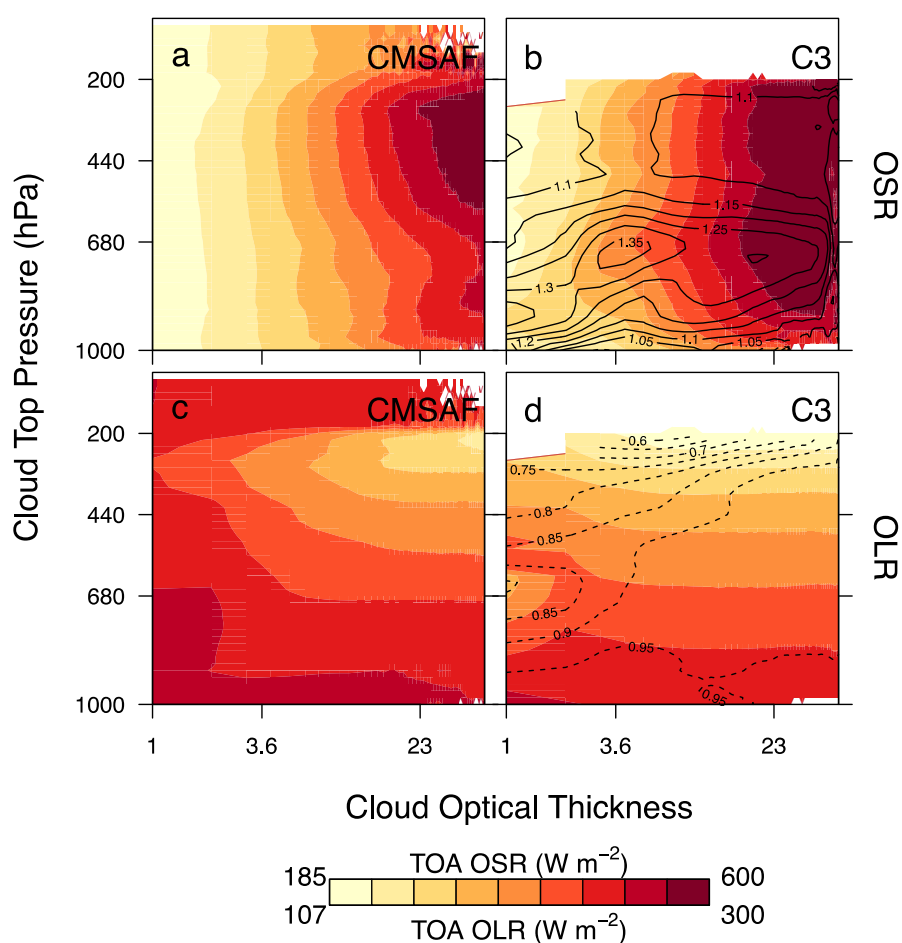


Figure 1.5 2D-histograms of outgoing radiative fluxes as retrieved by the CMSAF (left) at the Top Of the Atmosphere (TOA) and as simulated in C3 (right) for Summer (JJA) 2004-2010. Provided are the OSR (top) and OLR (bottom). The contours on the right-hand panels denote the relative bias between the radiation in C3 and the CMSAF. Solid (dashed) lines denote a positive (negative) bias in the simulations.

Section 2: Hail and Graupel in COSMO-CLM (deliverables: D2.1, D2.2, D2.3, D2.4, D2.5)

The implementation of graupel and hail in the two-moment microphysics scheme (Seifert and Beheng 2006) has been completed successfully. For the evaluation of the hail parameterization, and more specifically to test the number of prognostic moments in the Seifert and Beheng (2005) bulk microphysical scheme, the COSMO-CLM model was run at high resolution (~2.8 km grid spacing) driven by ERA-Interim boundary conditions and the same model configuration as in Van Weverberg et al. (2014). The 1-moment (1M) scheme was compared with two versions of the 2-moment microphysical scheme. In one of the 2-moment (2M) microphysical schemes, the particle size distributions are represented as negative exponentials ($2M_{EXP}$), whereas the other contained gamma size distributions with a diagnosed shape parameter ($2M_{GAM}$). For this study, covering the period 2002-2014, 12 additional cases were added to the original 20 intense convective cases discussed in the section 1, for a total of 32 intense convective cases with more than half having surface hail reports. Each case was simulated using one of the three versions of the microphysical scheme. The model was evaluated only within a 240 km range from the radar. The most important outcomes of this study is the improved simulated hail at the surface when using a 2M microphysical scheme, with potential implications for climate studies.

For the verification of surface precipitation in the model a careful processing of radar reflectivity measurements is performed after the clutter elimination. The radar-based accumulations are combined with a dense network of 90 hourly automatic rain gauge measurements. After adjustment of hourly radar rainfall accumulations by a dense rain gauge network, the long-term verification reveals a lower mean absolute error. The mean, the maximum and the exceedance probability are derived from this dataset. The annual mean rainfall for the period of 2005-2012 reveals a better accordance with the rain gauge network of RMI in terms of mean absolute error. This datasets could be highly useful for evaluation of very high resolution convection permitting model simulations over Belgium in future. Moreover, two hail detection algorithms are developed and used to identify the hail in the radar data. Both algorithms (Waldvogel et al. 1979, Witt et al. 1998) were applied on the corrected archived radar data from the volumetric scan of Wideumont's radar (2003-2012) and verified. Sensitivity of the hail detection algorithm to the quality of measurements was already published in Delobbe et. al. (2006). The algorithms analyse together the vertical profiles of reflectivity and the temperature profiles to estimate occurrence and severity of hail. The vertical profiles of reflectivity are extracted from the volume reflectivity data and the temperature profiles are extracted from ALARO weather model post analysis driven by ERA-Interim boundary conditions. The 10 years period is short from the climatological point of view, but provides reliable information for present day hail season, diurnal cycle identification and spatial distribution analysis. In the preparation for this analysis the thorough check of the quality of hail data from two hail detection algorithms was performed. The radar-based dataset of the occurrence and the severity of hail, achieved after all preparatory and post corrections, is essential for the statistical analysis and evaluation of any model. According to this dataset, the hail season for the territory in and around Belgium starts in April and lasts for 6 months until October with 6.6 times higher probability to have hail in July, than in September. In general, the probability to have hail in one of the 500x500m pixels of Wideumont's radar domain is 3.5 times higher between 15:00 and 18:00 UTC than between 9:00 and 10:00 UTC. ***Over the course of the project, two scientific papers have been written about this work and the results (Goudenhoofd and Delobbe, 2014; Lukach and Delobbe, 2015).*** The main questions addressed in this section are given below.

2.1. Can we improve the quality of the radar data?

Non-meteorological echoes are identified for each scan by the sequence of clutter detection techniques, developed at RMI in the scope of D2.2. At first, the static clutter maps were generated for each elevation of both scans of Wideumont's radar. At second, after the static clutter elimination, dynamic clutter was detected in the reflectivity data. That is done by comparing the data with a satellite cloud type image, by the detection of unrealistic vertical gradient of reflectivity between elevations or by detecting a typical 2D reflectivity texture.

For the verification of surface precipitation in the model a careful processing of radar reflectivity measurements is performed after the clutter elimination. The need of the corrections can be illustrated by comparing of 24h rainfall accumulation based on the uncorrected Pseudo Constant Altitude Plan Position Indicator (PCAPPI) data and the reflectivity data run through vertical profile (VPR) correction (see Figure 2.1). The benefit of the latter is clear observing the removal of concentric circles and increased rainfall at long range.

After a possible detection of a bright band, the Mean Apparent Vertical Profile of Reflectivity (MAVPR) is extrapolated to the ground. It is then applied to all stratiform precipitation taking into account beam broadening. The gaps in the lowest elevation are filled by higher elevations. A 3-way Z-R relationship from the German RADOLAN product is used to derive the rainfall rate. To deal with hail, the maximum reflectivity is limited to 55 dBZ (i.e. 88 mm/h). The rainfall accumulations over a given period are obtained by linear interpolation of the radar rain rate estimates.

After the identification of convective precipitation, a mean apparent vertical profile of reflectivity (MAVPR) is computed from stratiform precipitation close to the radar in a time window of 30 minutes. For the rainfall accumulation from Quantitative Precipitation Estimation (QPE) algorithms the radar data were processed even further.

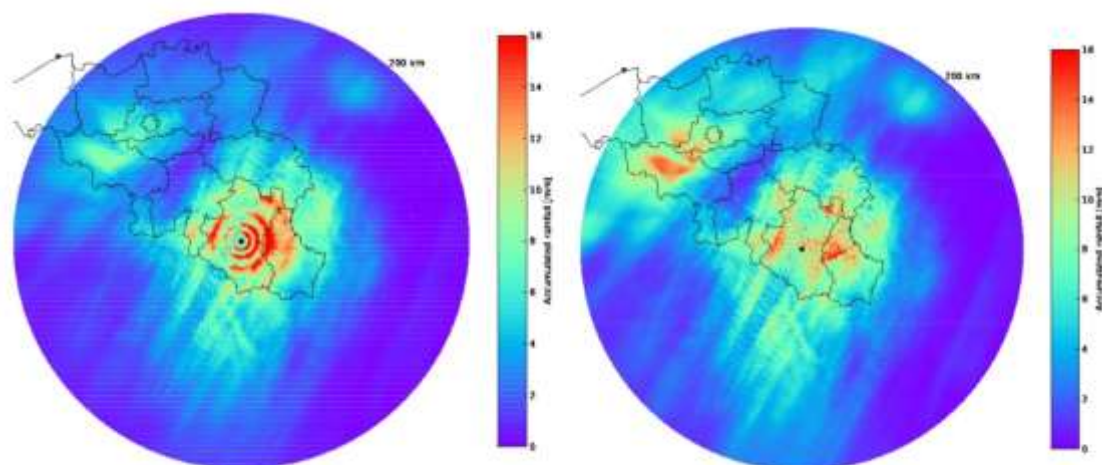


Figure 2.1: Case of 12 January 2008 : 24h accumulation based on PCAPPI (left) and VPR (right)

In a final step, the radar-based accumulations are combined with a dense network of 90 hourly automatic rain gauge measurements. If there is at least 10 radar-gauge pairs with values exceeding 0.1mm, a median correction factor is computed and applied. After adjustment of hourly radar rainfall accumulations by a dense rain gauge network, the long-term verification reveals a lower mean absolute error. The mean, the maximum and the

exceedance probability are derived from this dataset. In Figure 2.2 the result of described above corrections can be observed. The annual mean rainfall for the period of 2005-2012 reveals a better accordance with the rain gauge network of RMI in terms of mean absolute error.

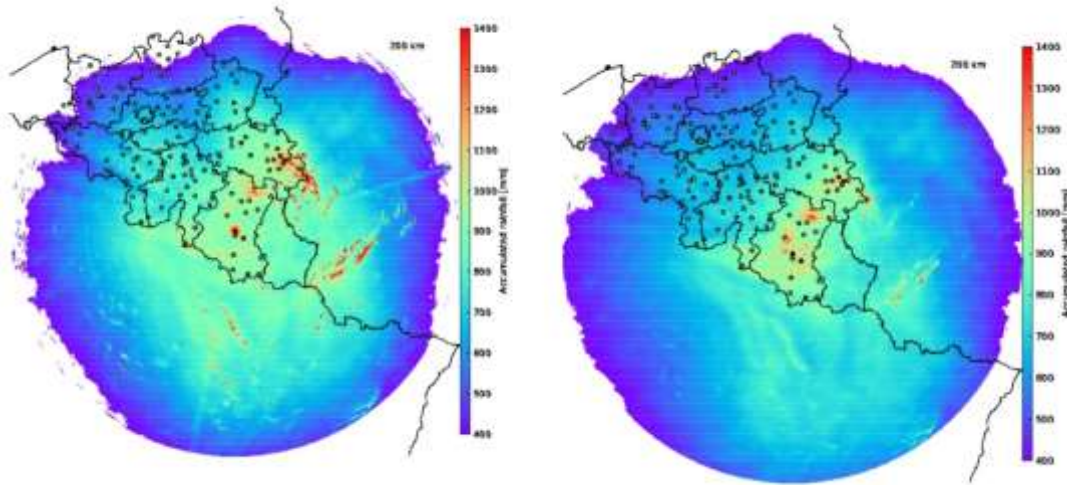


Figure 2.2: Annual mean rainfall for the period 2005-2013: 24h accumulation based on raw (a) and corrected (b) data of Wideumont radar.

2.2. How can we derive hail occurrence and intensity from the radar data?

The hail is identified in the radar data by two hail detection algorithms: the algorithm of Waldvogel and the algorithm of Witt (Waldvogel et al. 1979, Witt et al. 1998). Both algorithms were applied on the corrected archived radar data from the volumetric scan of Wideumont's radar (2003-2012) and verified in the framework of D2.2. Sensitivity of the hail detection algorithm to the quality of measurements was highlighted in Delobbe et. al. (2006). The algorithms analyse together the vertical profiles of reflectivity and the temperature profiles to estimate occurrence and severity of hail. The vertical profiles of reflectivity are extracted from the volume reflectivity data and the temperature profiles are extracted from ALARO weather model post analysis driven by ERA-Interim boundary conditions.

The radar-based occurrence and severity of hail are statistically analysed for 2003-2012. The 10 years period is short from the climatological point of view, but provides reliable information for present day hail season, diurnal cycle identification and spatial distribution analysis. In the preparation for this analysis the thorough check of the quality of hail data from two hail detection algorithms was performed. During this check the areas affected by the remaining ground clutter, related to anomalous propagation conditions of the radar beam (ANAPROP conditions), were determined. The statistical analysis of hail data allowed determining the optimal range interval from 33 km up to 163 km from the Wideumont's radar (see Figure 2.3).

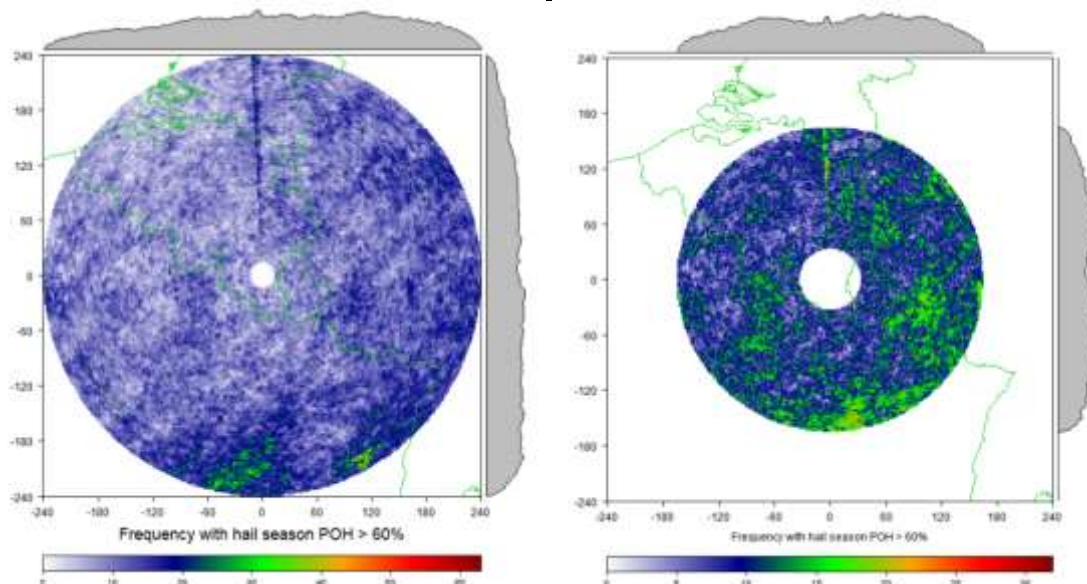


Figure 2.3: Frequency distribution of ten-year hail days (2003-2012) on the full range (left) and on the reduced radar domain (right). The reduced radar domain is defined as a range interval from 33 km up to 163 km from the Wideumont's radar.

For the spatial analysis of fast moving storms the 15 minutes temporal resolution of the volumetric scan of Wideumont's radar is insufficient. That produces the so-called “fish-bone” effect on the daily overview of the hail detection product (see Figure 2.4 left). This in its turn influences any type of spatial analysis whether it is verification or statistics. Applying an advection correction on the hail probability fields between successive scans can reduce this particular issue (see Figure 2.4 right). The advection correction applied to the hail data is based on the optical flow algorithm of Bowler et al. (2004).

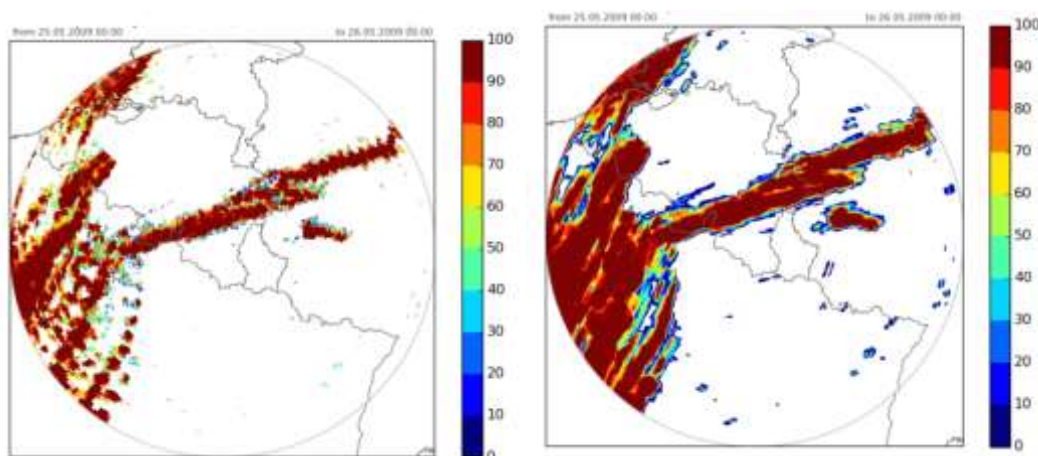


Figure 2.4: Daily overview of the hail detection product with a “fish-bone” effect (left) and after advection correction (right).

2.3. Does COSMO-CLM simulation show improvement in simulation of extreme hail and graupel events?

Another important aspect for accurate deep convective storm simulations is in the parameterization of hail within models, which can substantially impact precipitation and dynamical features within the cloud. Generally, hail formation depends on strong thunderstorms with high upward speeds and great vertical extent. Additionally, hailstorms require the presence of hail embryos such as frozen raindrops and regions of high liquid

water content where the hailstone will increase in size by either dry or wet growth mechanisms. Furthermore, the right conditions need to be present such that melting is minimized and the falling hailstones are able to reach the surface (i.e. large hail sizes, decreased height of the melting layer).

Many models have so far struggled to reproduce characteristic observational features of hail producing storms, due to weaknesses within microphysical parameterizations. Therefore, the work aimed to subsequently evaluate the new hail parameterization implemented within the model. Evaluation of the new hail parameterization consisted in using Belgian observational data of 32 intense convective cases on a daily basis for the period 2002-2014. Observational data was selected from the Wideumont radar (RMI). This dataset contained maximum expected hail size measurement (Witt et al. 1998), which it was used for the evaluation of the hail parameterization.

For the evaluation of the hail parameterization, and more specifically to test the number of prognostic moments in the Seifert and Beheng (2005) bulk microphysical scheme, the COSMO-CLM model was run at high resolution (~2.8 km grid spacing) driven by ERA-Interim boundary conditions and the same model configuration as in Van Weverberg et al. (2014). The 1-moment (1M) scheme was compared with two versions of the 2-moment microphysical scheme. In one of the 2-moment (2M) microphysical schemes, the particle size distributions are represented as negative exponentials ($2M_{EXP}$), whereas the other contained gamma size distributions with a diagnosed shape parameter ($2M_{GAM}$). For this study, covering the period 2002-2014, 12 additional cases were added to the original 20 intense convective cases presented in section 1, for a total of 32 intense convective cases with more than half having surface hail reports. Each case was simulated using one of the three versions of the microphysical scheme. The model was evaluated only within a 240 km range from the radar.

It was shown that the 2M scheme produced significant simulated hail at the surface as opposed to negligible amounts present in the model runs with the 1-moment version. The 2M scheme was able to reproduce the diurnal cycle of the mean area extent at the surface containing hail observed by the radar. However, the $2M_{GAM}$ size distributions for the precipitating hydrometeors showed better agreement with radar observations compared to the simulations with particle size distributions represented as negative exponential distributions. The $2M_{EXP}$ generally showed larger areas of hail reaching the surface together with greater hailstone sizes in comparison to the $2M_{GAM}$ and radar observations. Figure 2.5 shows the domain-time- and case-average vertical profiles of mean hail size for the three microphysical schemes. It shows that the average hail sizes in the 1M scheme were actually high within the upper part of the cloud. However, hail sizes decrease substantially to zero in the lower levels. This is not the case for the 2M scheme. A direct consequence of 2-moment schemes is the inclusion of particle size sorting that promotes faster fallout rates resulting in a reduction of evaporation for larger particle species. This increase the probability of larger particles to reach the surface as it is observed in the 2M cases.

To understand the differences observed in the model simulations when using different versions of the microphysical parameterizations, we initially analysed the microphysical processes that generally contribute the most to hail production within the model. As mentioned earlier, raindrop freezing potentially serves as initial hail embryos. These hail embryos subsequently grow by different microphysical mechanisms such as wet growth of graupel particles. Figure 2.6 shows the diurnal cycle of domain average hail production via these two newly implemented microphysical processes. The diurnal cycles of average

raindrop freezing rate (Figure 2.6a) for all three microphysical schemes are in better agreement with the diurnal cycle of the mean area containing hail at the surface (see RMI part of the final report). Wet growth production term is still important for the further increase in hail sizes within the storms given the larger hail production values. One of the most important outcomes of this study is the improved simulated hail at the surface when using a 2M microphysical scheme, with potential implications for climate studies.

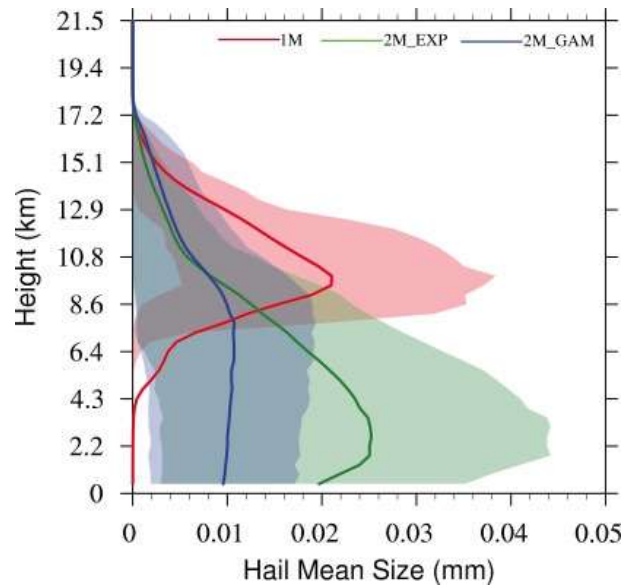


Figure 2.5: Domain-, time- and case-average vertical profiles of hail mean size. The shades represent the 10th and 90th percentile of the calculated mean with solid lines representing overall average for all cases.

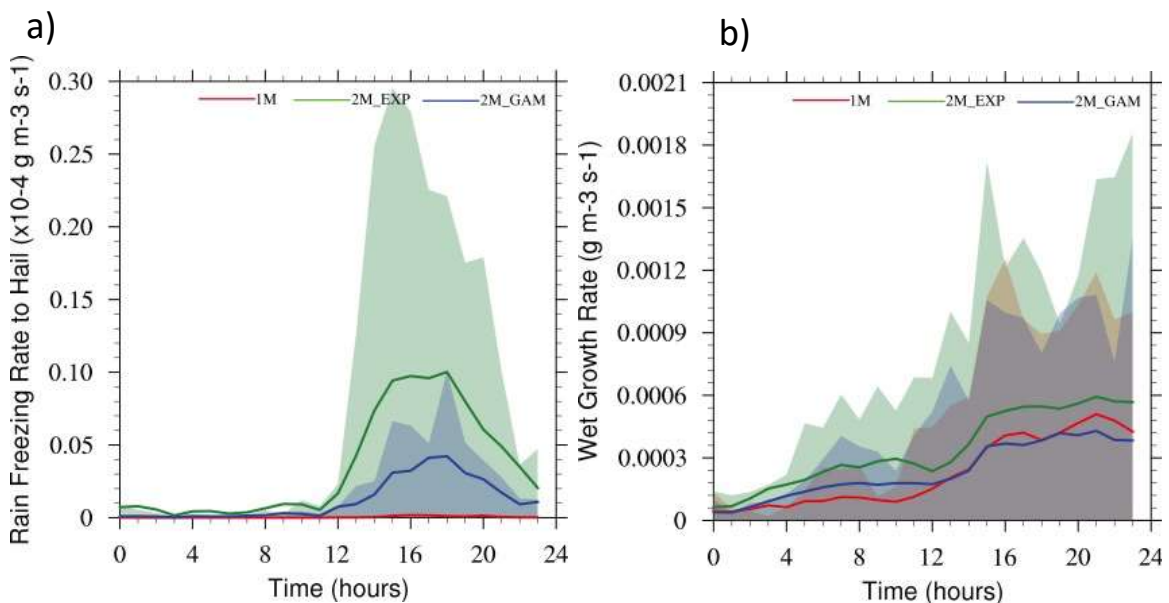


Figure 2.6: Domain- and case-average diurnal cycle of (a) rain freezing rate to produce hail embryos and (b) wet growth rate for all three microphysical schemes. As in Figure 2.1, the shades represent the 10th and 90th percentile of the calculated mean and the solid lines represent overall average for all cases.

2.4. To what extent have the extreme hail events varied since the middle of the last century?

Severe convection develops with local formation of hail larger than 2 centimetres is often observed over Belgium. This large hail events mainly take place during the months April until September. Regarding the daily time distribution, the highest amount of storms with large hail occur during the late afternoon and the evening. The main threats of large hail are damaging of crops (starting at a hail diameter of 0,6 cm), cars (from 2 cm on) and roofs (from 2,5 cm on) (Marshall et al., 2002; Stanley and Changnon, 1970; Waldvogel, 1980). From radar observations of the RMI (RMI, 2015), it can be estimated that during the period 2003-2012, hail larger than 2 centimetres felt on about 25% of the Belgian area. In recent years, hail larger than 5 cm has been observed several times with a record of 9,2 cm in 2009 (Hamid, 2009). The main aim was the examine the processes associated with hail over Belgium in the present day COSMO-CLM simulations and how these processes change in the future simulations.

For the period 2003-2012, an observation dataset with all convective cases was developed with use of radar data of the RMI (RMI, 2015) and data of ERA-interim (ECMWF, 2015). Based on this dataset, a hail index was developed to assess the geographical and temporal spread of large hail in Belgium. An analysis based on the ERA-interim (ECMWF, 2015) and NCEP/NCAR reanalysis (Kalnay e.a., 1996) can be seen on Figure 2.7 where the yearly amount of days with chance of large hail in central Belgium is visualized. During the second half of the 20th century and the beginning of the 21st century, there was a slight decrease in the yearly amount of days with chance of large hail. However, there is a large interannual variation and even the ten year average line shows clear decadal fluctuations. The yearly cumulative risk of large hail (not shown) gives a very similar trend. These results for the central part of Belgium can be extended to the most other regions of Belgium. Because of the rareness of giant hail (> 5 cm), it is very difficult to make an assessment of the trend in the frequency of this giant hail.

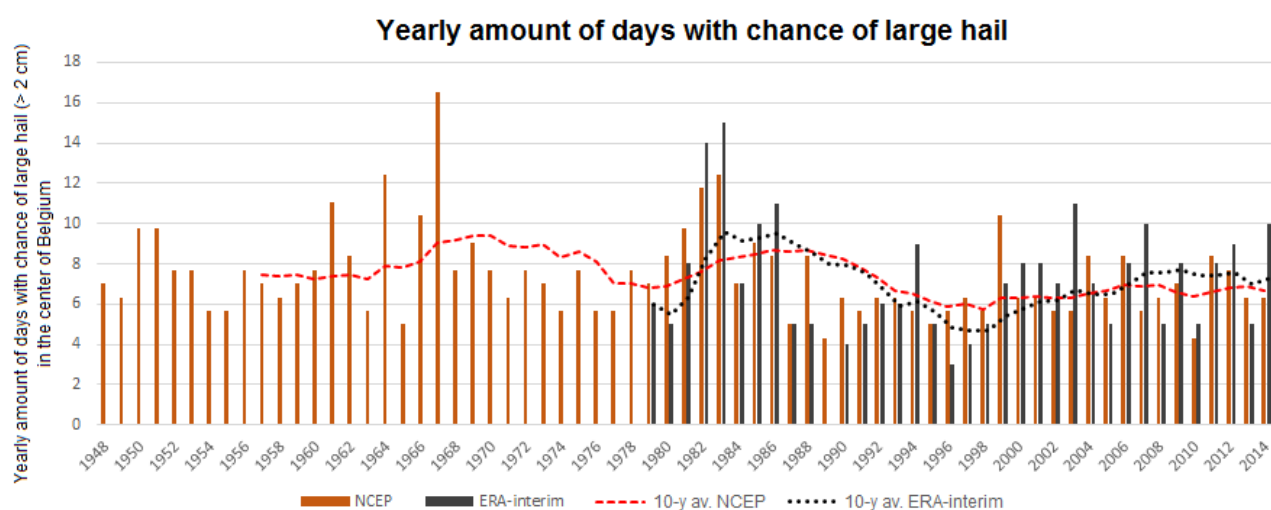


Figure 2.7: Yearly amount of days with chance of large hail in the central part of Belgium. Own simulation based on data of ERA-interim and NCEP reanalysis.

The hail index was applied on the COSMO-CLM present day (2001-2010) and future climate (2060-2069) simulations over Belgium. **The detailed analysis and results are published in the master thesis of Bart Verhaegen published by KUL (2015).**

Section 3: Impact of contrails in COSMO-CLM (deliverables D3.1, D3.2)

Given the significant implications of clouds in the climate system, it is imperative to fully understand how natural and artificial cloud formation affects the overall radiation budget in the atmosphere. One of the most visible human influences on Earth's climate system is the production of aviation contrails, which induces additional cloudiness in the upper troposphere potentially influencing surface air temperatures. Contrail formation is commonly described using the Schmidt-Appleman criterion (Schmidt 1941, Appleman 1953, Schumann 1996), as the aircraft passes at altitudes with temperatures of -40°C or lower. This mathematical formulation depends heavily on environmental conditions (i.e. temperature and pressure) and aircraft engine characteristics such as fuel content, overall airplane efficiency and water vapour emission. The produced contrails subsequently spread, becoming visually and microphysically indistinguishable from natural-occurring cirrus. It is therefore difficult to properly assess their influence on the climate system. Some climate models have incorporated contrail representations in their simulations in order to evaluate its impact, however uncertainties within overall model cloud representation can hinder the validity of the results.

In this work package, the contrail parameterization of Ferrone (2011) was incorporated into the newly implemented Seifert and Beheng (2006) 2-moment microphysical scheme within COSMO-CLM. ERA-Interim and realistic flight distribution data were used to drive the model to simulate two months, July 2006 and 2010, with a horizontal resolution of 0.22° ($\sim 25\text{km}$) for Central Europe, which is a high air traffic density area (simulation AV). In order to assess the impact of the contrail formation within the domain, additional simulations were done without the inclusion of the contrail parameterization (NOAV). These two months were characterized by heat waves with clear skies, especially July 2006. Thus, a greater impact was expected with the addition of aviation contrails in the simulations, due to the clear sky conditions.

Results were similar for both cases, thus for simplification we present results only for July 2006. The contrail parameterization essentially calculates an amount of ice, which is added to the ice category in the model. Once the contrails are present, microphysical processes dictate the evolution of this added ice within the domain depending on the environmental conditions. Figure 3.1 shows the total ice water content produced in the domain for each day of the month of July with and without contrail parameterization. An overall 6% increase of ice water content is observed for the simulations representing aviation contrails. However, in some instances (mid-month) the increase was negligible due to much drier conditions present in those days. Figure 3.2 shows the domain-time average change in high cloud cover and net downward radiation. Even though there is an increase of ice amount in the AV simulations, this does not necessarily translate to more cloudiness in all locations within the domain although the AV simulation showed on average an increase of $\sim 2\%$ in high cloud cover.

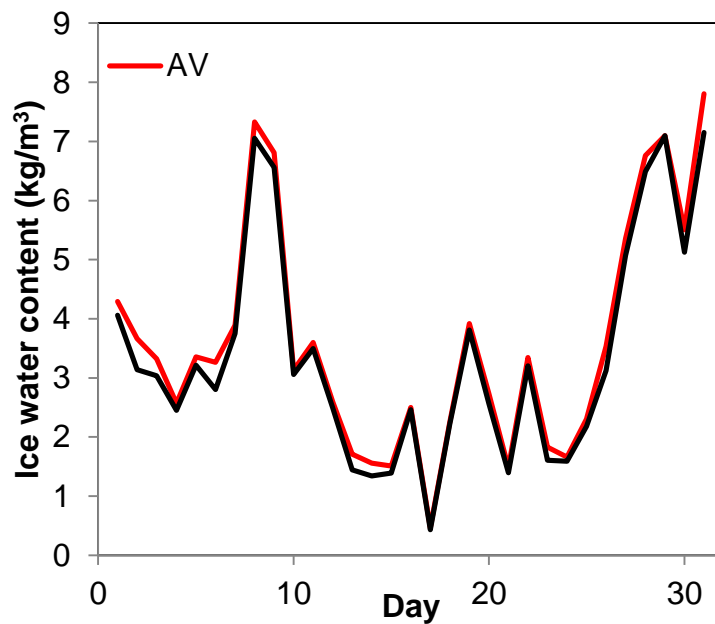


Figure 3.1: Total domain ice water content produced on each day of the month of June 2006 in both simulations with (AV) and without (NOAV) contrail parameterization.

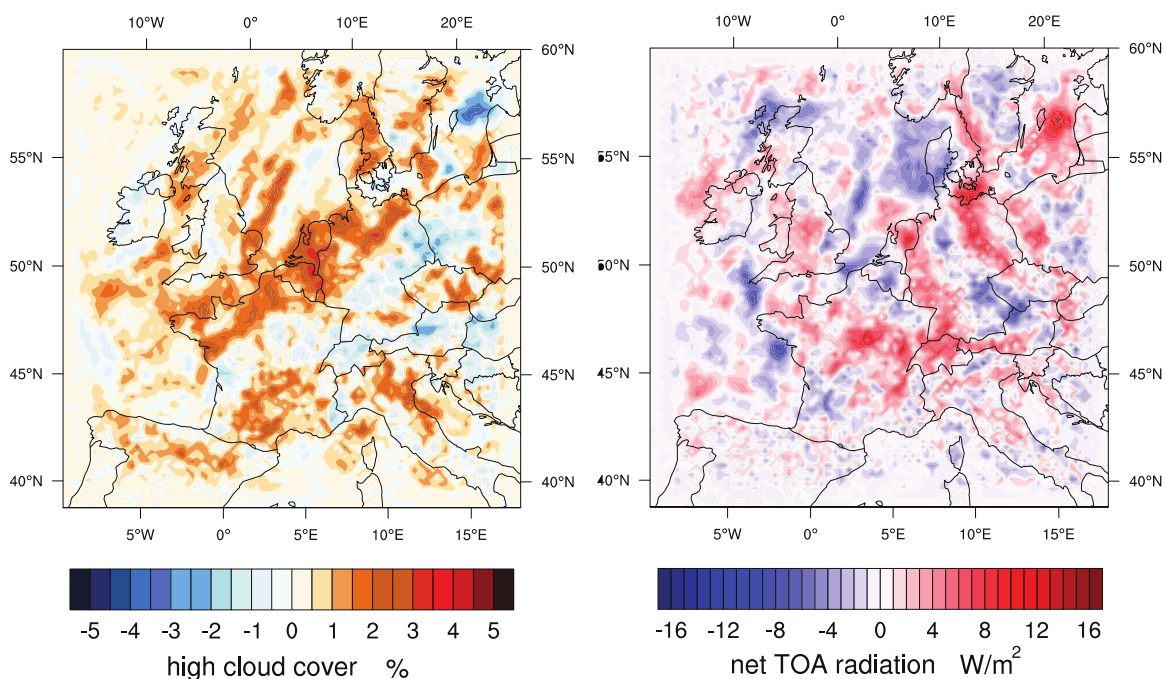


Figure 3.2: Domain-time average change of AV compared to NOAV simulations for high cloud cover (left) and net downward radiation at the top of the atmosphere (TOA, right).

With this increased cloudiness, the AV simulation showed an average increase of $\sim 0.4 \text{ W/m}^2$ in the TOA net downward radiation. This is expected since high cloud cover affects mostly the TOA outgoing longwave radiation. But high cloud cover does not necessarily coincide with higher TOA net downward radiation as observed in Figure 3.2. In Figure 3.3, the domain-time average change in the TOA outgoing longwave (OLR) and downward shortwave (DSR) radiation is shown separately. Comparing the left panels in both Figure 3.2 and 3.3, we can see that OLR follows the expected pattern of decreased amount when additional high cloud cover is present due to aviation contrail, which can lead to increased temperatures at the surface. However, the change in DSR is much more than in OLR and correlates much better with the TOA net downward radiation in Figure 3.2. Thus it seems that during the

simulated month characterized by a strong heat wave, the incoming shortwave radiation is so strong that it practically dominates the overall radiation at the top of the atmosphere even with increased high cloud cover present due to aviation contrails. Similarly to Figure 3.2 and 3.3, Figure 3.4 shows the change in surface temperature for the whole domain between AV and NOAV. Unlike other studies, there was a negligible change in surface temperature (~ -0.006 °C) attributed to aviation contrails in the model. This is probably due to the opposing effects in changes of the OLR and DSR.

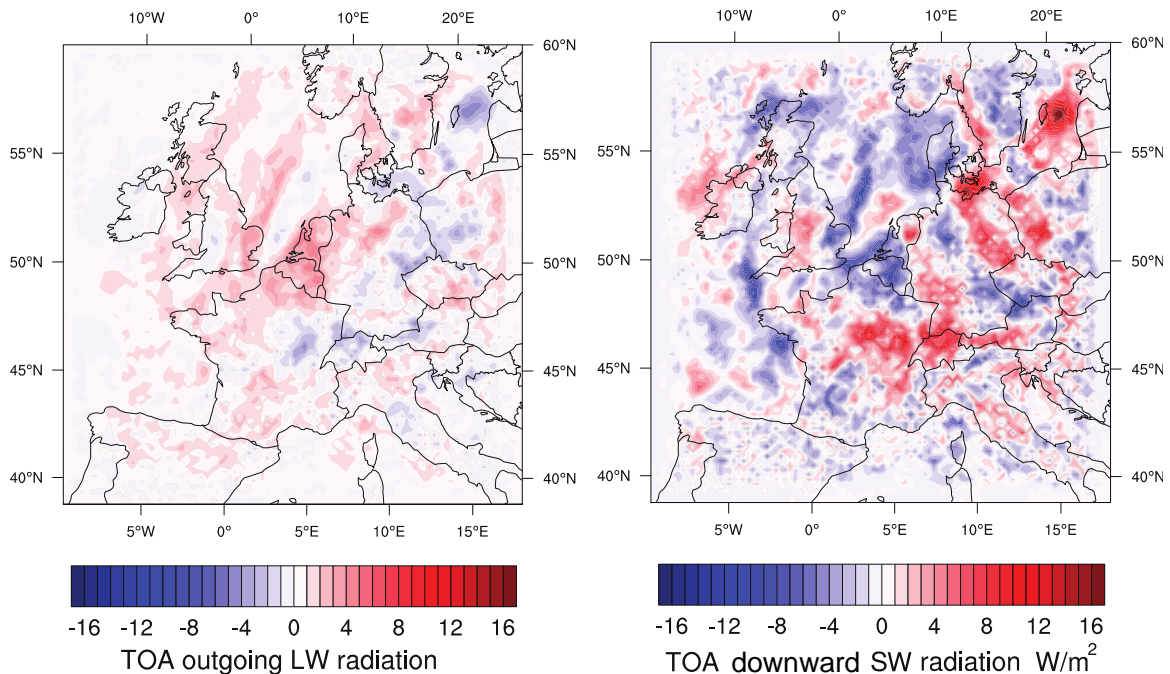


Figure 3.3: Same as in Figure 3.2 but for outgoing longwave (left) and downward shortwave (right) radiation at the Top Of the Atmosphere (TOA). For the TOA radiation, the frame of reference in the model is set so that downward radiation is identified as positive (outgoing radiation is thus indicated as negative). From this perspective a positive change in OLR (DSR) indicate less (more) outgoing (downward) LW (SW) radiation in the AV simulation compared to the NOAV run.

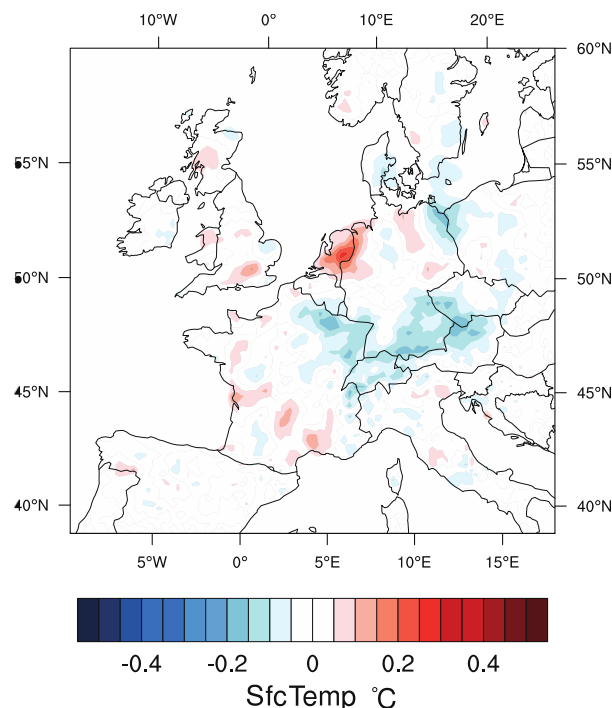


Figure 3.4: Similar to Figure 3.2 but for atmospheric temperature closest to the surface.

It is worth noting that an important aspect within the microphysical scheme that could affect the additional cloudiness attributed to aviation contrail is the rate of sources/sinks of ice within the model (e.g. rate of ice sublimation, snow formation due to ice, etc.). The rate magnitude of these microphysical processes will affect the contrail-induced ice residence time and further studies need to be done to assess the proper microphysical representation within the scheme. However, there exist many uncertainties regarding the science of cloud ice formation and so improvements done on this framework will inevitably affect these results.

Section 4: Urban climate modelling (deliverables D4.1-D4.4 and D5.1-D5.3)

In urban areas, there is always a risk of developing an urban heat island (UHI), thermal comfort stress during dry seasons or flooding when rainfall occurs. Within the MACCBET project, both the KU Leuven and VITO focus an important part of the modelling activities on urban areas, where approximately 50% of the global population resides. The KU Leuven uses the COSMO-CLM model to study the effect of future urban land use changes on the climate on a regional scale, whereas VITO develops a fast and very high resolution model to study the urban heat island phenomenon on a local scale. The basic aim of work package 4 (D4.1-4.4) was to the development and implementation of the urban parameterization TERRA_URB that is applicable for long-term regional climate simulations with COSMO-CLM. The next step was to perform long-term climate simulations for Belgium for present-day and future climatic conditions using this newly developed urban parameterization scheme. ***Over the course of the project, five scientific papers have been written about this work and the results (Wouters et al. 2012, 2013, 2015; De Ridder et al. 2015; Lauwaet et al. 2015).*** In the following chapters, the highlights will be presented.

4.1 Development of Urban Parameterization Scheme TERRA_URB:

An urban parameterization scheme in the soil module of COSMO-CLM has been developed and implemented in the COSMO-CLM model. This parameterization scheme has been used to estimate the effect of urban land use change scenarios on future climate change. The standard COSMO-CLM model uses the TERRA model as its SVAT (Soil-Vegetation-Atmosphere-Transfer) scheme (Majeski and Schröding, 1995). Based on the thermal properties of various types of vegetation and 8 different soil types, it simulates the exchange of energy and matter between the land surface and atmosphere. However, TERRA is not designed to simulate land use changes associated with urbanization. Two tracks were perused to take urbanization into account, first, a coupling attempt was done at ETH (Zurich) in which COSMO-CLM was coupled to the Community land model version 4.0 using the OASIS coupler via a subroutine coupling. Secondly, a direct urban parameterization has been developed and used. ***The results are published in a peer reviewed journal (Wouters et al 2012).***

A tile approach has been implemented in TERRA for which different surface types, including an urban fraction, can coexist within one horizontal grid cell. The urban tile adopts specific dynamic, radiative, thermal and aerodynamic parameters including roughness length, heat capacity, conductivity, albedo and emissivity. Furthermore, a bluff-roughness thermal roughness length parameterization of Zilitinkevich (1993) is adopted. New surface-layer transfer coefficients (Wouters et al., 2012) have been implemented which can deal with very small thermal roughness lengths typical for urban surfaces. Anthropogenic heat is at present

taken into account using electricity consumption and population density data (Flanner, 2009). All these changes to the COSMO-CLM SVAT model are summarized in Figure 4.1.

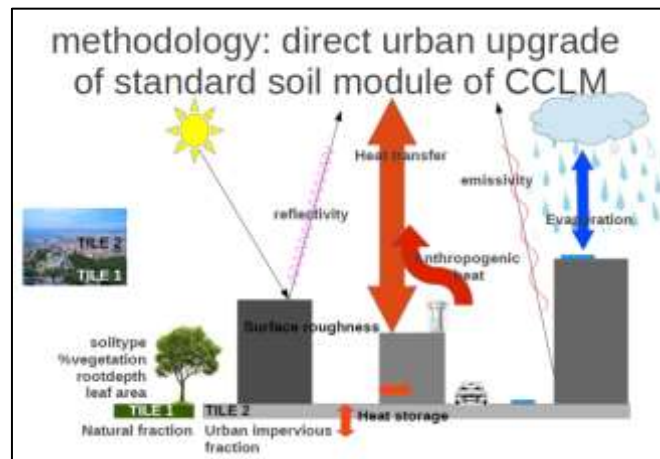


Figure 4.1. Schematic diagram showing the direct urban upgrade of standard soil module of COSMO-CLM

A more detailed description of TERRA-URB can be found in Wouters et al. (2015). TERRA-URB implements an efficient bulk representation for urban land in TERRA-ML. Herein, one takes additional land-surface parameters for representing buildings and streets in a surface grid-cell. Hereby, urban land is represented as a rough water-impermeable slab, that adopts urban bulk parameter estimates for surface roughness, albedo, emissivity and thermal inertia from Demuzere et al. [2008], Sarkar and De Ridder [2010] and De Ridder et al. [2012]. TERRA_URB employs a Monin-Obukhov-based surface-layer transfer scheme of Wouters et al. [2012] for a consistent treatment of the turbulent transport over the urban fabric. TERRA-URB takes into account the water reservoirs on impervious surfaces with the water-storage parameterization of Wouters et al. [2015]. The anthropogenic heat is considered as an additional heat source to the surface layer, following an methodology and dataset from Flanner [2009]. TERRA_URB is coupled to COSMO-CLM by means of a tile approach. Herein, the exchanges within the surface layer in terms of turbulent transport of momentum, heat, moisture, and radiative fluxes are determined separately for the building/street areas and the natural areas, and weighted according to the area fractions. TERRA_URB has a very low computational cost, and therefore it is suitable for long-term climate simulations. Two important questions addressed are given below.

4.1.1. Is TERRA_URB coupled to COSMO-CLM able to capture the urban heat island and its vertical extent in the boundary layer?

4.1.1.a. Comparison with flux-tower measurements

Obviously, urban climatic features such as the urban heat island are driven by the climatic response of urban land to the meteorological conditions. Therefore, it is investigated whether TERRA_URB is able to capture the particular response in terms of the surface energy balance according to an urban observation datasets. Hereby, TERRA_URB is decoupled from the regional-climate model. Instead, it is forced with continuous measurements for wind speed, temperature, humidity, downward radiation and precipitation during the campaigns “Basel UrBan Boundary Layer Experiment” (BUBBLE) in 2002 and “Canopy and Aerosol Particle Interactions in TOulouse Urban Layer” (CAPITOUL) in 2004-2005. This way, one focuses on the model performance in terms of the urban surface-energy balance alone, excluding any error arising from modelling the atmosphere above. For

instance, the evaluation at Toulouse centre in Rue de La Pomme during CAPITOU (see 'REF' in Figure 4.2) demonstrates that TERRA_URB is able to capture the different components of the urban surface energy balance, including the diurnal, daily and seasonal variability. In particular for the sensible heat flux, a correlation coefficient of 0.96 in summer and 0.80 in winter is obtained, and a bias of only 5 W/m² in summer and -25 W/m² in winter. This is in contrast to COSMO's original land-surface module TERRA-ML, which does not include an urban parameterization. As such, the latter was not capable to capture the surface energy balance (compare 'REF' with 'STD' in Figure 4.2).

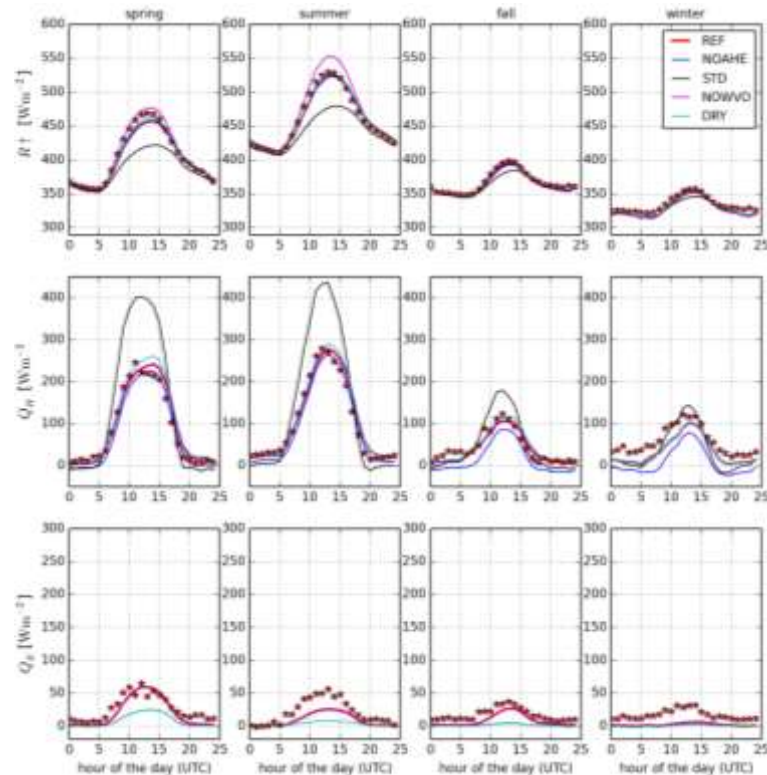


Figure 4.2: Observed (stars) and modelled (lines) diurnal averages for the infra-red upward radiation $R\uparrow$, sensible heat flux (QH) and latent heat flux (QE) for Toulouse Rue de la Pomme during the CAPITOU campaign 2004-2005 for the different seasons. REF (red) refers to the TERRA_URB reference simulation. NOAHE (blue line) is similar to REF, but ignores anthropogenic heat emission. In STD (black line), the standard land-surface module TERRA-ML is employed excluding urban parameterization. Additional sensitivity simulations are performed similar to REF, but excluding the effect of infra-red water-vapour opacity (NOWVO; cyan line) and impervious water-storage parameterization (DRY; light-blue line), respectively. From Wouters et al. [in prep.]

4.1.1.b. Comparison with vertical temperature profiles from tower observations

As shown by Wouters et al (2013) with an idealized boundary-layer advection model, the urban heat island intensity and its vertical extent, reaching their maximum during the night, are affected by several nocturnal boundary-layer properties. These boundary-layer properties also influence the vertical moisture, energy and pollutant transport and circulation in the atmosphere. At their turn, they largely affect air quality, and could modify (extreme) precipitation. A particularly important boundary-layer property is the vertical temperature profile in the lowest few hundreds of metres above the ground. Therefore, the modelled boundary-layer temperature profiles are compared with observations from 150 metre high towers located in the province of Antwerp, a first one from VMM in Zwijndrecht (industrial) and a second one from SCK/CEN in Mol (rural). This evaluation (see Figure 4.3) demonstrates that TERRA_URB coupled to COSMO-CLM (REF) is able to capture the

temperature profiles of both towers. In particular, the model results confirm the more neutral/unstable temperature slope in the industrial site in Zwijndrecht in contrast to the more stable temperature slope in the rural surroundings in Mol. This is again in contrast to the standard model version COSMO-CLM (STD) excluding the urban land-surface parameterization, which was not able to reproduce the tendency towards more neutral/unstable temperature profiles in Zwijndrecht.

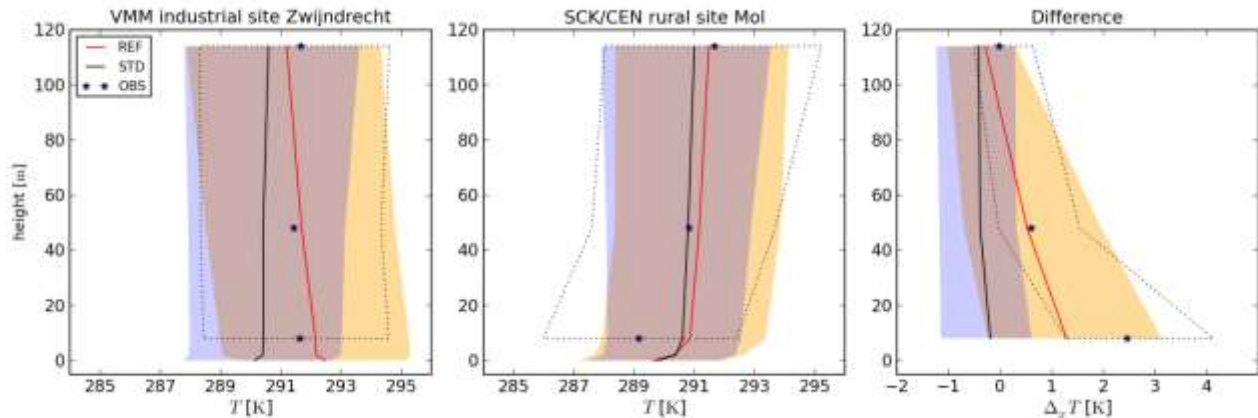


Figure 4.3 : observed (stars) and modelled (full lines) nocturnal (0H) vertical profiles for VMM industrial site in Zwijndrecht and the SCK/CEN rural site in Mol, averaged for the summer period 2012/07/21 → 2012/08/20. Hereby, both the reference simulations (REF; red) of COSMO-CLM coupled to TERRA_URB and the simulation (STD; black) with the standard model without TERRA_URB, and they are shown. The colour areas represent the spread between the 16th and 84th percentiles of the REF simulation (red) and the STD simulation (blue), and the dotted contour that of the observations. The right-hand panel shows the profile of the temperature differences between the two towers.

4.1.1.c. Comparison with urban climate observations

The model is compared with VITO's urban climate observations. Hereby, a good agreement is found with the in-situ measurements for air temperature in Antwerp (see Figure 4.4) and in Gent (not shown). Especially, the urban heat island intensity, calculated from the difference between the urban station at 'Koninklijk Lyceum van Antwerpen' (KLA) and the rural station at the organic farm 'Van LeeMputten' (VLM) in Vremde, are very well reproduced, including the diurnal and daily variability. For the latter, only a bias of -0.03K and high correlation coefficient of 0.78 are found in the UHI intensities. **A research paper on the above results is in progress (Wouters et al., 2015)**

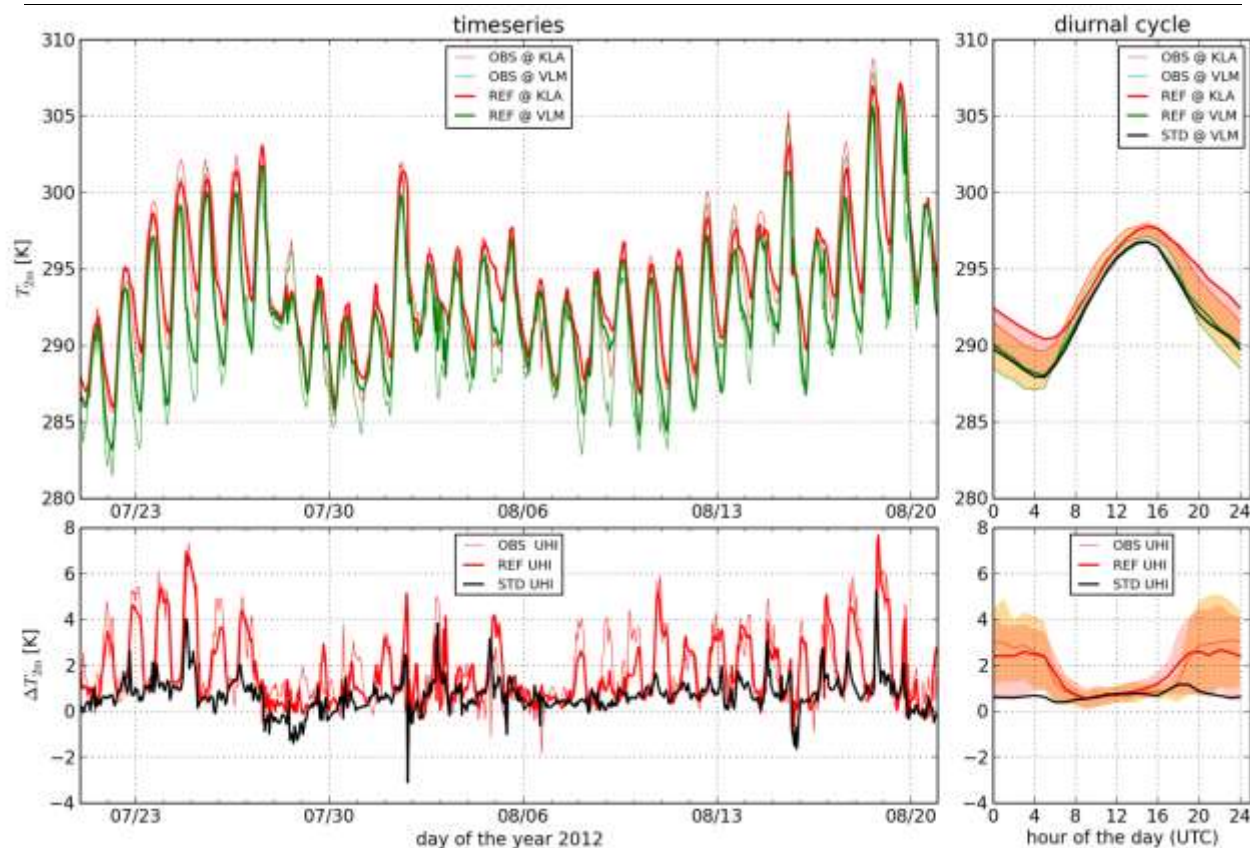


Figure 4.4: Time series and mean diurnal cycle for modelled (thick lines) and observed (thin lines) temperature at the urban site 'Koninklijk Lyceum Antwerpen' and the RURAL site (Vremde) for mid-summer (2012/07/21 until 2012/08/21). Model results for the reference simulation with TERRA-URB coupled to COSMO-CLM (REF) and the standard version of COSMO-CLM without urban parameterization (STD) are shown. The urban heat island (UHI) is calculated as the difference between the results for KLA and VLM. The orange and red areas in the upper-right panel represent the UHI for the observations and the model results for REF. The orange and red areas in the lower right panel represent the ranges between the 16th and 84th percentiles of the respective urban heat island intensities.

4.1.1.d. Intercomparison with other urban land-surface parameterizations

An Urban Model Intercomparison Project URBMIP has been established within the CLM community. The main partners herein are the KU Leuven, PIK Potsdam and the DWD. Herein, three urban land-surface parameterizations coupled to the same model COSMO-CLM have been compared, namely TERRA-URB, TEB and BEP-DCEP. The urban land-surface parameterizations vary in complexity, computational cost and needed input parameters. Each of the land-surface parameterizations have been coupled to exactly the same atmospheric model system of COSMO-CLM, and exactly the same model setup at very high resolution (1km) over Berlin. So in each of the three model setups, only the urban land-surface parameterization is altered. The resulted paper Trusilova et al. [in press] has shown that TERRA_URB is able to perform equally well as the other land-surface parameterizations for reproducing in-situ measurements for Berlin, even though the additional computational cost of TERRA_URB is more than 2 to 5 times lower than the other urban land-surface parameterizations.

4.1.2. What are the achievements and applications with TERRA_URB?

4.1.2.a. Out-of-the-box urban land-surface parameterization for high-resolution regional climate modelling and numerical weather prediction.

The development of TERRA_URB is accepted by the COSMO Scientific Steering Committee to be part of standard model code of the COSMO(-CLM) model (see CLM-community newsletter No5). As TERRA_URB was proven to be both reliable in capturing the city-scale urban-climate features and computationally inexpensive, application in numerical weather prediction at the DWD accounting for cities is expected by the end of this year. This also allows the CLM-community consisting of a (extra-) European scientific network with over 200 scientists working with COSMO-CLM to perform long-term urban-climate studies. Additional global urban external parameters have been introduced in COSMO(-CLM) surface-data preparation tool (EXTPAR3.0). This allows using TERRA_URB out-of-the-box for most cities in the world at high resolution for both numerical weather prediction and regional climate modelling.

4.1.2.b. projections of urban heat stress under future climatic conditions and future urban land use

10-year high-resolution urban climate simulations over Belgium have been performed with COSMO-CLM and TERRA_URB. Based on these results, a 'spatial' and 'climatological' heat-stress indicator have been developed for future heat-stress assessment in Belgium. Hereby, we did not only account for climate change scenarios, but also for the effect urban expansion. The latter are based on projections of urbanization towards 2060 by VITO spatial model (Engelen et al. 2011). The results are described in the VMM Research report (De Ridder et al. [2015], part 3: heat-stress indicator based on urban regional climate modelling) and the VMM climate report (Brouwers et al. [2015]), see also Figure 4.5. The heat stress is shown for urban land use in 2000 (urb: 2000, maps links) and for expected land use in 2060 (urb: 2060).

4.1.2.c. Assessment of urban climatic drivers for the regional climate

The seasonal dependency of urban heat islands (UHI) and their climatic drivers are studied with model-based sensitivity for Belgium using the TERRA_URB coupled to COSMO-CLM, see Wouters et al. [in prep]. Both the model results and observations indicate that nocturnal UHI intensities are larger during summer than during winter on average. Sensitivity experiments demonstrate that the existence of the Urban Fabric (UF; i.e., presence of streets and buildings), the Anthropogenic Heat Emission (AHE; i.e., combustion and other heat release into the atmosphere) as well as their synergic forcings determine UHI intensities at the scale of the cities.

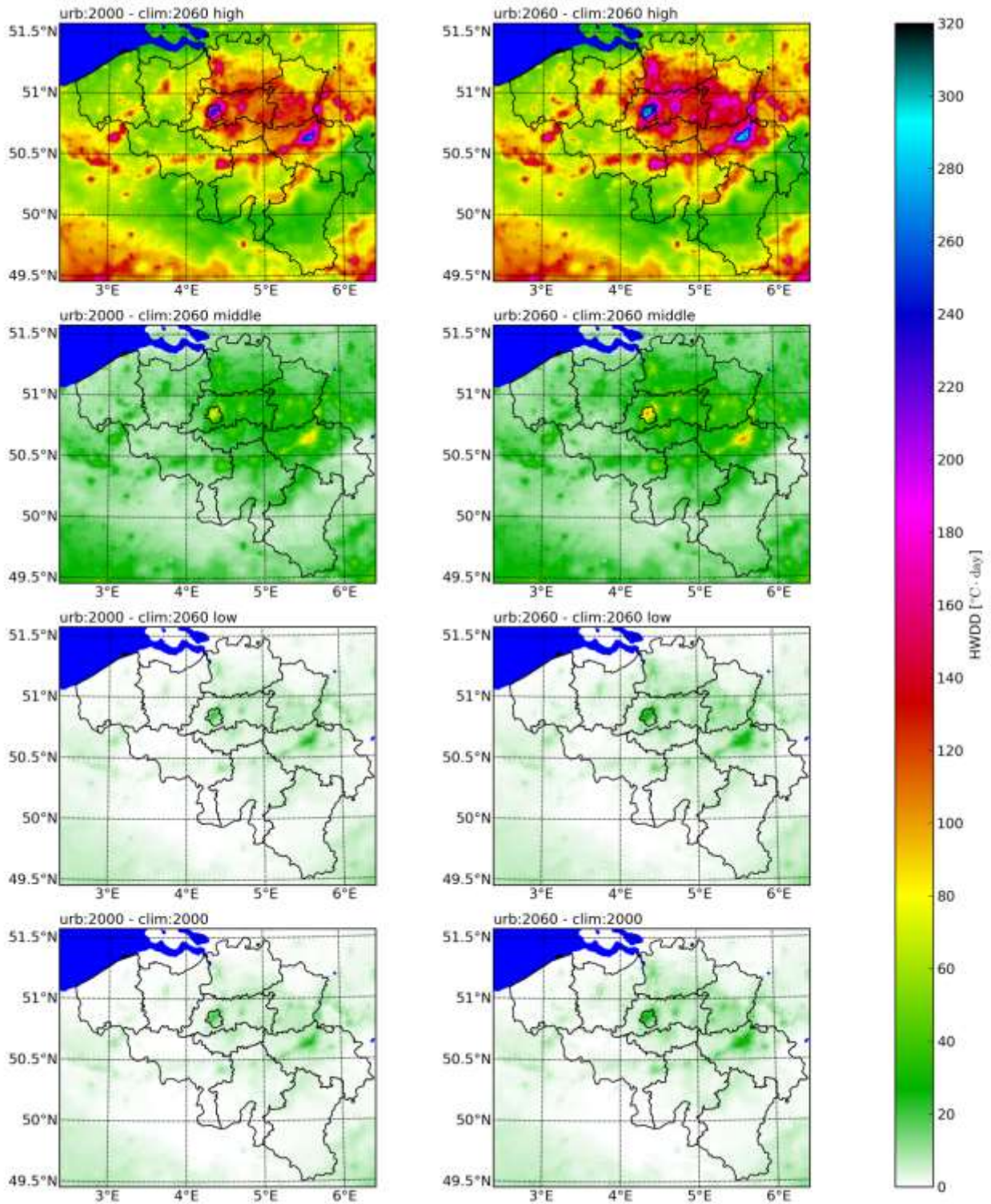


Figure 4.5: Based 10 year high-resolution climate simulations with TERRA_URB coupled to COSMO-CLM for Belgium , the annual-basis “heat-wave degree days (HWDD)” are calculated for: 1. the recent past 2000 - 2010 (clim: 2000, lowest maps), and 2. according to low, middle and high climate scenarios 2060-2070 (clim: 2060 – low/middle/high, maps above).

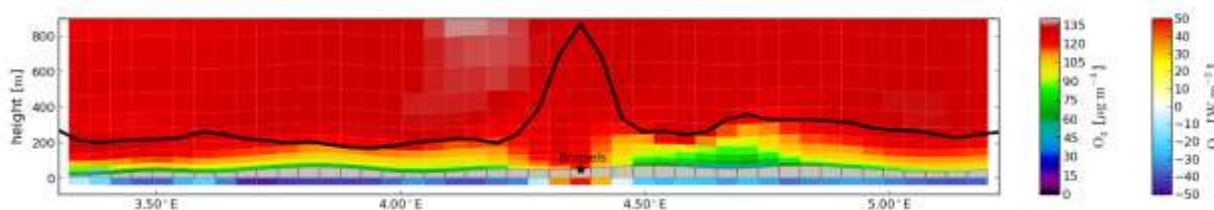


Figure 4.6. Air-quality modelling accounting for urban-climatic conditions taken from TERRA_URB coupled to COSMO-CLM. The figure shows a Zonal vertical transect through Brussels of ozone concentration modelled by AURORA (“Air quality modelling in Urban Regions using an Optimal Resolution Approach”; Mensink et al. [2001]). It is a snapshot (2009/08/16 21:00UTC, local time is 23:00) during the heat wave in august 2009. The z-axis shows the height above sea-level. The black line corresponds to the boundary-layer height simulated by COSMO-CLM+TERRA_URB. The lower colour bars below the grey orography bars represents the turbulent surface-heating or cooling at that time.

4.1.2.d. Assessment of impact urban climate on air quality

Urban climate largely affects the boundary layer properties and at its turn this affects air quality. Model results from VITO's AURORA model taking climatological input from COSMO-CLM + TERRA_URB indeed demonstrate that the urban climate largely affects air quality. In particular, high ozone concentrations during ozone peaks are prolonged in the evening and night in cities due to an enhanced vertical turbulent transport of pollutants in the urban boundary layer: The prolonged ozone concentrations are explained by the enhanced vertical transport of high ozone concentrations from aloft towards to surface above cities. This is despite the higher emissions that would lead to more ozone destruction in the evening. The enhanced vertical transport results from the urban heating which destabilized the boundary layer. Hereby, an urban boundary layer is formed for which a destabilization of the temperature profiles are found as shown earlier in Figure 4.3. The enhanced vertical transport also dilutes the NO_x concentrations, which would lead to less destruction of ozone at the surface. However, NO_x concentrations still remain high at the surface, because the NO_x dilution is (over)compensated by the higher NO_x emissions in urban areas such that it maintains the ozone destruction rate by NO_x in urban areas. As a consequence, the boundary-layer mixing-dilution process of NO_x could not explain the prolonged ozone concentrations.

4.1.2.e. Detailed impact of urbanization scenarios on the regional climate of Flanders

From VITO's spatial model, several detailed scenarios for the Flemish region have been employed in TERRA_URB coupled to COSMO-CLM. This way, address the impact of land-use change on the climate in Flanders. Hereby, the impact on temperature and precipitation has been studied, but also the associated spread and uncertainty. ***This work has been accomplished in the master thesis of Femke Faber.***

4.1.2.f What are the perspectives with TERRA_URB?

In the framework of the CORDEX.be (BELSPO) project, 30-year high-resolution climate simulations are performed with TERRA_URB coupled to COSMO-CLM. Because of the long-term datasets, they will allow to address the influence of urbanization on (extreme) temperatures, (extreme) precipitation statistics and air quality under future climate and land-use change scenario's for Belgium. The dataset will also represent one of the members of the high-resolution climate micro-ensemble climate archive.

The goal of the Work Package 5 was to create, evaluate, and apply a numerical model intended for downscaling atmospheric fields over cities. The focus is on the Urban Heat Island (UHI) phenomenon. An important prerequisite was that the model had to be much faster than traditional high-resolution mesoscale climate models, since we want it to be able to perform long simulations of current and future climate, at a spatial resolution of the order of a few hundred metres. Task 5.1 dealt with the development of the new urban climate model (UrbClim). Task 5.2 focused on the validation and on establishing a reference simulation for the city of Brussels. In Task 5.3 we then generated urban climate projections for Brussels.

4.2. Development of Urban boundary layer climate model UrbClim

VITO developed a new (and novel) urban boundary layer climate model, further referred to as UrbClim (Figure 4.7). The model domain typically covers urban agglomerations over a few tens of kilometres, in the vertical extending up to around 2-3 km height. It solves the discretized versions of the conservation equations for momentum, potential temperature, and specific humidity, and the incompressible form of the continuity equation. The pressure gradient force is not calculated internally but taken from a large-scale forcing model. In particular: the ECMWF model for current conditions, and the COSMO-CLM regional climate model (results from partner KUL in MACCBET) when considering future climate. Also cloudiness and the consequent short- and longwave radiation fields are adopted from the large-scale model. The calculation of land surface energy fluxes is done by means of the land surface scheme of De Ridder and Schayes (1997), modified to account for urban surface exchange processes (De Ridder, 2006; Demuzere et al., 2008; Sarkar and De Ridder, 2011; De Ridder et al., 2012).

4.2.1. Does UrbClim perform up to international scientific standards?

Before starting model experiments for Brussels, UrbClim was verified on two urban areas where good validation data are available: Toulouse (France) and Ghent (Belgium). In the case of Toulouse, the simulations were performed for the months of June and July 2004. UrbClim was able to model the measured fluxes with high accuracy, the bias was below 10 W/m² and the correlation coefficient was 0.9 (Figure 4.8). As a consequence, the UHI effect between the city centre and surrounding rural sites was captured very well by the model. Subsequently, UrbClim was applied to the wider area of Ghent. The reason for considering Ghent was the availability of high-quality validation data, which were collected in the course of a dedicated experimental campaign during the Summer of 2012 by VITO (within another project). We ran UrbClim on Ghent for the month of August 2012, and compared simulated 2-m air temperature with observed values, for a measurement station in the centre of the city (near the Vrijdagsmarkt), and another station in a rural area in Melle near Ghent (Figure 3.3). The root mean square error on the temperature difference was found to be 1°C, the bias 0.2°C, and the correlation coefficient 0.69. This is as good as - or better than - typical values previously obtained by us with more complex (hence also more CPU intensive) mesoscale models, see e.g. Sarkar and De Ridder (2011).

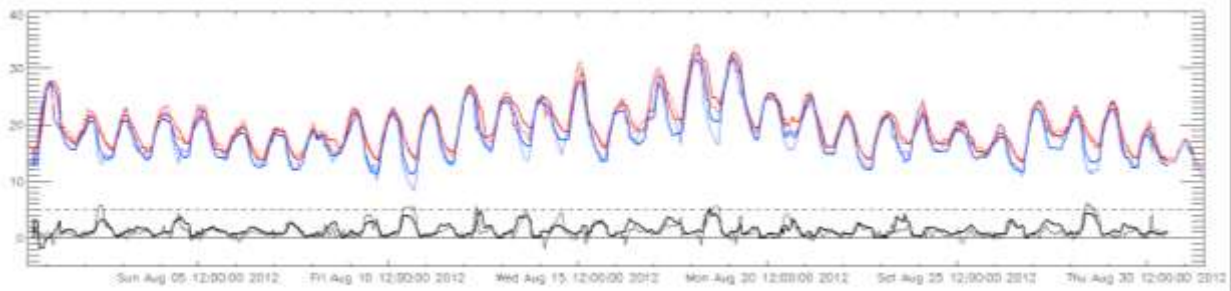


Figure 4.9: Simulated (thick lines) versus observed (thin lines) 2-m air temperature for an urban (red lines) and a rural (blue lines) site, for the month of August 2012, agglomeration of Ghent. The black lines in the lower part of the graph show the simulated and observed urban-rural temperature differences.

Afterwards, we shifted our focus back to Brussels, as was promised in the MACCBET proposal. It was a challenging task to find suitable air temperature measurements in and around the city to validate UrbClim, but we were able to get data from 3 meteorological stations (one inside the city centre) for the summer of 2008 in the Brussels area. The accuracy of the model results was assessed by comparing them to the time series of the validation data, focusing on capturing the temperature difference between the city centre and more rural locations. Figure 4.10 demonstrates that the UrbClim model is capable of reproducing the observed daily cycle and peak values, which reach 6°C during some nights. The error statistics are in line with the previously reported results for Ghent and Toulouse. We can thus conclude that the UrbClim model is certainly appropriate to study the urban climate in the Brussels region.

4.2.2. What are the characteristics of the current Urban Heat Island of Brussels?

To answer this question, we performed a reference UrbClim simulation for the period 1986-2005, driven with ECMWF ERA-Interim data, at an unprecedented horizontal resolution of 100m. In our analyses, we focus on the night time UHI of Brussels at 2300 LT, since this is the moment that the UHI is the strongest and has the biggest potential impact on human health, because the warmer urban night-time temperatures limit the recuperation of city inhabitants from heat stress during daytime. Figure 4.11 shows the resulting mean UHI map of Brussels for the summer period. Mean temperature differences between the city centre and the countryside can reach up to 4°C (note that this is a mean situation, some nights the differences can reach 10°C). The hottest areas are found in the industrial zones along Brussels' canal whereas the coolest place within the capital borders is the Zoniën forest.

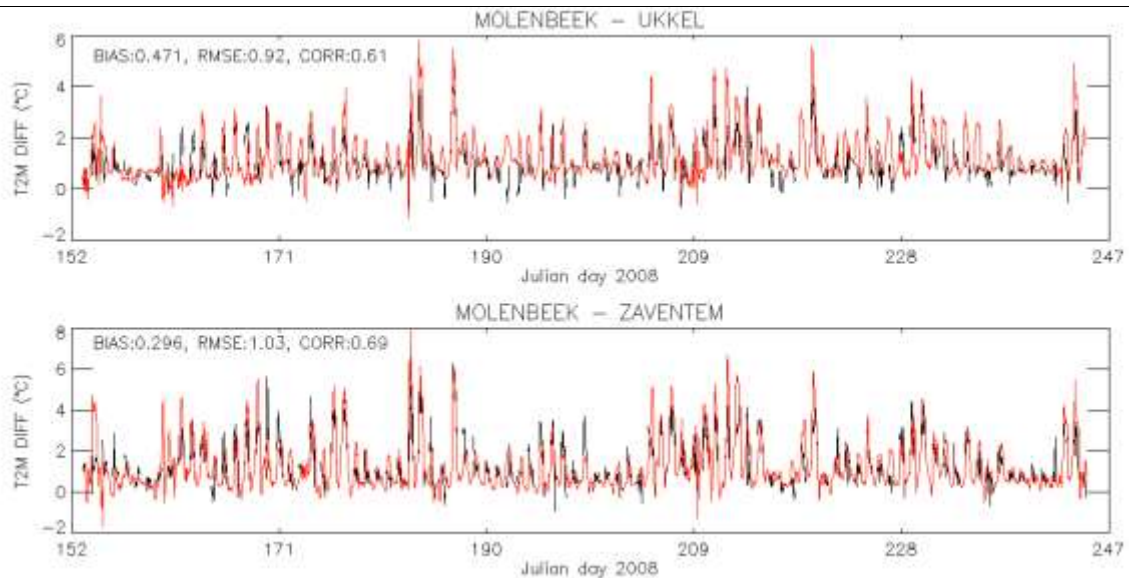


Figure 4.10: Comparison between the observed (black) and simulated (red) 2m air temperature differences between the city centre and the 'rural' locations. The error statistics (bias, root mean square error and Pearson's correlation coefficient) are included.

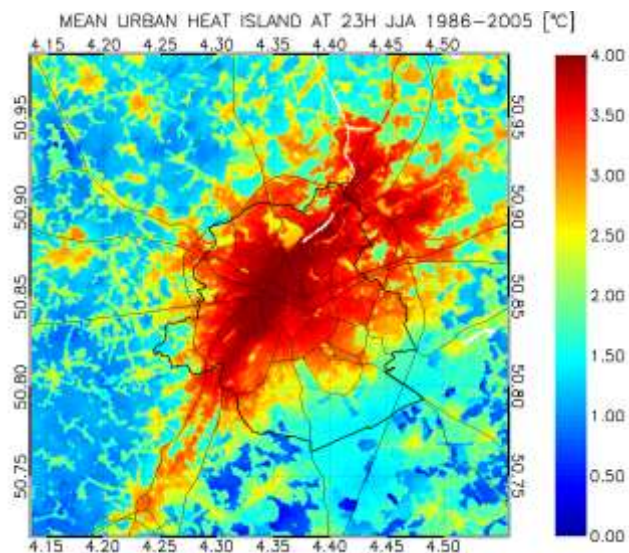


Figure 4.11: Brussels mean Urban Heat Island at 23h during the summer period (June-August).

Based on this data set, interesting analyses can be performed whereby several meteorological variables can be linked to the UHI intensity in Brussels (taken as the difference between the P90 (city centre) and P10 (countryside) value at midnight). Figure 4.12 shows the relationships between the daily night-time UHI values from the ERA-Interim driven simulations and several meteorological parameters that are expected to play a role in the formation and intensity of the UHI. As was the case in several observational studies, UHI intensity is found to be negatively correlated to the wind speed. Also positive correlations with incoming shortwave radiation (a measure for cloud cover), surface pressure and daily maximum temperatures are found, as well as negative correlations with soil water (a measure for recent precipitation) and incoming longwave radiation. Surprisingly, by far the strongest correlation (0.73) is found for the inversion strength in the lowest 100 m of the atmosphere. When taking a larger part of the temperature profile into account (1500m), the correlation decreases strongly to 0.13. An analysis of the wind direction revealed that the maximum UHI effects are reached when the wind is coming from the East (warm and dry air), as you would expect in Belgium.

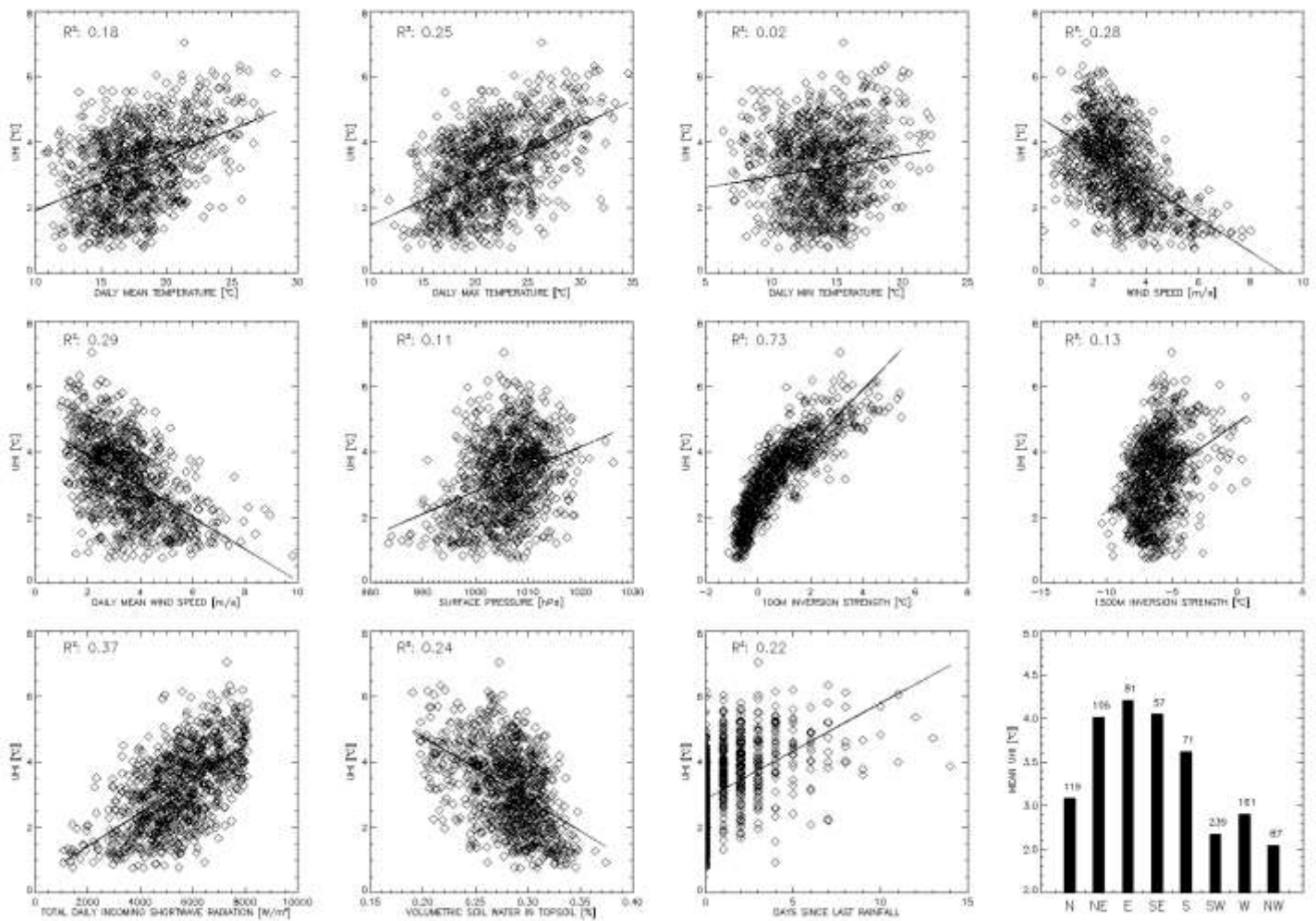


Figure 4.12: Correlation between several meteorological variables and the UHI intensity at midnight for Brussels. The lower right panel shows the dependency of the UHI intensity on the wind direction. The numbers above the bars indicate the number of cases that are included.

4.2.3. How does the Urban Heat Island of Brussels evolve under future climate conditions?

To assess the evolution of Brussels' UHI under plausible future climate conditions, results from the global climate model EC-Earth are dynamically downscaled with COSMO-CLM and UrbClim. The COSMO-CLM simulations are performed using one-way grid nesting up to a horizontal resolution of 3 km. This model chain is applied to simulate a 10-year reference period (2000-2009) (REF), driven with meteorological data from the base run of the global climate model EC-Earth. Secondly, a 10-year period in the future (2060-2069) is simulated, driven with EC-Earth model results for the Intergovernmental Panel on Climate Change (IPCC) RCP4.5 and RCP8.5, two of the RCPs used in the climate simulations of the Coupled Model Intercomparison Project (CMIP5).

In our analysis, the UHI intensity is calculated as the difference between the 90th and 10th percentile of the temperatures of the entire UrbClim domain at 0000 LT, in order to obtain a relatively general value of UHI intensity for the whole of Brussels, without taking only the extreme locations into account. Calculated this way, the mean UHI intensity of Brussels over all summer periods during 2000-2009 from the ERA-Interim driven simulations amounts to 3.15°C.

The impact of two plausible trajectories for future climate conditions, RCPs 4.5 and 8.5, on the UHI of Brussels and related meteorological parameters is shown in Table 4.1. Clearly, the UHI of Brussels is not increasing in response to greenhouse-gas induced climate change, with 10-year mean values changing not significantly (at a <1% level) in RCP4.5 and even decreasing slightly in RCP8.5. Interestingly, most related meteorological parameters do show changes that should benefit UHI formation (temperature, maximum temperature and wind speed) or do not change significantly (inversion strengths, rainfall and soil moisture). Only the radiation parameters show significant changes that have a negative effect on UHI formation.

Table 4.1: Overview of the 10-year mean values over all summer periods (June-August) for the UHI of Brussels and related meteorological variables for the reference and future climate simulations. Significant differences (at a <1% level) are indicated in bold.

	REF	RCP4.5	RCP8.5
UHI (°C)	3.22	3.20	3.08
Temperature (°C)	17.4	18.3	18.9
Daily max temperature (°C)	21.6	22.5	23.2
100m inversion strength (°C)	0.01	-0.07	0.08
Wind speed (m s ⁻¹)	2.55	2.21	2.17
Rainfall per summer (mm)	180	181	178
Volumetric water content topsoil (%)	0.28	0.29	0.28
Mean daily shortwave radiation (W m ⁻²)	220	201	210
Longwave radiation (W m ⁻²)	330	333	342

Whereas the changes in incoming solar radiation are not in line with the changes in the UHI, the slightly increasing incoming longwave radiation is found to play an important role. The increase in incoming longwave radiation in RCP8.5 is caused by higher air temperature and humidity values, since no significant changes in the night-time cloudiness were found. Indeed, when we use the overall temperature and humidity values from the reference and RCP8.5 simulations, we can calculate the expected changes in downward longwave radiation, which results in a difference of 11.6 W m⁻² between both simulations (314.5 and 326.1 W m⁻² respectively) that is clearly in line with the values in Table 4.1.

To explain the slight reduction of UHI intensities in the future scenarios, we have performed an additional analysis on the role of the extra longwave radiation. To isolate the impact of added longwave radiation, a case study is set up for the night from the 4th to the 5th of July 2008, during which a strong UHI formed (Day 187 in Figure 4.10). These two days are simulated again, driven with ERA-Interim data, but with an addition of 12 W m⁻² to the incoming longwave radiation in the input data, the mean difference between the RCP8.5 and REF scenario (Table 4.1).

Figure 4.13 presents the resulting potential temperature profiles for a rural and urban location at 0000 LT. In the urban location, the temperature profile is more or less neutral and the extra longwave radiation has a small but noticeable effect spread over the lowest 400m of the profile, only slightly warming the part of the profile closest to the surface. In the rural location, a strong inversion has formed and here the extra longwave radiation can only affect the lowest few meters of the profile, so the effect on the 2m temperature (+0.35°C) is much higher than in the urban location (+0.05°C). The resulting UHI intensity is thus reduced by 0.3°C. This mechanism can explain why we see a slight decrease in the overall UHI intensities in the RCP scenarios whereas other meteorological variables support an at least equally strong UHI.

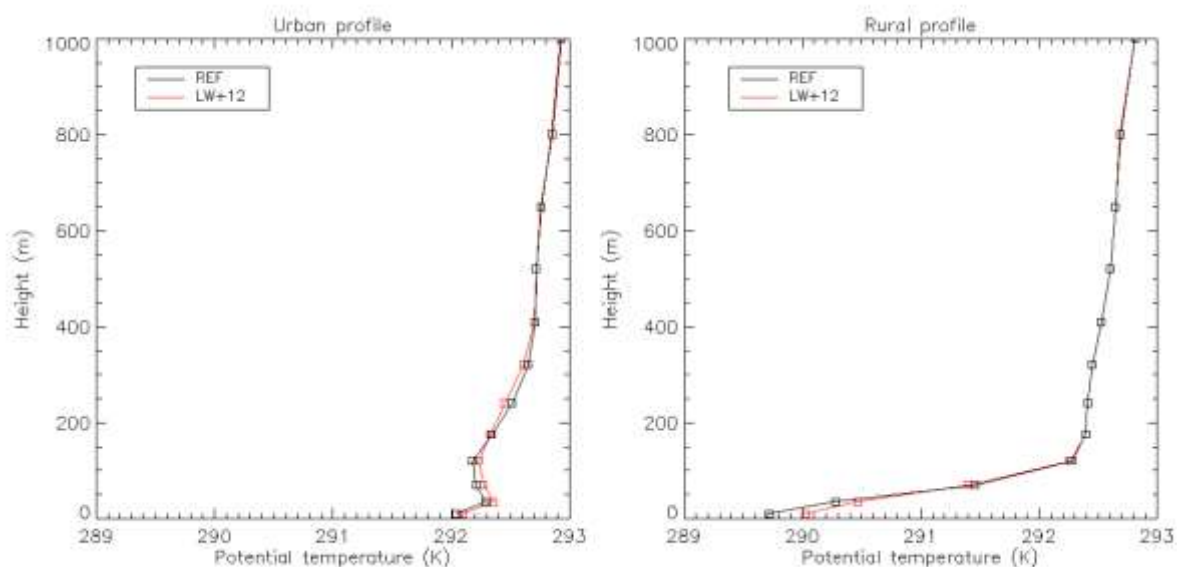


Figure 4.13: Potential temperature profiles at 0000 LT on 5 July 2008 at an urban and rural location for both the reference simulation (REF) and the simulation with 12 W m^{-2} added longwave radiation (LW+12). The urban and rural locations are defined as the location of respectively the 90th and 10th percentile of the 2 m air temperature map at 0000 LT.

Note that our simulations do not account for potential future urban growth, an effect that typically increases the urban-rural contrasts. Also, we use the results of only two RCP scenarios, calculated with one global climate model, coupled to one regional climate model, so we cannot estimate the resulting dispersion with respect to alternative climate change scenarios or global/regional climate models. Given these limitations and substantial uncertainties, the results presented here are not suited for local risk assessment but should rather provide a coherent picture of potential heat stress changes in the city area due to increasing greenhouse-gas emissions and resulting warming. Our results emphasize the need to focus on the unique aspects of urban climate in order to design well-informed adaptation strategies in urban areas.

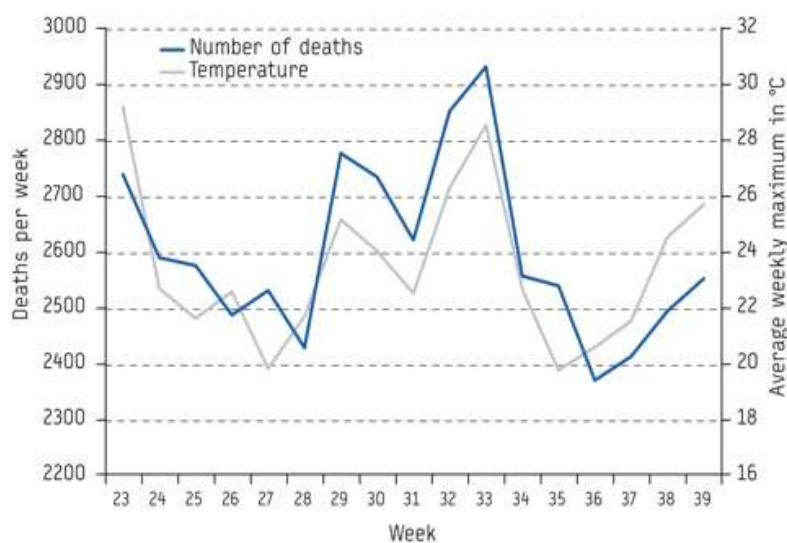


Figure 4.14: Relation between the air temperatures and the number of deaths during the heat wave of 2003 in France (Garssen et al., 2005).

4.2.4. Does the Urban Heat Island of Brussels affect the health of its citizens?

Although the magnitude of Brussels' UHI is not expected to change a lot in the (near) future, the presence of the urban heat island does have an impact on extreme temperatures, especially during the night, which are expected to occur more frequently in the future. This has important consequences for human health, since consecutive hot nights during which people cannot recuperate from extreme daytime temperatures may be most detrimental to the health of city inhabitants (Karl and Knight, 1997). Several studies have already demonstrated the link between high temperatures and mortality (Figure 4.14). With regard to human health and exposure mapping, the high spatial resolution of UrbClim provides much added value. A resolution of 100m is considerably finer than what is customarily used in climate modelling studies over cities, which generally employ resolutions of around 1 km or coarser. In this context, it should be noted that Sobrino et al. (2012), based on the analysis of aerial thermal-infrared imagery over Madrid, concluded that a spatial resolution of the order of a few hundred metres resolves the detail at the city neighbourhood scale much better than a 1km resolution. De Ridder et al. (2014) found that exposure, in their case to NO₂ concentrations over Brussels, decreased by 38% when degrading the resolution of their model several times by a factor of 4.

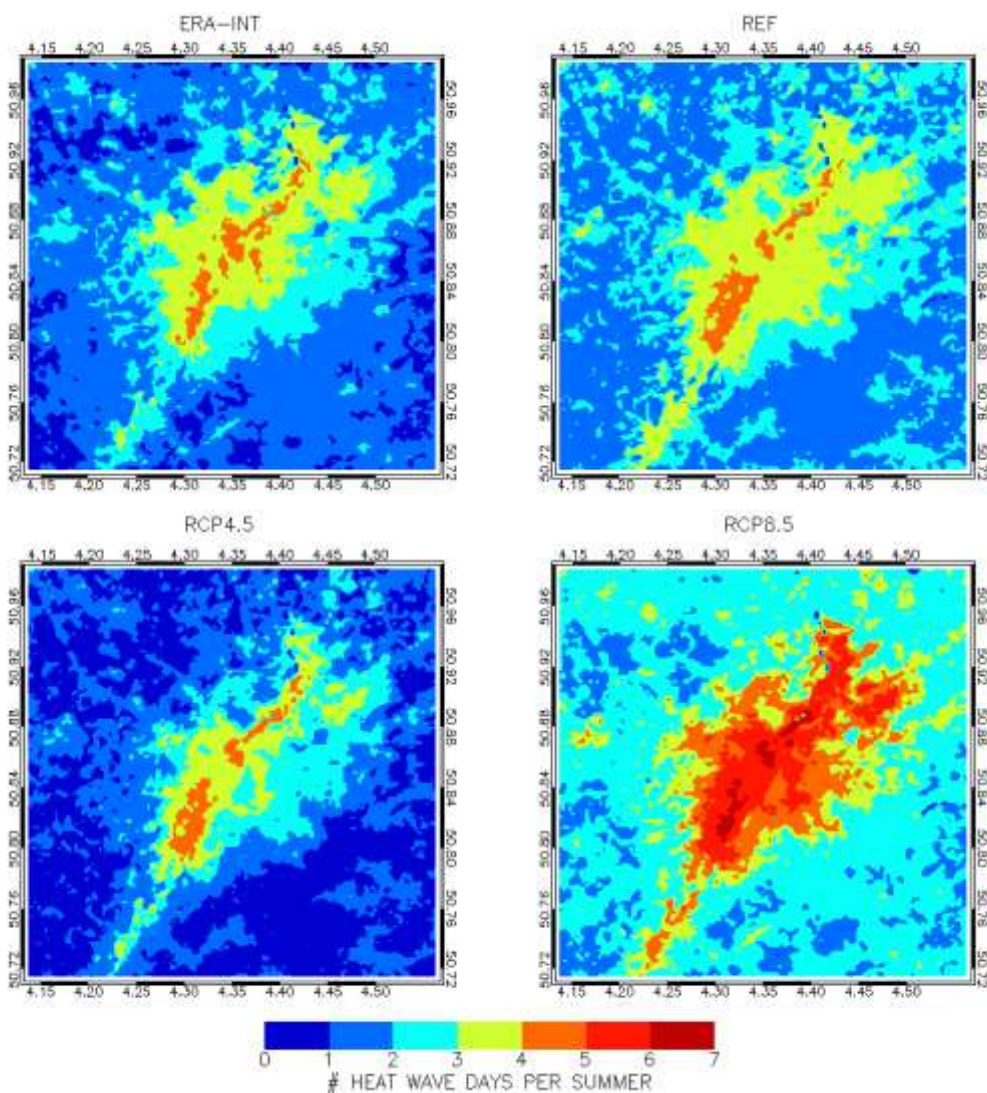


Figure 4.15: Maps of the number of Heat Wave Days per summer (June-August) for all 10-year simulations.

In the literature, a large number of definitions for extreme heat events exists, which all share some common properties. Since health effects become especially severe during prolonged periods of hot weather, most definitions consider multiple consecutive days of extreme weather. Mostly, the definitions also deal with minimum and maximum temperatures, since lack of cooling during the night is an important factor in health effects related to heat stress. Finally, definitions generally make use of statistically determined thresholds. In this project, we opted to apply the definition from the Federal Agency for Public Health in Belgium, which defines a Heat Wave Day (HWD) as a day that both the 3-day moving average minimal and maximal temperatures exceed a threshold value, listed as 18.2 °C and 29.6 °C, respectively. These values correspond to the 98th percentiles of the summer (JJA) temperatures in the observational station of Uccle, the national reference station.

Figure 4.15 shows the annual amount of HWDs for all 10-year simulations in this study. Clearly, in present day conditions, due to the UHI effect the city inhabitants experience 2 to 3 times as much Heat Wave Days as people living in the countryside. For the RCP4.5 simulation, the map looks fairly similar as the present day maps, as the changes in the temperatures apparently are too weak to trigger more extreme heat events, partly a consequence of using rigid thresholds. For the RCP8.5 simulation, where the temperature changes are larger, there is a strong increase in the number of HWDs in the city centre. Also the area where more than 4 HWDs per year occur, the maximum amount for present day conditions, is expanding by a factor around 5. In the rural areas, the increase is limited to 1-2 HWDs. Thus, although the UHI effect itself is slightly decreasing in this scenario, the future risk of extreme heat events in the city area is compounded by its presence.

Section 5: High resolution climate simulations over Belgium (D6.1; D6.2; D6.3)

The main aim of this work pack was to perform very high resolution regional climate model simulations for Belgium. To drive the high resolution nested regional climate model COSMO-CLM we use the initial time varying and lateral boundary condition from the EC-Earth model. EC-Earth is the global climate model composed of the ECMWFs Integrated Forecasting System (IFS), the OPA ocean and sea-ice model, the TESSEL land component and the TM atmospheric chemistry model (Krol et al., 2005). Being a fully coupled climate-chemistry model, EC-Earth is bound to become the absolute state-of-the-art in Earth system modelling in the coming years. The EC-Earth model provides coarse resolution (2 x 3°) lateral boundaries to drive the COSMO-CLM model, for both present-day and future periods. The coarser resolution GCM cannot capture realistically the spatial and temporal patterns of precipitation and temperature at regional scale (Figure 5.1). The basic strategy is, therefore to use the coarser global EC-Earth model simulations as boundary conditions to the COSMO-CLM to (i) account for sub-GCM grid scale forcings (e.g., complex topographical features and land cover inhomogeneity and land use change) in a physically-based way and (ii) to enhance the simulation of atmospheric circulations and climatic variables at fine spatial scales over Belgium for impact studies.

EC Earth Global Model Boundary condition data

The deliverable D6.1 was devoted to prepare EC-EARTH data as boundary conditions for COSMO-CLM. We developed a conversion scheme consisting of a set of shell scripts. These shell scripts read the coarser resolution EC-EARTH model data and prepare the data in a suitable format that can serve as an input for the COSMO-CLM model. This conversion

scheme has been implemented and tested on the high performance computing (HPC) facilities at KU Leuven (VIC3 – Linux cluster). The GRIB_filter and the necessary NetCDF libraries were installed on the HPC facilities to run the conversion scheme. The boundary conditions for current climate (2000-2010) and future climate (2024-2035; 2059-2069) for COSMO-CLM are prepared for RCP4.5 and RCP8.5. This work was facilitated by the experience we gained during the CLIMAQS project sponsored by IWT.

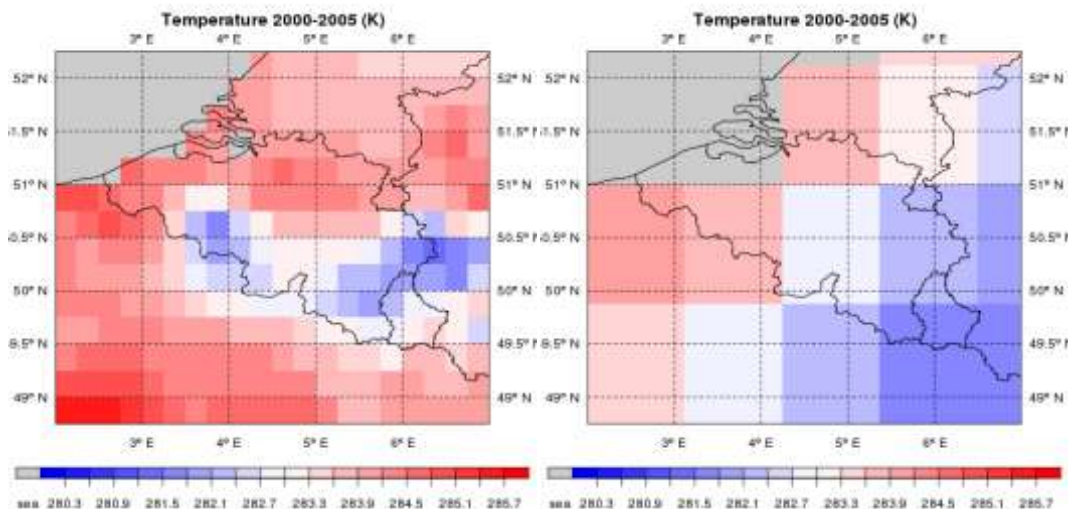


Figure 5.1: An example showing the mean temperature in Belgium for the period 2000-2005 from the E-OBS gridded dataset (left) and from the EC-Earth GCM (right). The coarser resolution GCM cannot capture realistically the spatial and temporal patterns of precipitation and temperature at regional scale. On the other hand high resolution RCM simulations take into account the complex, topography, land use change, vegetation dynamics and local land surface interaction etc.

Since the boundary conditions to a regional climate model are provided from the global model, it was therefore decided to first examine the large scale dynamics in the driving global model. The main aim of the deliverable D6.2 was to examine the performance of large-scale dynamics in the driving EC-Earth global climate model. The second deliverable (D6.3) aimed at performing high resolution climate simulations over Belgium. Table 5.1 gives a list of the high resolution multi-decadal convection permitting simulations performed over Belgium.

TABLE 5.1: High resolution regional climate model simulations performed for Belgium. The long-term climate simulations are named as LTS1, LTS2, LTS3 and so on. BC represents the boundary condition data from reanalysis or global EC Earth model data. All simulations are performed using the COSMO-CLM regional Climate Model.

	BC	RCM resolution	Period	Analysis	RCPs
LTS1	ERA Interim	2.8km	1999-2010	2000-2010	
LTS2	EC Earth	2.8km	1999-2010	2001-2010	RCP4.5
LTS3	EC Earth	2.8km	2026-2035	2026-2035	RCP4.5
LTS4	EC Earth	2.8km	2059-2069	2060-2069	RCP4.5
LTS4	EC Earth	2.8km	2059-2069	2060-2069	RCP8.5

Three main questions are addressed in this task:

- 1- Does the forcing global EC Earth model represent well the large scale atmospheric dynamics.
- 2- What are the added values of high resolution convection permitting models in simulation of regional climate over Belgium?
- 3- To what extent model horizontal grid spacing may precipitation extremes over Belgium.

A detailed description is given below:

5.1 Does the forcing global EC Earth model represent well the large scale atmospheric dynamics.

The climate change signal in Regional Climate Model (RCM) simulations is to a large extent determined by changes in atmospheric circulation, imposed by the host global climate model. For a correct assessment of precipitation sensitivity to climate change based on RCMs, it is therefore important to understand the large-scale atmospheric patterns that influence precipitation at the regional scale. Previous studies (e.g., Hazeleger W., et al. 2013a,b) show that EC_Earth simulates reasonably well the large scale dynamics.

The large scale circumglobal wave train (Branstator, 2002, Ding and Wang 2005; Saeed et. al 2010; Saeed et al 2011) is an important mode in the mid-latitude that influence the regional climate in the Northern Hemisphere. However, it was not known how the mid-latitude wave train influence the summer precipitation over European region. By using observed and NCEP reanalysis data, we found a circumglobal wavelike pattern in the mid-latitudes influencing summer precipitation over Europe. EC-Earth model reasonably simulates the circumglobal wavelike pattern and associated precipitation over Europe.

We applied Empirical Orthogonal Function (EOF) analysis to identify the mid-latitude circumglobal wave train (CGT) over European region during summer season (Figure 5.2). We first analysed NCEP reanalysis and the observed E-OBS precipitation data. We applied the correlation and composite analysis to examine the relationship between CGT and summer precipitation over Europe. Moreover, we also examined the CGT-European summer precipitation relationship in IPCC AR4 climate simulations carried out using ECHAM5MPIOM global climate model and a historical simulation carried out using global EC Earth model.

The leading mode EOF analysis (explained variance 15.2%) reveals a wave like pattern similar to CGT in mid-latitudes (Figure 5.2a). The associated precipitation shows a dipole like pattern with enhanced (reduced) precipitation over Western (Eastern) Europe during the positive (negative) phase of the wave train (Figure 5.2b-c). This pattern shows a different spatial structure to those associated with summer North Atlantic Oscillation (not shown here) suggesting CGT as another important mode in the mid-latitude associated with European summer precipitation. Moreover, the global models ECHAM5/MPIOM and EC Earth simulations captures essential observed CGT features and associated precipitation variability over Europe, allowing for a dynamical interpretation of the phenomenon and of its implications. ***The results of this study has already been published in a peer reviewed journal (Saeed et. al. 2013).***

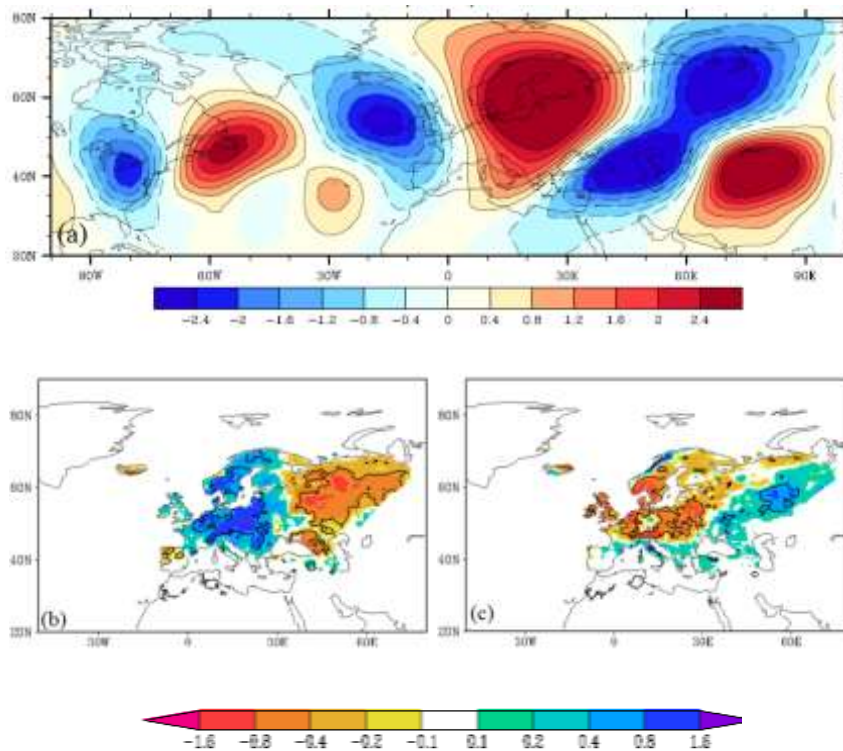


Figure 5.2: (a) The leading EOF mode using 200hPa meridional wind. (b-c) precipitation composites for positive (left) and negative (right) phases of CGT. The composites are based on the first principal component of leading EOF mode. Solid contours in b-c, show precipitation differences that are significant to 95% confidence level. The unit of precipitation is mm day^{-1}

5.2 What are the added values of high resolution convection permitting models in simulation of regional climate over Belgium?

Given the coarse scales of coupled atmosphere-ocean global climate models, regional climate models are increasingly relied upon for studies at scales appropriate for many impacts studies. The dynamical downscaling technique, in which a regional higher-resolution climate model (RCM) is nested into the GCM, can improve the simulation of hydrological cycle at regional scale. Increasing model resolution allows better description of the surface parameters such as land use, orography etc. In addition, the enhanced model resolution might allow better simulation of physical processes. For example at the km-scale resolution convection permitting simulations (CPS) can be performed which allows to model convection without relying on parameterization assumptions/approximations. In this section we addressed the question: What are the added values of the high resolution CPS models in simulation of regional climate over Belgium. For this purpose, we performed multi-decadal regional climate model simulations over Belgium using COSMO-CLM driven with ERAInterim boundary conditions (Table 5.1). The simulations are performed using a nesting strategy (shown in Figure 5.3) to reach a higher resolution of 2.8km, which is a lot higher than most other RCM studies.

First we downscaled the EC-Earth simulations to 25km grid. The 25km run is then nested to the 7km run and the 7km run is nested to the 2.8km run. The climate simulations performed for Belgium at a spatial resolution of 2.8km, yielding a level of detail that has rarely ever been achieved in regional climate simulations. The advantage of this 2.8km spatial resolution is that COSMO-CLM can then explicitly simulate deep convection, rather than having to use a sub-grid convection parameterization.

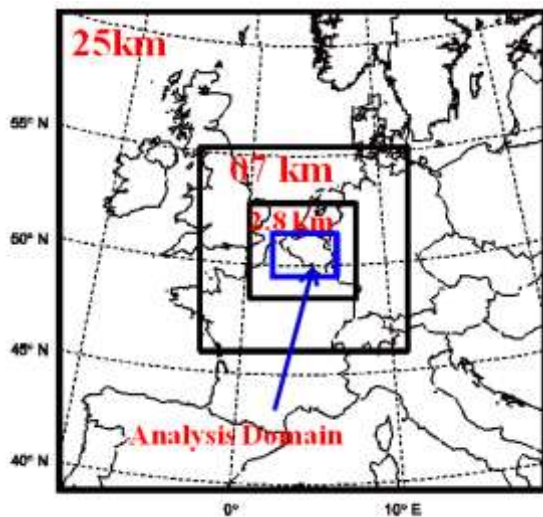


Figure 5.3: Model domain. The nesting domains for 07 km and 2.8 km resolutions are also shown inside the larger domain. The analysis domain cover only the Belgian territory.

We performed an evaluation of the CPS simulation for present day driven with ERAInterim datasets (Table 5.1). Several observational datasets are employed to evaluate the COSMO-CLM model over Belgium. Although, increasing model resolution is computationally more expensive, nevertheless, the enhanced resolution improves significantly the spatial distribution of precipitation (Figure 5.4). For temperature the benefits of using Convection permitting simulations (CPSs) are much smaller than for precipitation (Figure 5.5). Large improvements in the temperature simulations can be seen over the hilly areas. These improvements are likely to result from an improved description of orography in the hilly area of Belgium. We also found noticeable improvement in simulation of the daily precipitation cycle at 2.8km resolution (Figure 5.6). This suggests that the model captures well the timing of the daily convection in the CPSs. At higher resolution the model simulates less precipitation and temperature biases over Belgium.

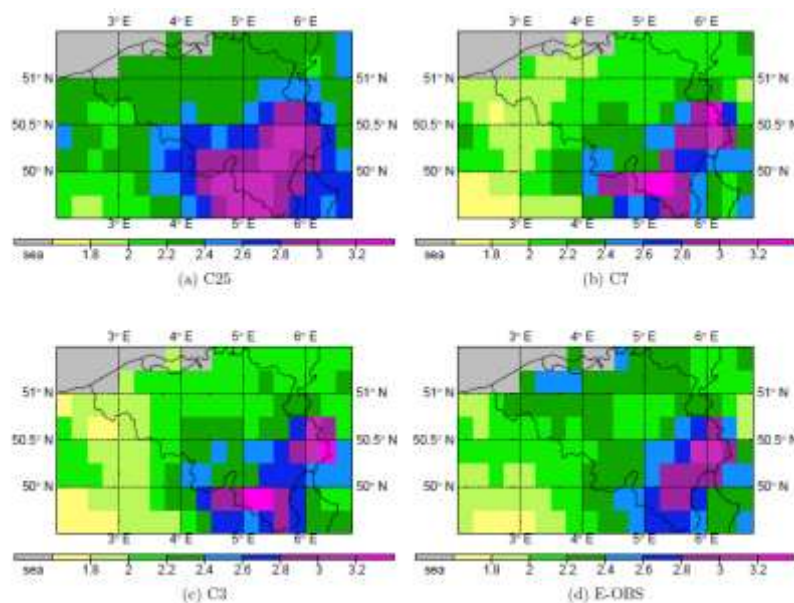


Figure 5.4: Observed and simulated mean annual precipitation over Belgium for present day (2000-2010). The three different resolutions shown by C25 (25km), C7 (7km) and C3 (2.8km), all aggregated to E-OBS dataset grid. The E-OBS dataset averaged over the same period is also shown in (d).

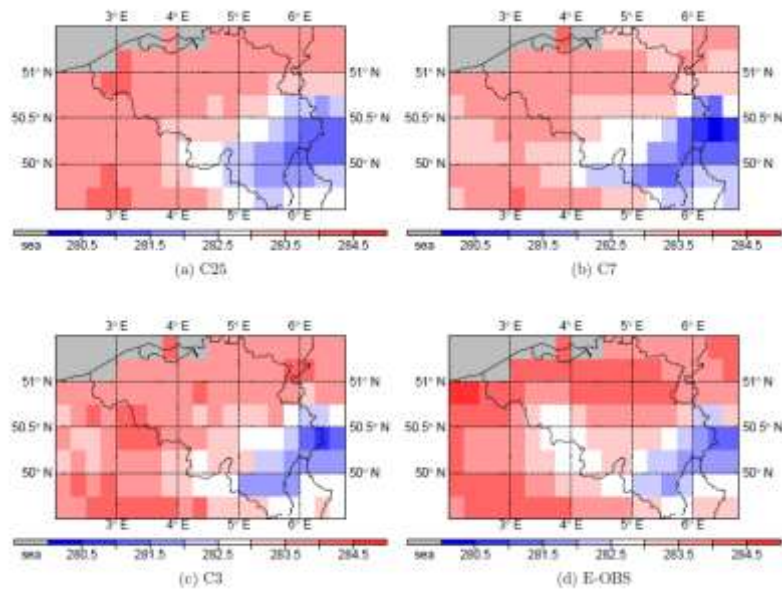


Figure 5.5: Same as Figure 5.4 but for 2-meter temperature.

A detailed evaluation of the simulated clouds at CPS against satellite information reveals a modest low bias in the top of the atmosphere outgoing short wave radiation, mainly during the summer season (Figure 5.7). This low bias originates from a significant over representation of the clear-sky conditions in the model, partly offset by too reflective clouds when they are present. Previous studies (Pfeifroth et al. 2012; Jaeger et al. 2008) show that the non-CPS model usually fail to capture the diurnal cycle of the cloudiness. In contrast, for most cloud types in our simulations, the diurnal cycle of the cloud fraction is well captured despite an underestimation of the total cloudiness. **A paper describing the detailed evaluation of the COSMO-CLM model has been submitted for publication to climate dynamics (Brisson et al 2015).** The results of this study show the potential of CPS simulations to increase confidence in the RCM simulation, not only in areas of steep topography but also in the flatter areas.

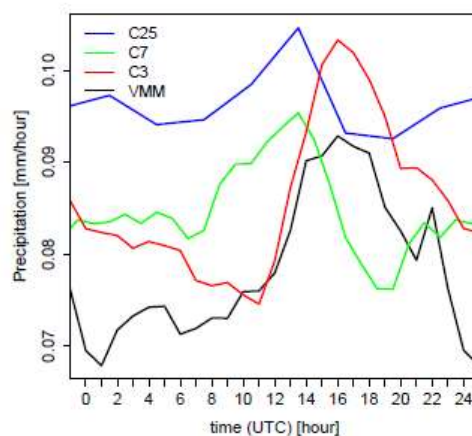
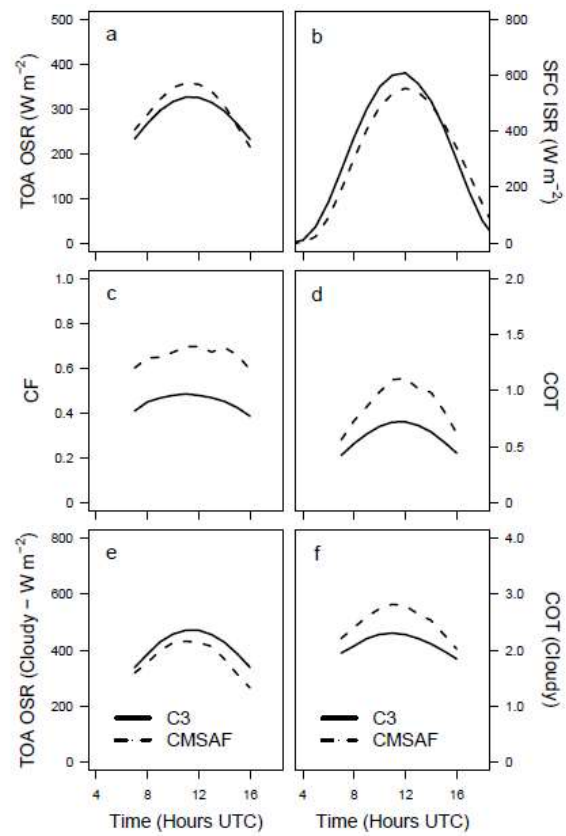


Figure 5.6: Daily cycle of hourly precipitation for the period 2000-2010. The simulations at C25 (25km), C7 (07km) and C3 (3km) and the VMM dataset are respectively shown in blue, green, red and black. The x-axis shows the local time (UTC +1).

Figure 5.7: Overview of domain and time averaged diurnal cycles as observed and as in the experiment. Provided as outgoing short wave radiation (a) at the Top Of the Atmosphere (TOA), station – averaged incoming short wave radiations (b), total cloud fraction (c), total cloud optical thickness (d), TOA outgoing short wave radiations for cloudy regions only (e), cloud optical thickness for cloudy regions only (f). The observations in all panel are obtained from the CMSAF, except for panel (b), which are from surface radiation station data. Only day hours (zenith angle < 65 degrees) are included for panels involving CMSAF data.



C3

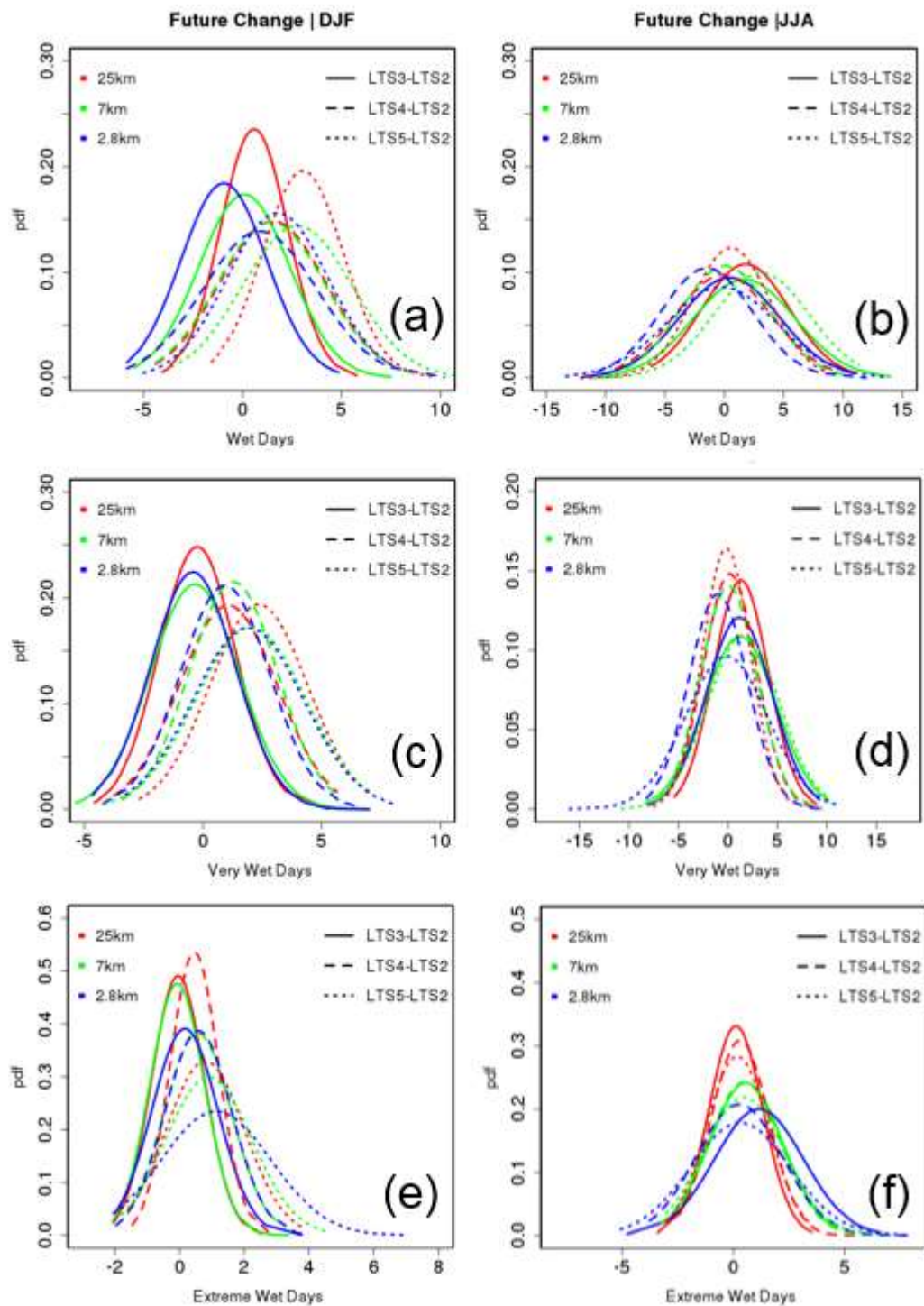


Figure 5.8: Future change in the wet, very wet and extreme wet days with respect to the reference period (2001-2010). Here wet, very wet and extreme wet days are defined as the days above 90th, 95th and 99th percentile of the reference period (2001-2010). Furthermore, LTS3-LTS2, LTS4-LTS2, LTS5-LTS2 display future change for three simulations covering the period (2026-35_rcp4.5; 2060-69_rcp4.5; 2060-69_rcp8.5) and are shown by red, green and blue colours. The future change in the wet, very wet and extreme wet days are computed for every grid-box and are shown by solid (LTS3-LTS2), dashed (LTS4-LTS2) and dotted (LTS5-LTS2) lines. The red, green and blue lines show the model resolutions mentioned on the upper left corner in each plot.

5.3 To what extent the horizontal grid-spacing may influence future precipitation extremes over Belgium

Extreme precipitation events largely influence the society through floods, infrastructure damage and even human casualties. These extremes have significant impacts in Europe in multiple economic sectors as well as adverse social and health effects. The IPCC AR5 (2014) suggest that the Climate change will increase the likelihood of systemic failures across European countries caused by extreme climate events affecting multiple sectors. Therefore understanding and quantifying the magnitude and frequency of these extremes in the present day climate and their pragmatic future projection is of great importance.

Convection permitting models (CPS) have shown to improve representation of extreme weather events. Due to the complexity of the CPS models and the computational costs such an approach cannot be performed for the whole time period (2000-2100). Therefore, shorter 10-year model integrations are performed for sub periods 1999-2010 (present-day reference period) and e.g. 2024-2035 and 2060-2069 using RCP4.5 member of EC Earth simulations. We further performed an additional 10-year simulation for future period (2059-2069) using the RCP8.5 member of EC Earth simulation (Table 5.1).

The results indicate a clear increase in the extreme wet days during both winter and summer seasons in the CPS model simulations for all cases (Figure 5.8e-f). However, we found mixed signals for wet and very days between CPS and non-CPS simulations (Figure 5.8a-d). Furthermore, during winter season the number of wet to extreme wet (Figure 5.8a,c,e) days are higher in the RCP8.5 realization (blue lines) compared to RCP 4.5 (green and red lines). This is in agreement with previous literature (e.g., IPCC AR5) that reports an increase in the future precipitation extremes over Europe for higher climate scenarios. However, during summer season this is less evident and both CPS and non-CPS model reveals blended future signals (Figure 5.8b,d,f).

As convection occurs at very small scale that may covers only few square kilometre, the domain averaged precipitation may be averaged out the actual information associated with precipitation extremes occurring over a particular grid scale area. We therefore analysed the individual gridcell precipitation extremes (Figure 5.9). For this purpose we first constructed a long time series containing data from every gridcell in the analysis domain (Figure 5.9). We first defined an extreme grid cell precipitation event as an event when daily precipitation exceeds 60 mm day^{-1} ($> 99^{\text{th}}$ percentile of reference period LTS2) over that grid. The upper limit of the precipitation imposed to define gridcell extreme events is subjective and a small variation in this limit does not affect the overall results. Figure 6.8 shows the number of extreme gridcell event simulated by CPS and non CPS models. During the summer season the CPS model simulations show increased frequency and intensity of gridcell extremes in future climate compared the non-CPS model simulations (Figure 5.9). This is clearly evident for very extreme grid cell events where all CPS model simulations show enhanced frequency and intensity future gridcell extremes compared to the driving non-CPS model simulations. We further found that the CPS model intensify the precipitation extremes compared to the forcing non-CPS simulations. The places where extremes increase, it increases more in the CPS and the places where extremes decrease, it decreases more in the CPS model simulations. This is especially evident for the summer season. ***A paper on the above results ben submitted to a peer reviewed journal for publication (Saeed et al. 2015)***

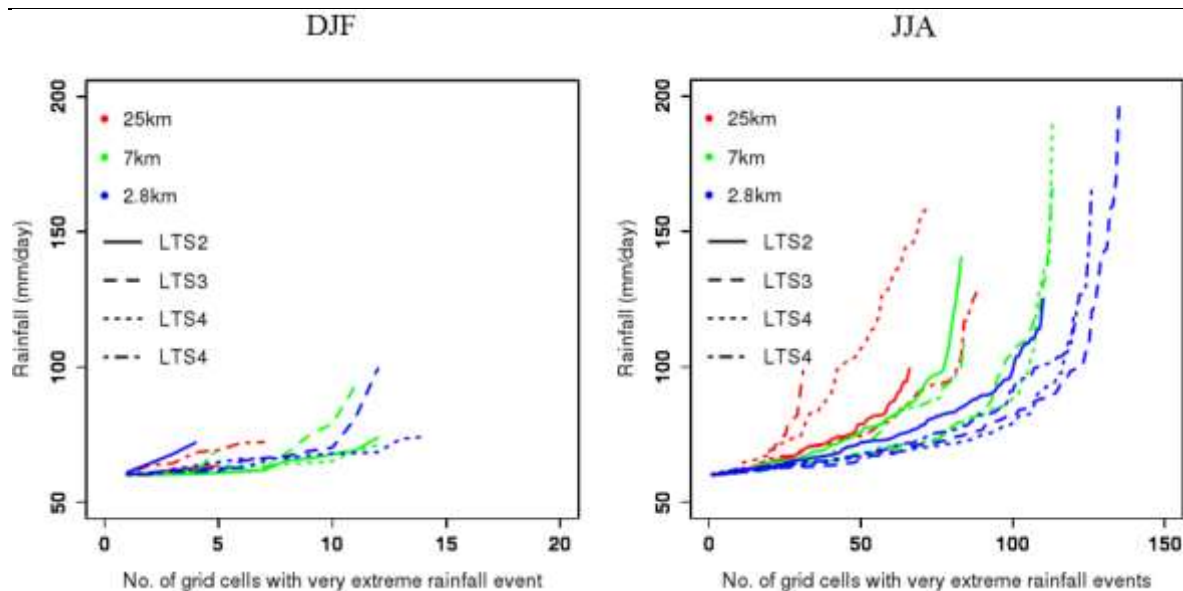


Figure 6.9: Simulated extreme grid-cell rainfall (mmday^{-1}) in present day and future simulations for winter (left) and summer (right). The daily rainfall above 60 mmday^{-1} in a grid cell is defined as extreme grid cell event. Here, present day (2001-2010); LTS3 (2025-2035; rcp4.5); LTS4 (2060-2069; rcp4.5) and LTS5 (2060-2069; rcp8.5) represent the climate simulations (period) performed in the present study (Table 1). The different simulations are shown by solid, long dashed, dotted and short dashed lines. The red, green and blue colours represents the model resolution shown in upper left corner in each plot.

Section 6: Air quality modelling (deliverables D7.1, D7.2, D7.3)

The regional air quality model AURORA has been applied to establish hourly air pollution fields for a reference period (2000-2009) and a future period (2026-2035). This is done for Europe, Belgium and the city of Brussels. In agreement with the project partners and the members of the steering committee, it was decided to model a future period from 2026-2035 with both the IPCC RCP4.5 emissions, the scenario that is used for all model simulations in the MACCBET project, and an emission scenario developed for the Flemish administration, the MIRA Europa scenario (Deutsch et al. 2010). The development of a spatially explicit emission data set with a horizontal resolution of 1 km has also been carried out. The AURORA air quality model was first validated using reference simulation and after validation the future projections regarding the impact of climate change on air quality over Belgium are produced. **Over the course of the project, three scientific papers have been written about these simulations and results (Lauwaet et al. 2012, Lauwaet et al. 2014 and De Ridder et al. 2014).** A detailed description of the questions addressed in this section is given below:

6.1. Is our model setup capable of reproducing the observed air quality parameters over Belgium?

The simulations in this Work Package are performed with the regional-scale air quality model AURORA (Air quality modelling in Urban Regions using an Optimal Resolution Approach), a limited-area Eulerian chemistry transport model, described in Van de Vel et al. (2009) and Lauwaet et al. (2012) and references therein. The AURORA model needs a specification of the position and strength of emission sources. The emission data are obtained with the Emission Mapping (Emap) Geographical Information Systems tool (Maes et al., 2009), which provides gridded emissions with a horizontal resolution of 1 km, based on the European Monitoring and Evaluation Programme (EMEP) dataset. E-MAP applies a top-down

methodology to spread the reported emission totals for a certain geographical unit (e.g. Brussels) to a 1 km grid, based on proxy data as roads, land use and population density.

Large-scale pollutant concentrations, which are required to account for remote emission sources, are interpolated from output generated by the chemistry-transport model TM5 (Huijnen et al., 2010) as shown in Figure 6.1. TM5 provides 3-hourly concentration levels of reactive gases and aerosols. AURORA also needs meteorological conditions as an input, which are taken from the COSMO-CLM simulations of Work Package 6, performed at the KULeuven. The COSMO-CLM simulations are performed using one-way grid nesting, similar to the AURORA simulations (Figure 6.1).

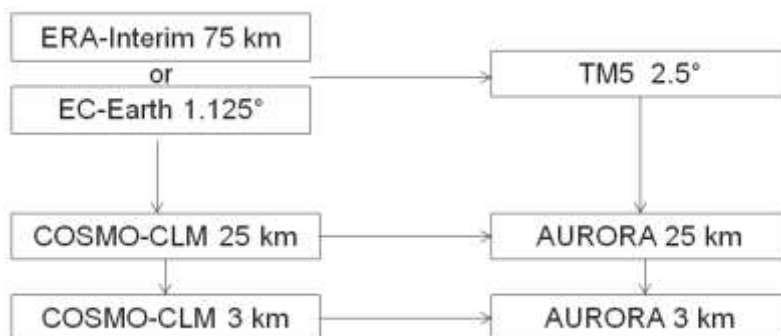
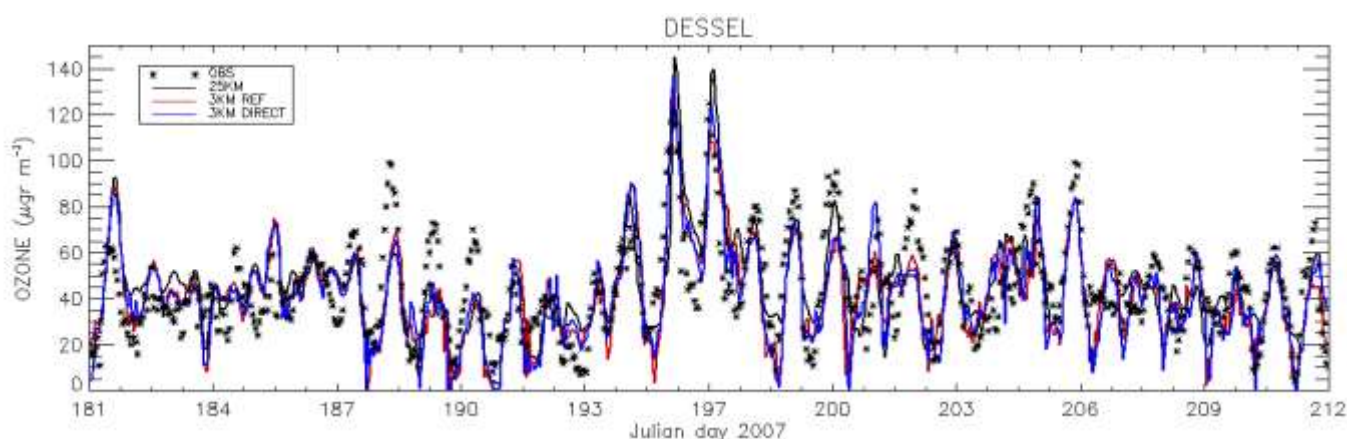


Figure 6.1: Schematic overview of the coupling between the different atmospheric models and their horizontal resolutions.

In order to evaluate the model performance, we selected 34 observation stations from the AirBase data archive (Mol et al., 2011). Given this model resolution, we only selected background stations, excluding traffic and industrial stations as these are generally not representative for the scale of a 3 km model grid cell. As an example, a comparison of the time series of modelled and observed concentrations at two different types of locations, the rural background station Dessel, where often the highest ozone concentrations in Belgium are measured during episodes, and the urban background station Gent, is presented in Figure 6.2. For these locations, the AURORA model is able to reproduce the daily cycle, and also the peak concentrations in the middle of the month are accurately simulated.



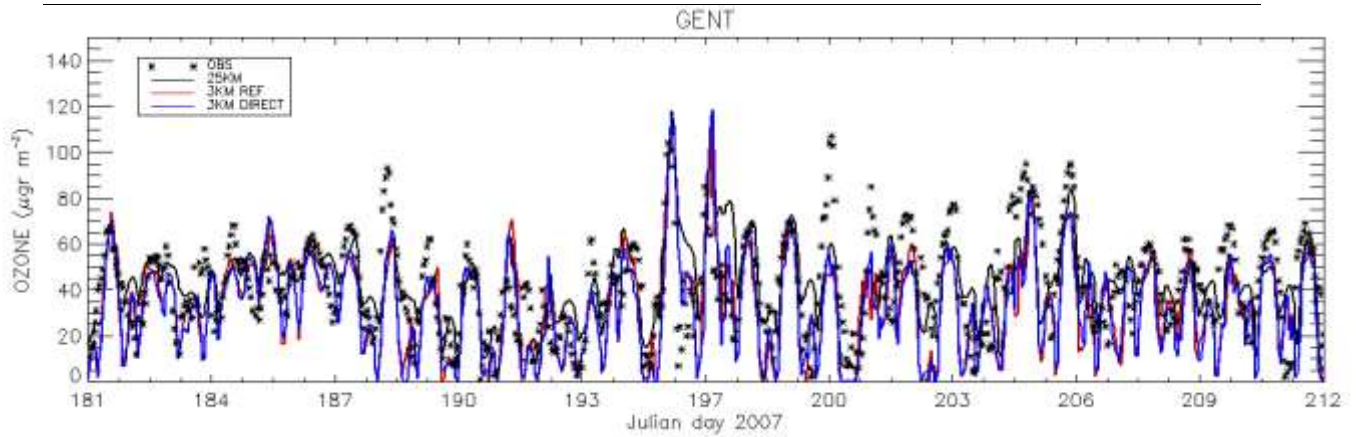


Figure 6.2: Time series of surface ozone concentrations for the rural background station Dessel (top) and the urban background station Gent (bottom).

Furthermore, Figure 6.3 demonstrates that the AURORA model with a horizontal resolution of 3 km is able to reproduce 10-year mean observed concentrations with a high spatial coefficient of determination of 0.86. The model has a slight and fairly constant positive bias at almost all locations. The right-hand side of Figure 6.3 shows the evaluation of the 25 km results for the same observations. Here, the spatial correlation is clearly lower (0.69) and the model has a slight negative bias, especially at the locations that are most polluted.

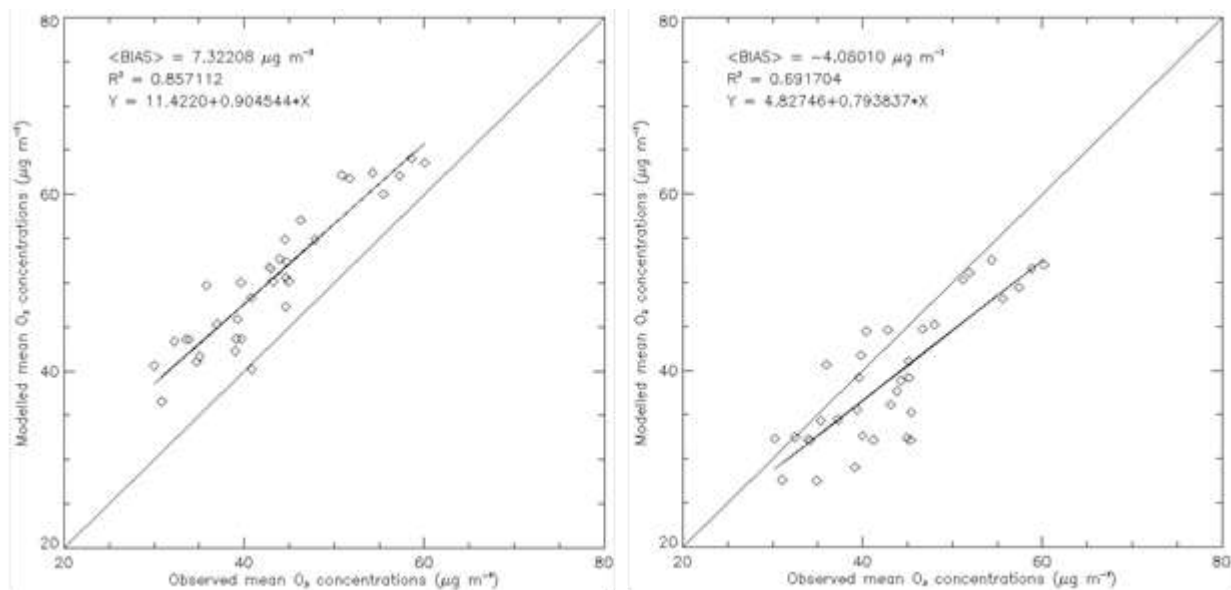


Figure 6.3: Evaluation of the 10-year (2000-2009) mean O_3 values for all observation stations. Left: Mean O_3 concentrations of the 3 km resolution simulations. Right: Mean O_3 concentrations of the 25 km simulations.

Overall, it can be concluded that the AURORA model performs satisfactorily and seems well suited to address the research questions of this Work Package.

6.2. What is the added value of the very high resolution simulations?

The added value of the high horizontal resolution is demonstrated in Figure 6.4 by evaluating the modelled peak concentrations, taken as the 95th percentile value of the 10-year time series. Clearly, the 3 km model results outperform the 25 km results, which have a strong negative bias and a lower spatial coefficient of determination. From these results we can conclude that the large computational demands that are needed for this high horizontal

resolution of 3 km pay off by significantly improving the spatial correlation and peak concentrations of the simulations.

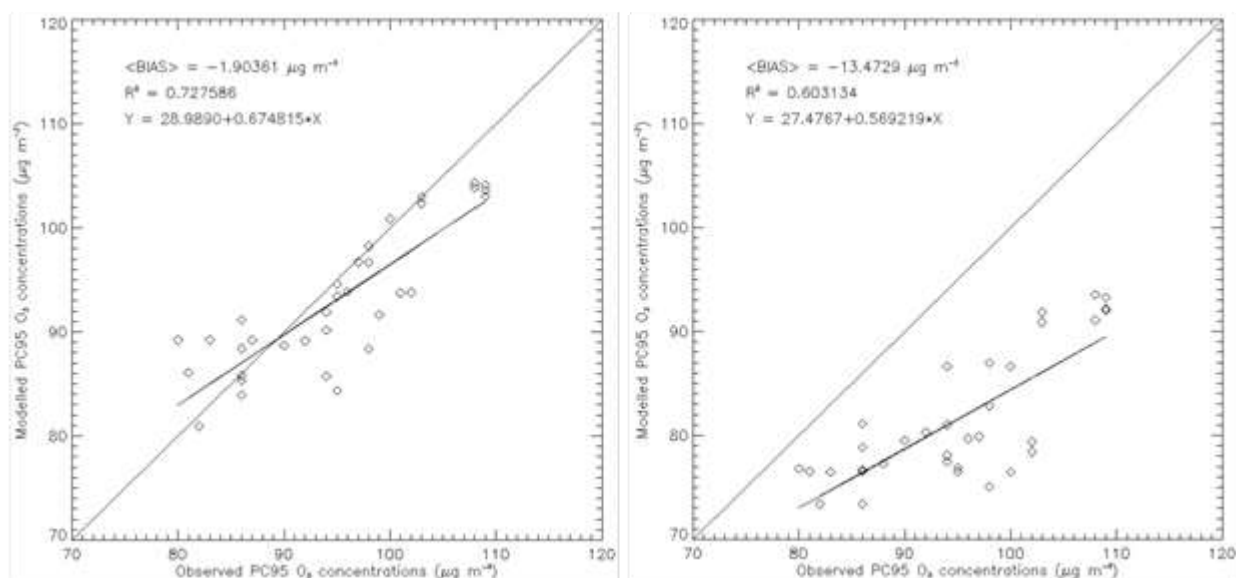


Figure 6.4: Evaluation of the 10-year (2000-2009) 95th percentile O₃ values for all observation stations. Left: 95th percentile O₃ values of the 3 km simulations. Right: 95th percentile O₃ values of the 25 km simulations.

Furthermore, we have taken the modelling work a step further and performed simulations for Brussels and its surroundings at a very high horizontal resolution of 1 km. To demonstrate the added value of using such a high resolution, the effect of the modelling resolution on the exposure of the population to NO₂ concentrations above a threshold of 40 µg m⁻³ is calculated. Figures 6.5, 6.6 and 6.7 show the results of this experiment. Clearly, such a high modelling resolution is needed to get a correct estimate of the number of people that are affected by peak concentrations.

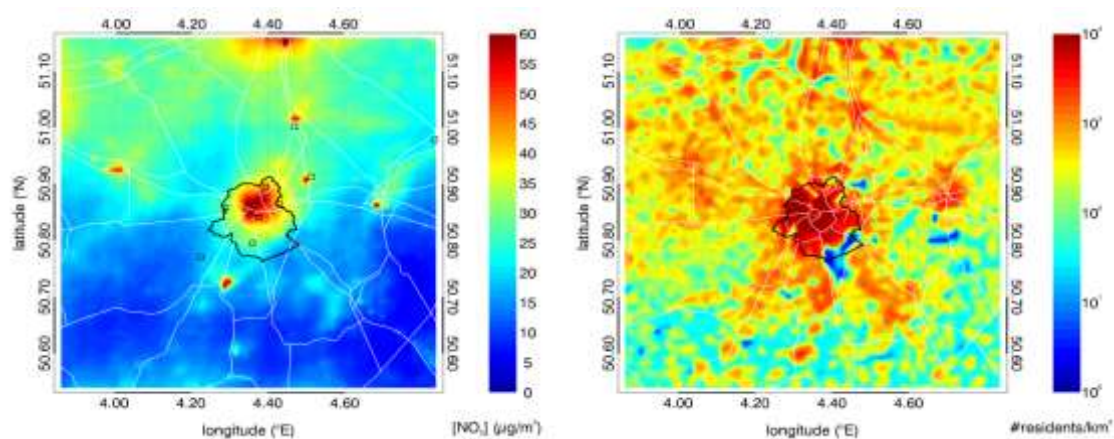


Figure 6.5: The left panel shows the simulated annual mean NO₂ concentration field for Brussels and surroundings. The right panel shows population density expressed as number of residents per km².

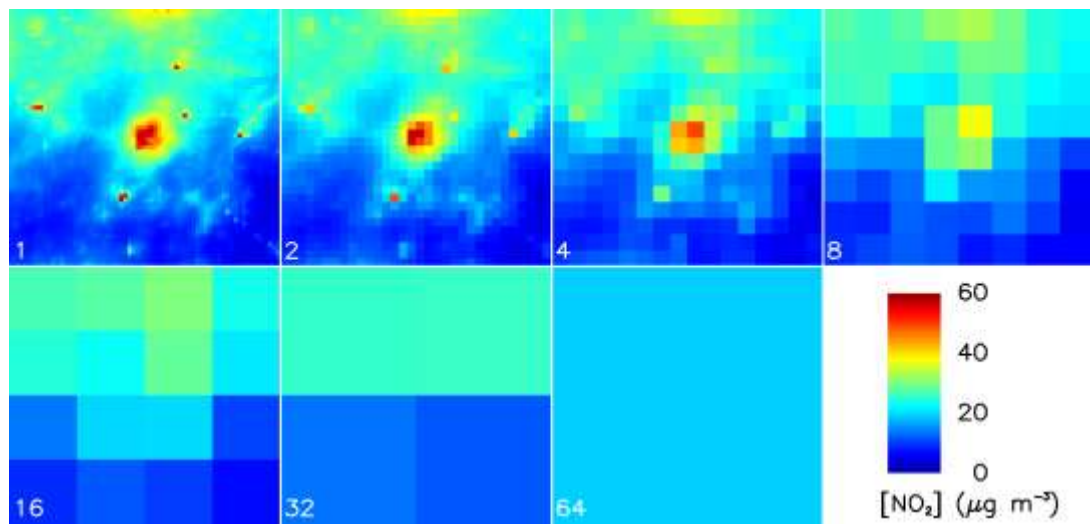


Figure 6.6: Annual mean NO_2 concentrations with decreasing model resolution from left to right and top to bottom.

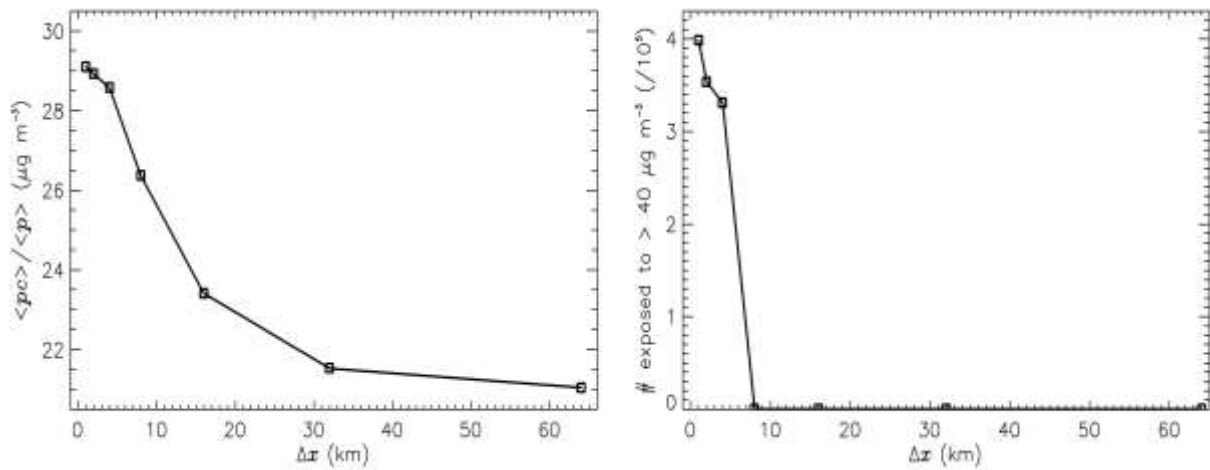


Figure 6.7: Left panel: population-weighted NO_2 concentration $E \equiv \langle pc \rangle / \langle p \rangle$ (i.e., exposure) for the $64 \times 64 \text{ km}^2$ sub-domain considered in the exposure-versus-resolution analysis. Right panel: The number of persons exposed to annual mean NO_2 concentrations above a value of $40 \mu\text{g m}^{-3}$. Both quantities are shown as a function of spatial resolution (Δx).

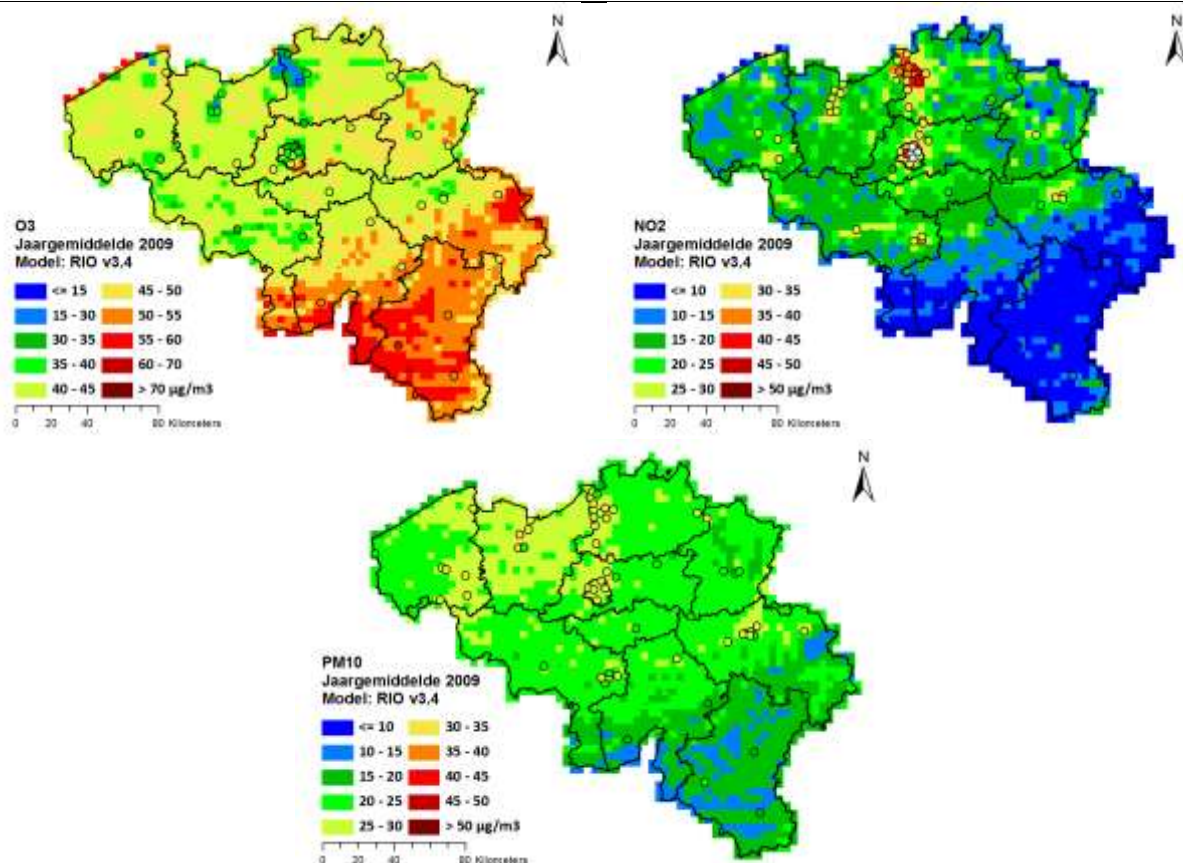


Figure 6.8: Example RIO output maps for the reference year 2009.

6.3. Which model produces the best air quality maps for Belgium?

One of the objectives of this Work Package was to deliver the best possible retrospective high resolution air quality maps applying advanced statistical data assimilation techniques (e.g. optimal interpolation, kalman filter,...). During the course of the project, an enhanced comparison was made between the standard RIO maps that are officially used by the Flemish authorities and AURORA related products from the MACCBET project for the reference year 2009 (Maiheu et al. 2013). RIO (Hooyberghs et al, 2006; Janssen et al., 2008) is a land use regression model for the interpolation of hourly pollutant concentrations as measured by the official monitoring network in Belgium. The model is based on a residual kriging interpolation scheme using a land use (CORINE) derived covariate. The RIO model produces hourly concentration maps for the pollutants PM₁₀, PM_{2.5}, NO₂ and O₃ on a 4x4 km² grid over Belgium (Figure 6.8).

The RIO model is compared to the raw AURORA output maps (AUR) and several statistically enhanced results: applying a simple mean bias correction (AURBIAS), a more advanced bias correction based on orthogonal regression (AURORTHO), a Kalman Filter based correction (AURKF) and an Optimal Interpolation based correction (AUROI). For three pollutants (O₃, NO₂ and PM₁₀) the error statistics of both a temporal and spatial validation are calculated, using all 34 AirBase observation stations (Mol et al., 2011). The results for NO₂ are shown in Figure 6.9.

In order to clearly define which model produces the best results, an advanced scoring system is developed. When comparing the numbers for a specific indicator, the best scoring model gets a value of 10. The mean value for the indicator over all models gets a value of 5. Between these two points, a linear fit is employed to translate the numbers to a score from

0 to 10. Values lower than 0 are set to 0. The result of this exercise for both the temporal and spatial validation is shown in Tables 6.1 and 6.2.

Regarding the temporal validation, the RIO model clearly performs better than the AURORA derived products. The more advanced data assimilation system as Optimal Interpolation and Kalman Filter pay off and score much higher than the more simple bias correction methods. The AURORA model itself is worst, as could be expected. The spatial validation has a more well-balanced outcome: RIO still performs best overall but the gap is closer and all models have their strong points.

Based on these results, it was decided by the Flemish authorities that RIO remains the reference model for producing retrospective air quality maps. It should be noted though that such a geostatistical modelling technique lacks the ability for scenario analysis and future projections, for which a deterministic model as AURORA is needed.

6.4. What is the impact of climate change on air quality over Belgium?

The MACCBET model chain described above is applied to simulate a 10-year reference period (2000-2009), driven with meteorological data from the base run of the global climate model EC-Earth (Hazeleger et al., 2010; Hazeleger et al., 2012). Secondly, a 10-year period in the near future (2026-2035) is simulated, driven with EC-Earth model results for the IPCC Representative Concentration Pathway RCP4.5 (Van Vuuren et al., 2011), one of the RCPs used in CMIP5. To increase the relevance of our results for local policy makers, the 2026-2035 period is also simulated by AURORA with a second emission scenario (called MIRA), that was compiled by the Flemish administration (Table 6.3).

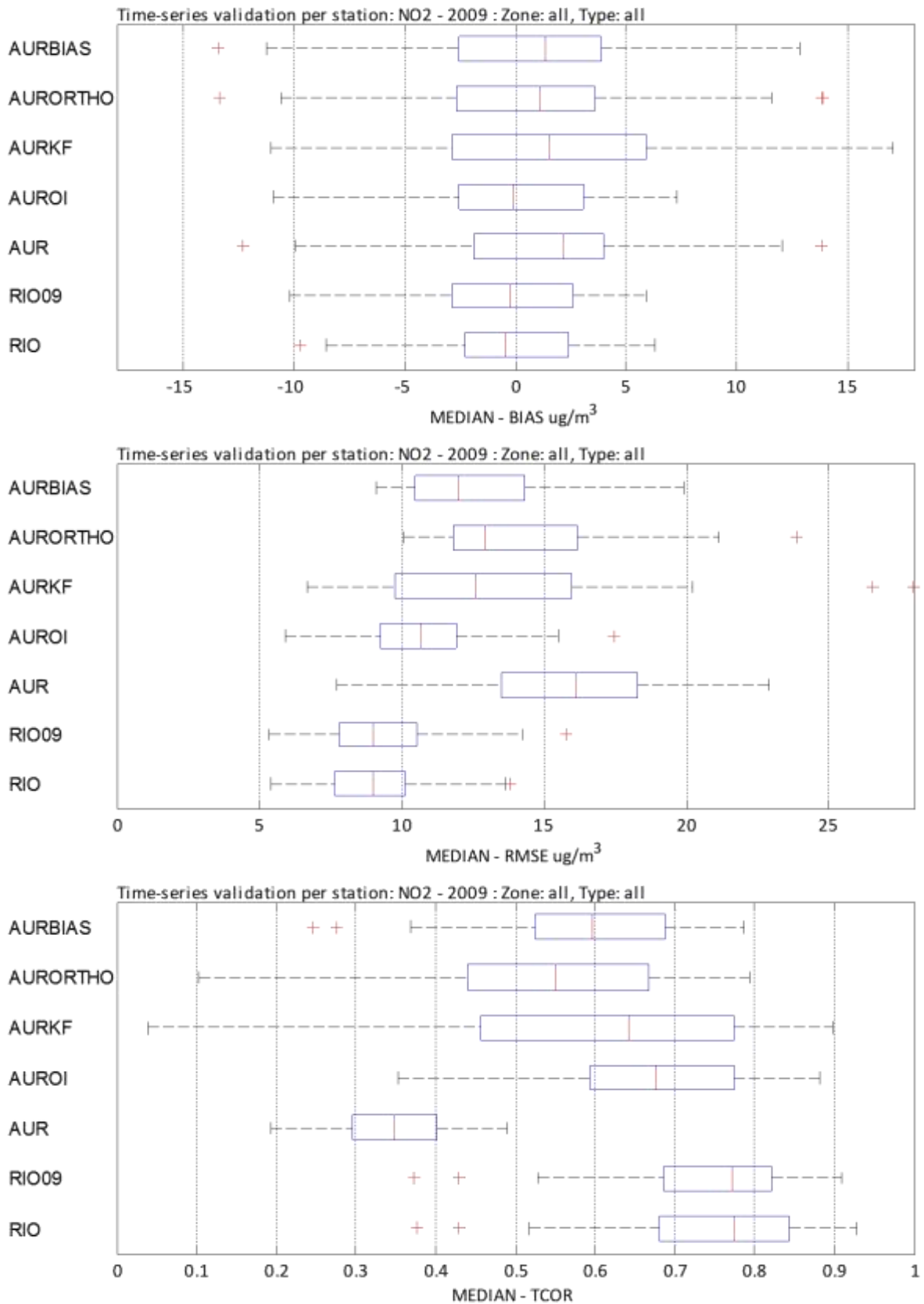


Figure 6.9: Temporal validation of the different models for NO₂ using 34 stations from the AirBase network. From top to bottom: Median Bias, Median Root Mean Square Error and Median Correlation Coefficient.

Table 6.1: Score table for the temporal validation of the different models.

		RIO	AUR	AUROI	AURKF	AURORTHO	AURBIAS
O ₃	BIAS	8.36	0.00	5.00	10.00	0.00	2.74
	RMSE	10.00	0.00	6.98	5.00	0.00	3.33
	CORR	10.00	0.00	5.61	5.00	0.00	0.00
NO ₂	BIAS	8.36	0.00	10.00	2.75	5.00	3.74
	RMSE	10.00	0.00	7.25	4.08	3.47	5.00
	CORR	10.00	0.00	6.33	5.00	1.54	3.27
PM ₁₀	BIAS	7.28	0.00	10.00	2.75	5.00	3.74
	RMSE	10.00	0.00	7.25	4.08	3.47	5.00
	CORR	10.00	0.00	6.33	5.00	1.54	3.27
SCORE		84.00	0.00	64.75	43.66	20.02	30.09

Table 6.2: Score table for the spatial validation of the different models.

		RIO	AUR	AUROI	AURORTHO	AURBIAS
O ₃	BIAS	8.32	0.00	2.35	5.90	10.00
	RMSE	4.99	0.00	10.00	9.83	5.01
	CORR	0.00	10.00	4.73	5.27	7.79
NO ₂	BIAS	10.00	0.00	9.89	0.00	2.65
	RMSE	10.00	9.34	2.65	6.42	3.58
	CORR	10.00	4.21	5.79	3.39	3.83
PM ₁₀	BIAS	4.60	0.00	9.14	3.92	10.00
	RMSE	8.00	0.00	7.14	0.00	2.86
	CORR	10.00	3.81	6.19	3.54	1.31
SCORE		65.91	27.36	57.88	38.27	47.03

Table 6.3: Emission totals Mton/year for the different pollutants for the reference year (2000) and the two future scenario's RCP4.5 and MIRA-Europe.

pollutant	EUROPE			Belgium		
	2000	2030 RCP4.5	2030 MIRA- EU	2000	2030 RCP4.5	2030 MIRA-EU
CO	40.19	10.11	10.12	0.503	0.086	0.086
NH ₃	4.50	4.35	3.35	0.055	0.064	0.041
NM ₁₀ VOC	11.91	7.04	6.96	0.118	0.050	0.080
NO _x	15.57	8.19	9.13	0.203	0.062	0.070
PM _{2.5}	2.09	1.02	1.78	0.018	0.007	0.012
PM _{coarse}	1.11	0.60	1.16	0.023	0.024	0.009

As an example, the results for surface O₃ concentrations are discussed here. Figure 6.10 shows the reference yearly mean concentrations over Belgium, a very polluted area with high NO_x emissions which favours O₃ formation. However, when the abundance of NO_x emissions is too high (in big cities and along highways), it enhances O₃ titration, and thus leads to lower O₃ concentrations in these areas, so the highest concentrations are found in more remote areas in the South of the country.

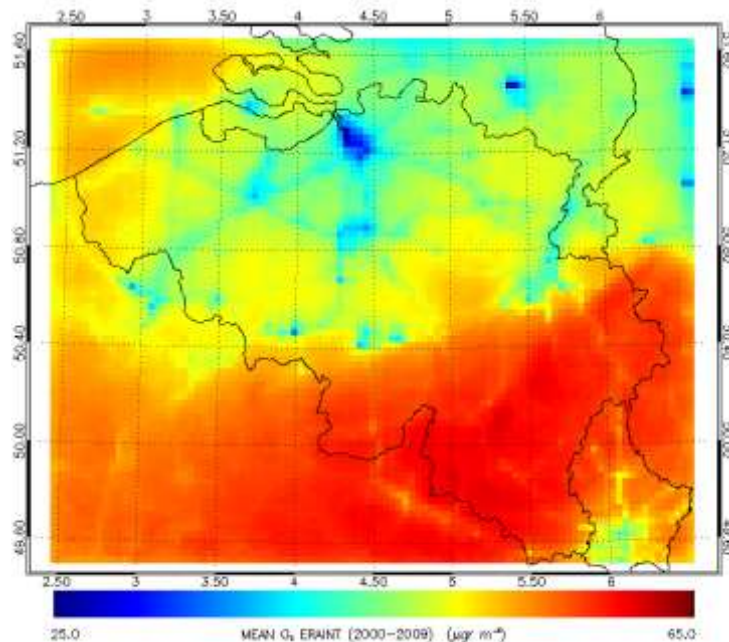


Figure 6.10: Reference yearly mean O_3 concentrations.

The results for the near future (2026-2035) show that the surface O_3 concentrations are expected to increase significantly over Belgium, especially in the most polluted areas (Figure 6.11), due to less O_3 titration by lower NO_x emissions, in accordance with the results of related international studies. Applying an alternative local emission scenario with less drastic emission reductions is found to have little impact on the outcome of the simulations. The domain-wide O_3 concentrations for a region such as Belgium seem to be dominated by the background concentrations.

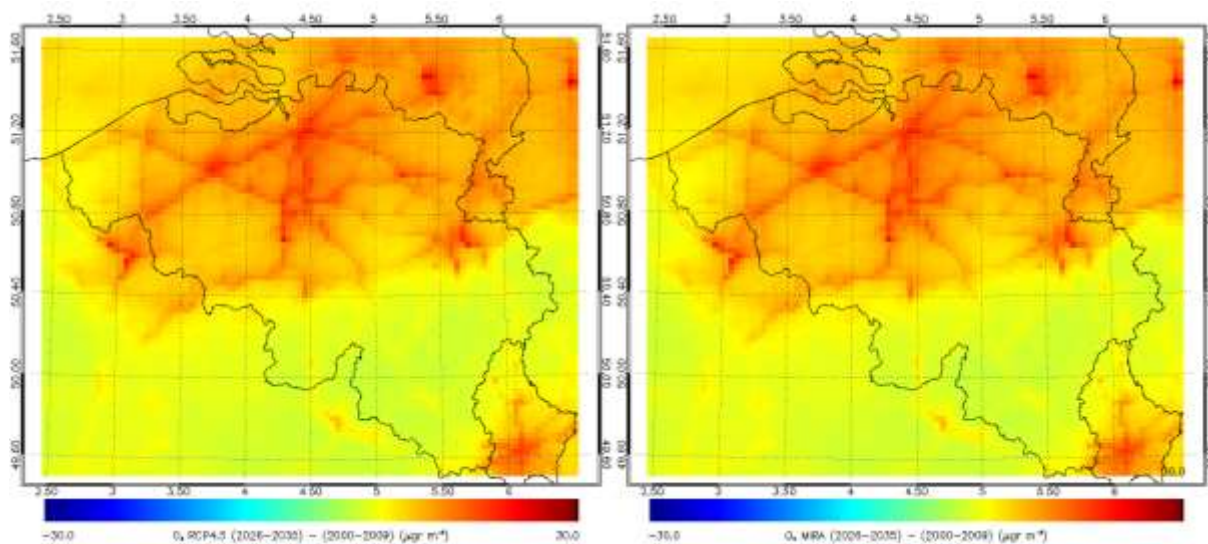


Figure 6.11: Change in yearly mean O_3 concentrations for the RCP4.5 (left) and MIRA-EU (right) scenarios.

When investigating the effects of the applied climate change alone, the impact on the O_3 concentrations is much smaller than the combined effect of emission and climate changes (Figure 5.12). The climate change (higher temperatures and less precipitation) results in slightly lower overall concentrations, due to changes in the background concentrations. However, in the most polluted regions the warmer and drier conditions increase the O_3 production.

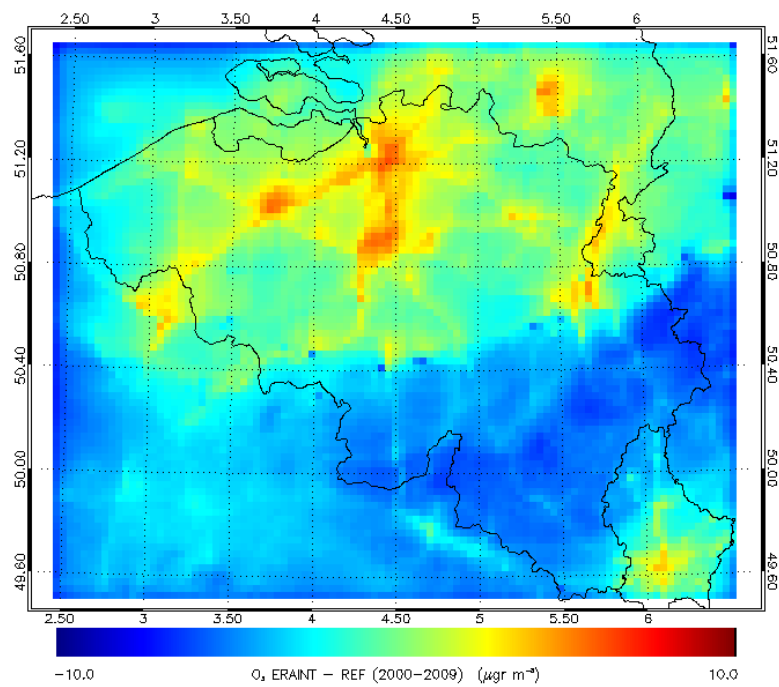


Figure 6.12: Change in yearly mean O3 concentrations when only including climate change effects.

An overview of the results for all pollutants is given in Table 6.4. These results confirm the findings of several other regional modelling studies that future pollutant concentrations are dominated by projected emission changes rather than climatic changes.

Table 6.4: Effect of climate and emission changes on the yearly mean pollutant concentrations over Belgium.

	O ₃ (µg/m ³)	NO ₂ (µg/m ³)	PM ₁₀ (µg/m ³)
Reference yearly mean concentrations	54.6	19.3	16.0
Effect of climate change only	-1.4	-4.6	-1.1
Effect of climate change and RCP4.5 emissions	+11.2	-11.6	-5.4
Effect of climate change and MIRA emissions	+12.8	-12.8	-2.1

3. POLICY SUPPORT

The MACCBET work laid the basis for a recently published climate assessment of Flanders (MIRA klimaatrapport 2015). This report is an authoritative policy support document for Flanders. This was the most important leverage of the MACCBET work that was performed towards policy and society in general. In addition, this report led to publicity for the MACCBET results in the national media and press. For example the VRT devoted a news item. The full reference to the report is:

Brouwers, J. , Peeters, B. , Van Steertegem, M. , van Lipzig, N., Wouters, H. , Beullens, J. , Demuzere, M. , Willems, P. , De Ridder, K. , Maiheu, B. , De Troch, R. , Termonia, P. , Vansteenkiste, T. , Craninx, M. , Maetens, W. , Defloor, W. , Cauwenberghs, K., 2015. MIRA klimaatrapport 2015: over waargenomen en toekomstige klimaatveranderingen. Publisher Aalst: Vlaamse Milieumaatschappij, 147 pp.

The report tries to give scientifically correct policy relevant answers to the questions: "To what extent is climate change already visible in Flanders and Belgium?" and "What are the expectations for the future?". The report starts with an explanation of the mechanism that is at the root of global climate change. Then specifically for Flanders and Belgium, the report describes the observed climate change signals. The future scenarios are based on the latest scenarios of the IPCC (the Intergovernmental Panel on Climate Change of the United Nations). But in addition to that, the report describes the spatial differences (including the urban heat island effect) of the climate change signal. This part of the report heavily supports on the MACCBET results. The report further continues to describe the potential impacts of climate change on human health and the water management. Subsequently, the importance of so-called tipping points is pointed out. The report concludes with some reflections on how the policy can deal with the uncertainties.

The report was the result of an excellent collaboration between the project partners of MACCBET together with other researchers: Johan Brouwers, Bob Peeters, Marleen Van Steertegem, Dienst MIRA, VMM; Nicole van Lipzig, Hendrik Wouters, Jochem Beullens, Matthias Demuzere, Departement Aard- en Omgevingswetenschappen, KU Leuven; Patrick Willems, Afdeling Hydraulica, KU Leuven; Koen De Ridder, Bino Maiheu, Afdeling Ruimtelijke Milieu-aspecten, VITO; Rozemien De Troch, Piet Termonia, RMI; Thomas Vansteenkiste, Michel Craninx, Willem Maetens, Willem Defloor, Kris Cauwenberghs, Dienst Hoogwaterbeheer, VMM The report comes together with five scientific reports:

- De Ridder K., Maiheu B., Wouters H. & van Lipzig N. (2015) Indicatoren van het stedelijk hitte-eiland in Vlaanderen², studie uitgevoerd in opdracht van de Vlaamse Milieumaatschappij, MIRA, MIRA/2015/05, VITO en KU Leuven.
- van Lipzig N.P.M. & Willems P. (2015) Actualisatie en verfijning klimaatscenario's tot 2100 voor Vlaanderen, studie uitgevoerd in opdracht van de Vlaamse Milieumaatschappij, MIRA, MIRA/2015/01, KU Leuven i.s.m. KMI.
- Beullens J. & van Lipzig N.P.M. (2015) Actualisatie en verfijning klimaatscenario's tot 2100 voor Vlaanderen - Appendix 1: Nieuwe modelprojecties voor Ukkel op basis van Europese en Belgische fijnmazige klimaatmodellen. Studie uitgevoerd in opdracht van de Vlaamse Milieumaatschappij, MIRA, MIRA/2015/02, KU Leuven.
- Tabari H., Taye M.T. & Willems P. (2015) Actualisatie en verfijning klimaatscenario's tot 2100 voor Vlaanderen - Appendix 2: Nieuwe modelprojecties voor Ukkel op basis van

globale klimaatmodellen (CMIP5). Studie uitgevoerd in opdracht van de Afdeling Operationeel Waterbeheer van de Vlaamse Milieumaatschappij en MIRA, MIRA/2015/03, KU Leuven.

- Beullens J. & van Lipzig N.P.M. (2015) Actualisatie en verfijning klimaatscenario's tot 2100 voor Vlaanderen - Appendix 3: Ruimtelijke patronen voor België op basis van Europese en Belgische fijnmazige klimaatmodellen. Studie uitgevoerd in opdracht van de Vlaamse Milieumaatschappij, MIRA, MIRA/2015/04, KU Leuven.

With respect to urban climate, MACCBET(-related) results have found their way into policy in Antwerp, Ghent, and Brussels. For Antwerp, it was even BELSPO's MACCBET web page that was the trigger of the use of project results in policy. After getting in touch with us (VITO), environment administrators of the City of Antwerp used the information we provided on the city's heat island phenomenon to enforce certain heat-alleviating measures in the Building Code, including the obligation to establish:

- green roofs on flat roofs extending over 20 m² or more
- green parking space on private property (pavement with green joints or concrete tiles with openings for vegetation)
- green (i.e., permeable) gardens of private areas larger than 20 m²

Subsequently, VITO carried out a heat map study and, currently, is establishing a heat warning system in Antwerp's Ecohuis.

With respect to the City of Ghent, VITO also conducted a heat map study. In addition, through the Postgraduate Programme on Weather and Climate Modelling of Ghent University, in which several MACCBET partners are involved, we are involved in setting up a heat island monitoring network, in which the City authorities as well as the Flemish Environmental Agency have expressed a strong interest. Results of the measurements will be publicly available, and thus increase awareness in the general public and policy makers alike. Ghent is also taking several measures to alleviate the urban heat island phenomenon.

In the case of Brussels, MACCBET results have been employed in the EU-FP7 Stratego project, to estimate the cooling energy requirements under future climate conditions. This has been communicated to the Brussels Agency for the Environment (IBGE/BIM).

In addition, participation to MACCBET has certainly facilitated VITO's involvement in the European FP7 projects NAACLIM and RAMSES, which both consider urban climate and adaptation, and which are considering city case studies throughout Europe and beyond. The concerned cities (Berlin, Almada, Barcelona, Bilbao, London, Skopje, New York, Rio de Janeiro, Hyderabad...) are involved in these projects as user partners, and keen on employing project outcomes in the development of their climate-related policy. Hence, indirectly MACCBET also contributes to the development of new policy in (at least some of) those cities.

4. DISSEMINATION AND VALORISATION

The MACCBET work laid the basis for a recently published climate assessment of Flanders (MIRA klimaatrapport 2015). More information can be found in section 3. The full reference to the report is:

Brouwers, J., Peeters, B., Van Steertegem, M., van Lipzig, N., Wouters, H., Beullens, J., Demuzere, M., Willems, P., De Ridder, K., Maiheu, B., De Troch, R., Termonia, P., Vansteenkiste, T., Craninx, M., Maetens, W., Defloor, W., Cauwenberghs, K., 2015. MIRA klimaatrapport 2015: over waargenomen en toekomstige klimaatveranderingen. Publisher Aalst: Vlaamse Milieumaatschappij, 147 pp.

This event led to extensive media coverage. All press coverage of this report is listed below:

17-9-2015	Eerste Vlaams Klimaatrapport	VRT Radio (EEN, MNM, Radio 2 enz.)
17-9-2015	Eerste Vlaams Klimaatrapport	VRT Journaal 19u
17-9-2015	Klimaatrapport 2015 confronteert waargenomen en toekomstige klimaatveranderingen	BELGA-bericht
17-9-2015	Vlaamse Klimaatrapport	Karrewiet (jeugdjournaal VRT)
17-9-2015	Eerste Vlaams Klimaatrapport	VRT Radio
17-9-2015	Eerste Vlaams Klimaatrapport	VRT Website
17-9-2015	Eerste Vlaams Klimaatrapport	Diverse websites (Nieuwsblad, HLN, ...)
17-9-2015	Confronterend filmpje over klimaatverandering in ons land	Website De Morgen
17-9-2015	Eerste Vlaams Klimaatrapport	Diverse radiozenders
17-9-2015	Klimaatrapport 2015: meer regen en minder sneeuw	website De Standaard
17-9-2015	Hoe we de klimaatverandering (zullen) voelen in Vlaanderen	Knack-website en dagelijkse nieuwsbrief
17-9-2015	Dit filmpje maakt duidelijk welke gevolgen van de klimaatverandering we in Vlaanderen al zien	Newsmonkey.be
18-9-2015	Vlaanderen lijdt al onder verandering klimaat	De Standaard* pagina 10
18-9-2015	Overstromingen en hittegolven veranderen het leven	De Standaard* pagina 11
18-9-2015	Antwerpen is een hitte-eiland geworden	De Standaard* pagina 10
18-9-2015	Aantal hittedagen zal in eeuw tijd verdrievoudigen	Het Nieuwsblad pagina 10
18-9-2015	Dijlestad is hitte-eiland	Het Laatste Nieuws/Mechelen-Lier, pagina 21
18-9-2015	Klimaatverandering nu al te merken in Vlaanderen	Het Laatste Nieuws pagina 5

18-9-2015	België schaart zich achter 'zwak' Europees klimaatplan	De Morgen pagina 3
18-9-2015	Wat doet het nieuws met Sepideh Sedaghatnia?	Radio 1
18-9-2015	Meer regen én meer droogte. Het klinkt tegenstrijdig, ...	Nieuwsblad
18-9-2015	Meer regen én meer droogte. Het klinkt tegenstrijdig, ...	Gazet van Antwerpen
19-9-2015	Een klimaatbeleid kost geld, maar minder dan geen klimaatbeleid	Opiniestuk in De Morgen
25-9-2015	Hoe zal het klimaat in Vlaanderen veranderen	Boerenbond, Boer & tuinder
9-10-2015	Waterbewuster en -robuuster bouwen	Krant van West-Vlaanderen
16-10-2015	Blijft opwarming van de aarde beneden 2°C	Visie (ACV weekblad, p. 8-9)

Further, in order to provide access to the dataset/results to project partners, research institutions and other users for planning purposes a MACCBET website has been launched <https://ees.kuleuven.be/maccbet/>.

This website is hosted by the Department of Earth and Environmental Science of the KU Leuven. The website provides a brief overview of the project aims, news items related to the project and the partners and users involved. Furthermore, a protected area is developed to store all internal information (e.g. minutes) as to insure a central and secure archive. The website host all relevant data for members of the Follow-Up committee or research institutions. The direct access to the data is requested and may be acquired upon request.



The introduction page of the operational MACCBET website

Furthermore, two symposiums were arranged by the MACCBET partners. The first symposium was arranged in KU Leuven during November 08, 2013 in the middle of the project and the second in RMI during June 02, 2015 at the end of the project. Several scientists from and outside Belgium and stakeholders attended these symposiums. The progress of the MACCBET project and key findings were presented in the symposiums. Further details about the symposium is given below

Mid- Term Workshop/Symposium

The mid-term Workshop/symposium was arranged by KU Leuven on November 08, 2013. Several participants and stakeholder from Belgium participated in the symposium. Four invited speakers delivered key lectures on climate change and regional climate modelling. The invited speakers include

- **Prof. Dr. Daniela Jacob** (Climate Service Centre, Germany):
Topic of presentation: How to refine the knowledge derived from climate research in a practice-orientated way.
- **Prof. Nicole van Lipzig** (KU Leuven - Department of Earth and Environmental Sciences):
Topic of presentation: **The MACCBET project: Modelling atmospheric composition and climate for the Belgian territory** (PDF, 5.0MB)
- **Prof Dr. Jean-Pascal van Ypersele** (Université catholique de Louvain):
Topic of presentation: Main outcomes of the IPCC fifth assessment report (AR5) – working group I
- **Prof. Dr. Filippo Giorgi** (Abdus Salam International Centre for Theoretical Physics, Italy)
Topic of presentation: The future of regional climate modelling

Beside the invited speaker, several other presentations were delivered by the scientists working on the MACCBET project. A detailed description of the MACCBET mid-term symposium can be found on <http://ees.kuleuven.be/maccbet2013/index.html>

Final conference/Symposium

Royal Meteorological Department (RMI) arranged a final one-day MACCBET symposium on June 01, 2015. Participants and stakeholder from Belgium attended in the MACCBET final symposium. Following invited speakers delivered key lectures on climate change and regional climate modelling.

- Prof. Dr. Erik van Meijgaard – KNMI
Topic of Presentation: [Climate Change scenarios for the 21st Century for the Netherlands](#)
- Dr. Markel García-Diez – Institut Català de Ciències del Clima (Barcelona)
Topic of Presentation: [Towards a more complete climate model evaluation.](#)
- Prof. Dr. Nicole van Lipzig – KULeuven
Topic of Presentation: [Overview of the MACCET project](#)
- Dr. Kwinten Van Weverberg – MetOffice
Topic of Presentation: [Evaluation strategies to advance cloud and precipitation processes in models of the atmosphere](#)

Beside the invited speaker, several other presentations were delivered by the scientists working on the MACCBET project. A detailed description of the MACCBET final symposium can be found on <http://www.meteo.be/meteo/view/en/19389622-MACCBET+Final+Symposium.html>

Furthermore, MACCBET, together with other projects, has allowed VITO to develop and verify the novel urban climate model UrbClim (De Ridder et al., 2015). Following the

publication of the model, we have received several expressions of interest from across the globe to establish collaborations based on this model. So far, one such collaboration has been initiated with the Catalan Institute for Climate Science (IC3) in Barcelona (research group of Xavier Rodo, which is working on the health effects of climate change). This has resulted in a one-month stay of one of their postdocs (Markel García) at VITO in May-June 2015, including the presentation by Markel of an invited talk at the MACCBET final conference in Brussels (June 2015). We have also received a request for collaboration from Dr Rong Zhu, Chief Scientist of the National Climate Center of the China Meteorological Administration. VITO staff will have a meeting with her in Beijing in mid-October 2015, to discuss possible avenues for collaboration.

5. PUBLICATIONS

Peer review

KU Leuven

Saeed, S., N. Van Lipzig, W. A. Müller, F. Saeed, D. Zanchettin, 2013: Influence of Circumglobal wave-train on European summer precipitation, *Climate Dynamics*, doi: 10.1007/s00382-013-1871-0.

Demuzere, M., Oleson, K., Coutts, A., Pigeon, G. and van Lipzig, N.P.M., 2013, Simulating the surface energy balance over two contrasting urban environments using the Community Land Model Urban (CLMU). *International Journal of Climatology* 33 (15), pp. 3182-3205.

Brisson, E., M. Demuzere, and N. P. M. van Lipzig, 2015. Modelling strategies for performing convective permitting climate simulations. *Meteorologische Zeitschrift*. DOI: [10.1127/metz/2015/0598](https://doi.org/10.1127/metz/2015/0598).

Trusilova, K., Schubert, S. Wouters, H., Früh, B., Demuzere, M., Großmann-Clarke, S., Becker, P., 2015. The urban land use in the COSMO-CLM model: a comparison of three parameterizations for Berlin. *Meteorologische Zeitschrift* (in press).

Prein, A. F., W. Langhans, G. Fosser, A. Ferrone, N. Ban, K. Goergen, M. Keller, M. Tölle, O. Gutjahr, F. Feser, E. Brisson, S. Kollet, J. Schmidli, N. P. M. van Lipzig, R. Leun, et al. (2015). A review on regional convection-permitting climate modelling: Demonstrations, prospects, and challenges, *Rev. Geophys.*, 53, 323–361. doi:10.1002/2014RG000475.

VITO

Lauwaet D., Viaene P, Brisson E., van Noije T., Strunk A., Van Looy S., Maiheu B., Veldeman N., Blyth L., De Ridder K., Janssen S., 2012. Impact of nesting resolution jump on dynamical downscaling ozone concentrations over Belgium. *Atmospheric Environment* 67, 46-52.

De Ridder, K., D. Lauwaet, B. Maiheu, 2015. UrbClim – a fast urban boundary layer climate model. *Urban Climate*, 12, 21-48.

De Ridder, K., P. Viaene, K. Van de Vel, O. Brasseur, A. Cheymol, and F. Fierens, 2014. The impact of model resolution on simulated ambient air quality and associated human exposure. *Atmósfera*, 27, 403-410.

UCL

Van Weverberg, K., 2013: Impact of environmental instability on convective precipitation uncertainty associated with the nature of the rimed ice species in a bulk microphysics scheme. *Monthly Weather Review*, 141, 2841-2849.

RMI

Goudenhoofd, E., and L. Delobbe, (2013): Statistical Characteristics of Convective Storms in Belgium Derived from Volumetric Weather Radar Observations. *J. Appl. Meteor. Climatol.*, 52, 918–934. doi: <http://dx.doi.org/10.1175/JAMC-D-12-079.1>.

Co-publications

Peer review

KU Leuven and VITO

Wouters, H., De Ridder, K. and van Lipzig, N.P.M., 2012. Comprehensive parametrization of surface-layer transfer coefficients for use in atmospheric models. *Boundary-layer meteorol.*, DOI 10.1007/s10546-012-9744-3.

Wouters, Hendrik, Koen De Ridder, Nicole P.M. van Lipzig, Matthias Demuzere, Dirk Lauwaet, 2013. The diurnal evolution of the urban heat island of Paris: a model-based case study during Summer 2006. *Atmospheric Chemistry and Physics*.

Wouters, H., M. Demuzere, K. De Ridder, N.P.M. van Lipzig, 2015. The impact of impervious water-storage parametrization on urban climate modelling. *Urban Climate*, **11**, 24-50.

Lauwaet, D., P. Viaene, E. Brisson, N.P.M. van Lipzig, T. van Noije, A. Strunk, S. Van Looy, N. Veldeman, L. Blyth, K. De Ridder, and S. Janssen, 2014. The effect of climate change and emission scenarios on ozone concentrations over Belgium: a high-resolution model study for policy support. *Atmospheric Chemistry and Physics*, **14**, 5893-5904.

KU Leuven and UCL

Van Weverberg, E. Goudenhoofd, U. Blahak, E. Brisson, M. Demuzere, P. Marbaix, and J. P. van Ypersele, 2014: Comparison of one-moment and two-moment bulk microphysics for high-resolution climate simulations of intense precipitation. *Atmos. Res.*, **147-148**, 145–161.

Brisson, E., K. Van Weverberg, M. Demuzere, A. Devis, S. Saeed, M. Stengel, and N.P.M. van Lipzig (2015) How well can a convection permitting model reproduce decadal statistics of precipitation, temperature and cloud characteristics? *Climate Dynamics* (in press).

Submitted

KU Leuven

Sajjad Saeed, Erwan Brisson, Matthias Demuzere, Nicole van Lipzig (2015), Multi-decadal convection permitting climate simulations over Belgium: Sensitivity of future precipitation extremes to the convection permitting model, *Geophysical Research Letters* (submitted).

KU Leuven and VITO

Lauwaet D., De Ridder K., Maiheu B., Hooyberghs H., Saeed S., Brisson E., van Lipzig N.P.M. 2015 Assessing the current and future urban heat island of Brussels. *Urban Climate*, in revision.

Wouters, H., Demuzere, M., De Ridder, K., van Lipzig, N.P.M., Vogel, G. Exploring water-storage and evaporation for urban impervious land cover. Urban Climate 2015, in review.

RMI

Lukach M., Loris Foresti and Laurent Delobbe, to be submitted: Occurrence and severity of hail in Belgium based on weather radar observations (In Prep.).

9.1.2 Others

KU Leuven

Sajjad Saeed, Erwan Brisson, Matthias Demuzre, Nicole van Lipzig, (2015), To what extent convection permitting scale models may modify the future precipitation extremes? CLM Community Assembly, 29 September - 02 October 2015, Luxembourg.

N. van Lipzig, A. Prein, W. Langhans, G. Fosser, A. Ferrone, N. Ban, K. Goergen, M. Keller, M. Tölle, O. Gutjahr, F. Feser, E. Brisson, S. Kollet, J. Schmidli, R. Leung A review on regional convection-permitting climate modelling: demonstrations, prospects, and challenges. CLM Community Assembly, 29 September - 02 October 2015, Luxembourg.

Sajjad Saeed, Erwan Brisson, Matthias Demuzre, Nicole van Lipzig, (2015), [Climate extremes: do model projections for the future depend on the grid spacing?](#) MACCBET Final Symposium, June 01, 2015, Brussels, Belgium.

Nicole van Lipzig, Sajjad Saeed, Hendrik Wouters, Matthias Demuzere, Erwan Brisson, Koen De Ridder, Dirk Lauwaet, Jean-Pascal van Ypersele de Strihou Philippe Marbaix, Kwinten van Weverberg, Cecille Villanueve ,Laurent Delobbe, Maryna Lukach (2015), MACCBET: Modelling atmospheric composition and climate for the Belgian territory. MACCBET Final Symposium, June 01, 2015, Brussels, Belgium.

Sajjad Saeed, Nicole van Lipzig, Erwan Brisson,, High resolution future climate simulations over Belgium using the regional climate model COSMO-CLM. COSMO-CLM User Seminar, March 17-20,2014, Frankfurt, Germany.

Saeed, S, N. Van Lipzig B. Erwan (2013): Evaluation of very high resolution regional climate model over Belgium. CORDEX 2013, November 4-7, 2013, Brussels, Belgium.

Saeed, S, N. Van Lipzig B. Erwan (2013): CCLM Assessment of very high resolution regional climate mode simulations over Belgium: Part I. Present day climate. CCLM Assembly, August, 27-30, 2013, Zurich, Switzerland.

Saeed, S, N. Van Lipzig B. Erwan (2013): CCLM evaluation using E-Tool-VIS: Illustrative examples. COSMOCLM-User Seminar, March, 05-08, 2013, Offenbach, Germany.

Saeed S., van Lipzig, N., Muller, A. W., Saeed, F., Zanchettin, 2012, Summer precipitation variability over Europe and associated tele-connections, CLM-community Assembly, Leuven, Belgium, September 17-20, 2012.

Demuzere, M., Oleson, K., Coutts, A., van Lipzig, N.P.M., 2012, Offline evaluation of the Community Land Model-Urban for Toulouse (France) and Melbourne (Australia). In: 12th EMS Annual Meeting & 9th European Conference on Applied Climatology (ECAC) | 10 – 14 September 2012 | Łódź, Poland

Demuzere, M., Coutts, A., Oleson, K., van Lipzig, N.P.M., 2012, Urban climate mitigation strategies in a regional climate modelling context. In: ICUC Dublin 2012, August 2012, Dublin, Ireland.

Demuzere, M., Oleson, K., Coutts, A., van Lipzig, N.P.M., 2012, Offline evaluation of the Community Land Model-Urban for Toulouse (France) and Melbourne (Australia). In: Geophysical Research Abstracts, General Assembly of the European Geophysical Union, April 2012, Vienna, Austria.

Demuzere, M., Coutts, A., Oleson, K., van Lipzig, N.P.M., 2012, Modelling the surface energy balance characteristics of two contrasting urban settings with the Community Land Model – Urban (CLMU). In: COSMO User Seminar, WG3b SOILVEG, 6-9 March 2012, Offenbach, Germany.

Hendrik Wouters, Kristina Trusilova, Sebastian Schubert, Matthias Demuzere, Susanne Grossmann-Clarke, Barbara Frueh. `URB-MIP: the URBan Model Intercomparison Project. 29-Aug-2013. CLM Assembly 2013, Zürich, Switzerland.

Brisson, E., Van Lipzig, N.P.M. (2011). Downscaling precipitation at convective resolving scale in Belgium. 4th CLM-Community Assembly, 30 August – 2 September, Cava De' Tirreni, Italy.

Demuzere, M., 2011, Offline evaluation of the Community Land Model-Urban for Toulouse (France) and Melbourne (Australia). In: Science Day Monash University 2011, Monash University, Clayton Campus, Melbourne (Australia).

Master/Bachelor Thesis (KU Leuven):

Thomas Vanhamel (2012-2013): Bepaling van de vochtbronnen van de neerslag in België, Master of Science in Geographie, KU Leuven.

Enyo Vanmontfort (2013-2014): Evolution of COSMO-CLM simulated temperature and precipitation over Belgium in the future. Bachelor in de Geographie, KU Leuven.

Bart Verhaegen (2014-2015): Klimatologie van grote hagel in België. Master of Science in Geographie, KU Leuven.

UCL

Cecille M. Villanueva-Birriel, Kwinten Van Weverberg, Philippe Marbaix, Jean-Pascal van Ypersele, 2015: "Impact of Aviation Contrail within Central Europe using COSMO-CLM". CLM Assembly, Belvaux, Luxembourg, September 2015.

Cecille M. Villanueva-Birriel, Kwinten Van Weverberg, Maryna Lukach, Philippe Marbaix, Jean-Pascal van Ypersele, 2015: "Performance Assessment of Surface Hail Simulations using a High-Resolution Regional Climate Model". MACCBET Symposium, RMI, Brussels, June 2015.

Cecille M. Villanueva-Birriel, Kwinten Van Weverberg, Maryna Lukach, Philippe Marbaix, Jean-Pascal van Ypersele, 2015: "Surface hail simulations in a high-resolution regional climate model". Seminar, Université catholique de Louvain, May 2015.

Cecille M. Villanueva-Birriel, Kwinten Van Weverberg, Maryna Lukach, Philippe Marbaix, Jean-Pascal van Ypersele, 2015: "Surface Hail Simulations in a High-Resolution Regional Climate Model". European Geosciences Union General Assembly, Vienna, Austria, April 2015.

Cecille M. Villanueva-Birriel, Kwinten Van Weverberg, Maryna Lukach, Philippe Marbaix, Jean-Pascal van Ypersele, 2015: "Effects of Hail Parameterization within the COSMO-CLM in Simulated Convective Storms". COSMO / CLM / ART User Seminar, Offenbach, Germany, March 2015.

Van Weverberg, K. E. Brisson, M. Stengel, 2014: "Evaluation of clouds and radiation in a high-resolution climate model using CMSAF-information". 4th CMSAF User Workshop, Grainau, Germany, March 2014.

Van Weverberg, K., A. M. Vogelmann, W. Lin, E.P. Luke, A. Cialella, P. Minnis, M. Khaiyer, E.R. Boer, M.P. Jensen, 2013: The role of cloud microphysics in the simulation of mesoscale convective systems (MCS) in the tropical western pacific. Atmospheric System Research Program Science Team Meeting, March 18-21, 2013, Potomac, Maryland, U.S.A.

Van Weverberg K., 2013: Cloud and precipitation microphysics in cloud-resolving models. Brookhaven National Laboratory Atmospheric Science Division Seminar, March 27, 2013, Upton, New York, U.S.A.

Van Weverberg, K., E. Brisson, P. Marbaix, J.-P. van Ypersele, 2013: Impact of microphysics complexity on surface precipitation characteristics in CLM. COSMOCLM-User Seminar, March, 05-08, 2013, Offenbach, Germany.

Van Weverberg, K., E. Goudenhoofd, U. Blahak, E. Brisson, P. Marbaix, J.-P. van Ypersele, 2013: Microphysics complexity and surface precipitation characteristics in CCLM. CCLM Assembly, August, 27-30, 2013, Zurich, Switzerland.

Van Weverberg, K., E. Goudenhoofd, U. Blahak, M. Lukach, E. Brisson, M. Demuzere, P. Marbaix, J.-P. van Ypersele, 2013: Sensitivity of convection-permitting regional climate simulations to the level of microphysics parameterization complexity. CORDEX 2013, November 4-7, 2013, Brussels, Belgium.

Van Weverberg, K., 2013: High-resolution precipitation modeling in a regional climate model for Belgium. MACCBET User Symposium, November 8, 2013, Leuven, Belgium.

Van Weverberg K., P. Marbaix, J.-P. van Ypersele: 2012: "Microphysics and the simulation of precipitation extremes in Belgium", CLM-community Assembly, Leuven, Belgium, September 17-20, 2012.

VITO:

Lauwaet D., Viaene P, Brisson E., van Noije T., Strunk A., Van Looy S., Maiheu B., Veldeman N., Blyth L., De Ridder K., Janssen S., 2012. Impact of nesting strategy on dynamical

downscaling ozone concentrations over Belgium, Belgium Meteorology and Climate conference Meteoclim, Liège, June 2012.

Lauwaet D., Viaene P., Brisson E., van Noije T., Strunk A., Van Looy S., Maiheu B., Veldeman N., Blyth L., De Ridder K., Janssen S., 2012. Impact of climate change on air quality over Belgium in the near future, CLM-community Assembly, Leuven, Belgium, September 17-20, 2012.

Lauwaet D., Viaene P., Brisson E., van Noije T., Strunk A., Van Looy S., Veldeman N., Blyth L., De Ridder K., Janssen S., 2013. The impact of climate change and emission scenarios on ozone concentration over Belgium: A high resolution model study for policy support, International Conference on Regional Climate – CORDEX 2013, Brussels, November 2013.

Lauwaet D., Hooyberghs H., Lefebvre W., Maiheu B. and K. De Ridder, 2014. Urban Heat Islands in Europe: analysis with a high resolution model. Belgium Meteorology and Climate conference Meteoclim, Antwerpen, June 2014.

RMI:

Lukach M., Delobbe L., (2013), Radar-based Hail statistics over Belgium, 2003-2012, June, 30 – July, 3, 2013 ,11th International Precipitation Conference, Ede-Wageningen, the Netherlands.

Lukach M., Delobbe L., (2013), Radar-based Hail Statistics Over Belgium, June 3-7, 2013, 7th European Conference on Severe Storms, Helsinki, Finland.

Goudenhoofd E., Delobbe L., (2013), Statistics of extreme areal rainfall depths based on radar observations, 7th European Conference on Severe Storms, Helsinki, Finland.

Goudenhoofd E., Delobbe L., 2012, Statistical characteristics of convective storms in Belgium derived from volumetric weather radar observations, PhD symposium METEOCLIM, l'Université de Liège, Liège, Belgium, June 2012.

Goudenhoofd E., Delobbe L., Radar-based statistics of point and areal rainfall, *ERAD 2012, 7th European Conference on Radar in Meteorology and Hydrology, June 2012, Toulouse, France.*

Huuskonen A., Delobbe L., EUMETNET OPERA: Achievements of OPERA-3 and challenges ahead, *ERAD 2012, 7th European Conference on Radar in Meteorology and Hydrology, June 2012, Toulouse, France.*

KU Leuven, VITO, UCL, RMI

Erwan Brisson, Sajjad Saeed, Matthias Demuzere, Kwinten Van Weverberg, Nicole van Lipzig, Multivariable evaluation of a decadal convective permitting simulation over Belgium using the regional climate model COSMO-CLM, COSMO-CLM User Seminar, March 17-20, 2014, Frankfurt, Germany.

Nicole van Lipzig, E. Brisson, D. Lauwaet, M. Demuzere, K. de Ridder , S. Saeed , K. Van Weverberg (2013): A common strategy to reduce systematic model errors in the CLM model? COSMOCLM-User Seminar, March, 05-08, 2013, Offenbach, Germany.

Hendrik Wouters, Matthias Demuzere, Koen De Ridder, Gerd Vogel, Nicole van Lipzig. Evaporation from urban areas: model sensitivity and results with TERRA-URB standalone. 4-Mar-2013. COSMO User Seminar, DWD, Offenbach, Germany.

Demuzere, M., Vanweverberg, K., Brisson, E., van Lipzig, N.P.M., 2013, First steps towards a common regime-dependent error analysis In the COSMO-CLM model. In: CLM Assembly, August 2013, Zurich (Switzerland).

Demuzere, M., Nicole van Lipzig, Sajjad Saeed, Dirk Lauwaet, Koen de Ridder, Kwinten van Weverberg, Philippe Marbaix, Jean-Pascal van Ypersele, Laurent Delobbe, Maarten Reyniers, Maryna Lukach, 2012. MACCBET: Modelling atmospheric composition and climate for the Belgian territory. COSMO/CLM User Seminar, 06 to 08 March 2012, Offenbach, Germany.

Hendrik Wouters, Koen De Ridder, Matthias Demuzere, Bino Mahieu, Nele Veldeman, Felix Deutch, Peter Viaene, Erwan Brisson, Nicole van Lipzig. `How much spatial details in meteorological parameters is needed for modelling urban air-quality? 6-Mar-2013. COSMO User Seminar, DWD, Offenbach, Germany.

Hendrik Wouters, Koen De Ridder, Matthias Demuzere, Bino Mahieu, Nele Veldeman, Peter Viaene, Dirk Lauwaet, Nicole van Lipzig. `How much spatial detail in meteorological parameters is needed to model air-quality in a city? A case study for the city of Antwerp, Belgium. 8-Apr-2013. EGU General Assembly, Vienna Austria.

Hendrik Wouters, Matthias Demuzere, Koen De Ridder, Gerd Vogel, Nicole van Lipzig. Implementation of a new urban surface-ux and impervious water-storage parameterization TERRA-URB: evaluation and sensitivity analysis for Toulouse city. 8-Apr-2013. EGU general assembly, Vienna, Austria.

Hendrik Wouters, Dirk Lauwaet, Peter Viaene, Shaun Carl, Matthias Demuzere, Nele Veldeman, Felix Deutsch. How much detail in meteorological parameters is needed for urban air-quality modelling. 28-Aug-2013. CLM Assembly 2013, Zürich, Switzerland

Rozemien De Troch, Olivier Giot, Rafiq Hamdi, Sajjad Saeed, Hossein Tabarim Meron Teferi Taye, Piet Termonia, Nicole van Lipzig and Patrik Willems, 2014: Overview of a few regional climate models and climate scenarios for Belgium. Wetenschappelijk en technische publicatie Nr 65. Uitgegeven door het KMI van BELGIE.

6. ACKNOWLEDGEMENTS

The MACCBET project was funded by the Belgian Science Policy Office (BELSPO). We also acknowledge the COSMO-CLM community for providing the regional climate model COSMO-CLM. We also acknowledge the Royal Meteorological Institute of Belgium (RMI) for providing the station observational dataset, the EU-FP6 project ENSEMBLES (<http://ensembles-eu.metoffice.com>) and the data providers in the ECA&D project (<http://www.ecad.eu>)" for providing the E-OBS dataset. We thank all members of follow-up committee for providing useful information/guidance that helped greatly in achieving the overall goals of the project.

7. REFERENCES

Brouwers J., Peeters B., Van Steertegem M., van Lipzig N., Wouters H., Beullens J., Demuzere M., Willems P., De Ridder K., Maiheu B., De Troch R., Termonia P., Vansteenkiste Th., Craninx M., Maetens W., Defloor W., Cauwenberghs K. (2015) MIRA Klimaatrapport 2015, over waargenomen en toekomstige klimaatveranderingen. Vlaamse Milieumaatschappij i.s.m. KU Leuven, VITO en KMI. Aalst, Belgium, 147 p.

Branstator G., 2002: Circumglobal teleconnections, the jet stream waveguide, and North Atlantic Oscillation. *J Clim* 15:1893–1910.

Bowler, N. E. H., Pierce, C. E., and Seed, A. W., 2004: Development of a precipitation nowcasting algorithm based upon optical flow techniques, *J. Hydrol.*, **288**, 74–91.

Brisson E., K. Van Weverberg, M. Demuzere, A. Devis, S. Saeed, M. Stengel, N. P.M. van Lipzig (2015) How well can a convection-permitting climate model reproduce decadal statistics 2 of precipitation, temperature and cloud characteristics? Submitted to *Climate Dynamics*.

Ding, Q., Wang, B., 2005: Circumglobal teleconnection in northern hemisphere summer. *J Clim* 18:3482–3505.

Delobbe L., Holleman I., 2006: Uncertainties in radar echo top heights used for hail detection. *Meteorological Applications*, **13**, 361-374.

Saeed S, Müller W. A., Hagemann S., Jacob, D. 2010: Circumglobal wave train and summer monsoon over northwestern India and Pakistan; the explicit role of the surface heat low. *Clim. Dyn.* DOI:10.1007/s00382-010-0888-x.

Saeed S, Müller W. A., Hagemann, S., Jacob, D., Mujumdar, M., Krishnan, R., 2011: Precipitation variability over the South Asian monsoon heat low and associated teleconnections. *Geophys. Res. Lett.* 38: L08702. DOI: 10.1029/2011GL046984.

Saeed S., Van Lipzig N., Müller WA., Saeed F., Zanchettin D., (2013) Influence of the circumglobal wave-train on European summer Precipitation. *Clim Dyn.*, DOI 10.1007/s00382-013-1871-0.

Seifert A., Beheng K. D., 2005: A two-moment cloud microphysics parameterization for mixed-phase clouds. Part 1: Model description. *Meteorology and Atmospheric Physics*, Volume 92, Issue 1-2, pp. 45-66

Pfeifroth, U., R. Hollmann, and B. Ahrens (2012). Cloud Cover Diurnal Cycles in Satellite Data and Regional Climate Model Simulations. *Meteorologische Zeitschrift* 21(6), 551-560.

Jaeger, E. B., I. Anders, D. Lüthi, B. Rockel, C. Schar, and S. I. Seneviratne (2008). Analysis of ERA40-driven CLM simulations for Europe. *Meteorologische Zeitschrift* 17(4), 349-367.

Maraun, D., Wetterhall, F., Ireson, A.M., Chandler, R.E., Kendon, E.J., Widmann, M., Brienen, S., et al., (2010), Precipitation downscaling under climate change: Recent developments to

bridge the gap between dynamical models and the end user. *Reviews of Geophysics* 48, RG3003, doi:10.1029/2009RG000314.

Walther, A., J.-H. Jeong, G. Nikulin, C. Jones, and D. Chen (2013, January). Evaluation of the warm season diurnal cycle of precipitation over Sweden simulated by the Rossby Centre regional climate model RCA3. *Atmospheric Research* 119, 131-139.

Willems, P., Olsson, J., Arnbjerg-Nielsen, K., Beecham, S., Pathirana, A., Gregersen, I. B., Madsen, H., Nguyen, V.-T.-V. (2012) *Impacts of Climate Change on Rainfall Extremes and Urban Drainage*. IWA Publishing, London, UK.

Mearns, L.O., Giorgi, F., Whetton, P., Pabon, D., Hulme, M., Lal, M. (2004) *Guidelines for use of climate scenarios developed from regional climate model experiments*. Data Distribution Centre of the Intergovernmental Panel on Climate Change.

Hohenegger, C., P. Brockhaus, C. S. Bretherton, and C. Schär (2009). The Soil Moisture-Precipitation Feedback in Simulations with Explicit and Parameterized Convection. *Journal of Climate*, 22, 5003-5020.

De Troch R., Hamdi R., Van de Vyver H., Jean-Franc, Geleyn O., Termonia P (2013) Multiscale Performance of the ALARO-0 Model for Simulating Extreme Summer Precipitation Climatology in Belgium. *Journal of Climate*, 26, 8895-8915. DOI: 10.1175/JCLI-D-12-00844.1.

Christensen, J.H., Christensen, O.B. (2007) A summary of the PRUDENCE model projections of changes in European climate by the end of this century. *Climatic Change* 81: 7–30.

Fowler, H. J., and M. Ekström, 2009: Multi-model ensemble estimates of climate change impacts on UK seasonal precipitation extremes. *Int. J. Climatol.*, 29, 385–416, doi:10.1002/joc.1827.

Clark, A. J., W. a. Gallus, and T.-C. Chen (2007, October). Comparison of the Diurnal Precipitation Cycle in Convection-Resolving and Non-Convection-Resolving Mesoscale Models. *Monthly Weather Review* 135(10), 3456-3473.

Weisman, M. L., W. C. Skamarock, and J. B. Klemp (1997, April). The Resolution Dependence of Explicitly Modeled Convective Systems. *Monthly Weather Review* 125(4), 527-548.

Ban, N., J. Schmidli, and C. Schär (2014). Evaluation of the convection-resolving regional climate modeling approach in decade-long simulations. *Journal of Geophysical Research. Atmospheres* 119(13), 7889-7907.

Prein, a. F., a. Gobiet, M. Suklitsch, H. Truhetz, N. K. Awan, K. Keuler, and G. Georgievski (2013). Added value of convection permitting seasonal simulations. *Climate Dynamics*, 41(9-10), 2655-2677.

Kendon, E. J., N. M. Roberts, C. a. Senior, and M. J. Roberts (2012, September). Realism of Rainfall in a Very High-Resolution Regional Climate Model. *Journal of Climate* 25(17), 5791-5806.

Hohenegger, C., P. Brockhaus, C. S. Bretherton, and C. Schär (2009). The Soil Moisture-Precipitation Feedback in Simulations with Explicit and Parameterized Convection. *Journal of Climate*, 22, 5003-5020.

Fosser, G., S. Khodayar, and P. Berg (2014). Benefit of convection permitting climate model simulations in the representation of convective precipitation. *Clim Dyn*, 44, 45–60. DOI 10.1007/s00382-014-2242-1

Demuzere, M., K. De Ridder, and N. van Lipzig, 2008. Modelling the energy balance in Marseille: Sensitivity to roughness length parameterizations and thermal admittance. *Journal of Geophysical research*, 113, doi:10.1029/2007JD009113.

Demuzere, M., De Ridder, K., van Lipzig, N. P. M., 2008. Modeling the energy balance in Marseille: Sensitivity to roughness length parametrizations and thermal admittance. *J. Geophys. Res.* 113, 1–19.

De Ridder, K., Bertrand, C., Casanova, G., Lefebvre, W., Sep. 2012. Exploring a new method for the retrieval of urban thermophysical properties using thermal infrared remote sensing and deterministic modeling. *Journal of Geophysical Research* 117 (D17), 1-14.

De Ridder K., Maiheu B., Wouters H. & van Lipzig N. (2015), Indicatoren van het stedelijk hitte-eiland in Vlaanderen, studie uitgevoerd in opdracht van de Vlaamse Milieumaatschappij, MIRA, MIRA/2015/05, VITO. Raadpleegbaar op www.milieuraapport.be.

De Ridder, K., and G. Schayes, 1997. The IAGL land surface model. *Journal of Applied Meteorology*, 36, 167-182.

De Ridder, 2006. Testing Brutsaert's temperature roughness parameterization for representing urban surfaces in atmospheric models. *Geophysical Research Letters*, 33, L13403, doi:10.1029/2006GL026572.

De Ridder, K., 2010. Bulk transfer relations for the roughness sublayer. *Boundary-Layer Meteorology*, 134, 257-267.

De Ridder, K., C. Bertrand, G. Casanova, and W. Lefebvre, 2012. Exploring a new method for the retrieval of urban thermophysical properties using thermal infrared remote sensing and deterministic modelling, *Journal of Geophysical Research*, 117, doi:10.1029/2011JD017194.

De Ridder et al., 2014, The impact of model resolution on simulated ambient air quality and associated human exposure. *Atmosfera* 27 (4), 403-410.

De Ridder, K., D. Lauwaet, and B. Maiheu, 2015. A new urban boundary layer climate model. *Urban Climate* 12, 21-48.

Karl T., Knight R., 1997. The 1995 Chicago heat wave: how likely is a recurrence? *Bulletin of the American Meteorological Society* 78, 1107–1119.

Lauwaet D., De Ridder K., Maiheu B., Hooyberghs H., Saeed S., Brisson E., van Lipzig N.P.M. ASSESSING THE CURRENT AND FUTURE URBAN HEAT ISLAND OF BRUSSELS. *Urban Climate*, in revision.

Sarkar, A., and K. De Ridder, 2011. The urban heat island intensity of Paris: a case study based on a simple urban surface parameterisation. *Boundary-Layer Meteorology*, 138, 511-520.

Sobrino J.A., Oltra-Carrió R., Sòria G., Bianchi R., Paganini M., 2012. Impact of spatial resolution and satellite overpass time on evaluation of the surface urban heat island effects. *Remote Sensing of Environment* 117, 50-56.

Van Vuuren, D.P., Edmonds, J., Kainuma, M., Riahi, K., Thomson, A., Hibbard, K., Hurtt, G. C., Kram, T., Krey, V., Lamarque, J.-F., Masui, T., Meinshausen, M., Nakicenovic, N., Smith, S. J., and Rose, S. K. 2011. The representative concentration pathways: an overview. *Climatic Change*, 109, 5-31.

Wouters, H., De Ridder, K., Van Lipzig, N. (2012). Comprehensive Parametrization of Surface-Layer Transfer Coefficients for Use in Atmospheric Numerical Models. *Boundary-Layer Meteorology*, 145(3), 539-550.

Wouters, H., De Ridder, K., Van Lipzig, N., Demuzere, M., Lauwaet, D. (2013). The diurnal evolution of the urban heat island of Paris: a model-based case study during Summer 2006. *Atmospheric Chemistry and Physics*, 13, 8525-8541.

Wouters, H., Demuzere, M., De Ridder, K., van Lipzig, N.P.M., Vogel, G. Exploring water-storage and evaporation for urban impervious land cover. *Urban Climate 2015*, in review.

De Ridder et al., 2014, The impact of model resolution on simulated ambient air quality and associated human exposure. *Atmosfera* 27 (4), 403-410.

Deutsch F., Veldeman N., Vankerkom J., Peelaerts W., Buekers J., Torfs R., Fierens F., Vanpoucke C., Trimpeneers E., Vancraeynest L., Bossuyt M. (2010), Zwevend stof en fotochemische luchtverontreiniging. Visionair scenario Milieuverkenning 2030, studie uitgevoerd in opdracht van de Vlaamse Milieumaatschappij, MIRA, MIRA/2010/09, VITO.

Hazeleger, W., Severijns, C., Semmler, T., Stefanescu, S. and Yang, S., Wang, X., Wyser, K., Dutra, E., Baldasano, J. M., Bintanja, R., Bougeault, P., Caballero, R., Ekman, A. M. L., Christensen, J. H., van den Hurk, B., Jiminez, P., Jones, C., Kållberg, P., Koenigk, T., McGrath, R., Miranda, P., Van Noije, T., Palmer, T., Parodi, J. A., Schmith, T., Selten, F., Storelymo, T., Sterl, A., Tapamo, H., Vancoppenolle M., Viterbo, P., and Willén, U. 2010. *EC-Earth: A Seamless Earth System Prediction Approach in Action*. *Bulletin of the American Meteorological Society*, 91, 1357-1363, doi: 10.1175/2010BAMS2877.1.

Hazeleger, W., Wang, X., Severijns, C., Stefanescu, S., Bintanja, R., Sterl, A., Wyser, K., Semmler, T., Yang, S., van den Hurk, B., van Noije, T., van der Linden, E. and van der Wiel, K. 2012. EC-Earth V2.2: description and validation of a new seamless earth system prediction model. *Climate Dynamics*, 39, 2611-2629.

Hedegaard, G.B., Christensen, J.H. and Brandt, J. 2012. The relative importance of impacts from climate change vs. emissions change on air pollution levels in the 21st century. *Atmospheric Chemistry and Physics*, 12, 24501–24530.

Hooyberghs, J., Mensink, C., Dumont, G. and Fierens, F.: Spatial interpolation of ambient ozone concentrations from sparse monitoring points in Belgium., *Journal of environmental monitoring* : JEM, 8(11), 1129–35, doi:10.1039/b612607n, 2006.

Huijnen, V., Williams, J., vanWeele, M., van Noije, T., Krol, M. and Dentener, F., et al. 2010. The global chemistry transport model TM5: description and evaluation of the tropospheric chemistry version 3.0. *Geoscientific Model Development*, 3, 445-473.

Janssen, S., Dumont, G., Fierens, F. and Mensink, C.: Spatial interpolation of air pollution measurements using CORINE land cover data, *Atmospheric Environment*, 42(20), 4884–4903, doi:10.1016/j.atmosenv.2008.02.043, 2008.

Lauwaet D., Viaene P, Brisson E., van Noije T., Strunk A., Van Looy S., Maiheu B., Veldeman N., Blyth L., De Ridder K., Janssen S., 2012. Impact of nesting resolution jump on dynamical downscaling ozone concentrations over Belgium. *Atmospheric Environment* 67, 46-52.

Lauwaet D., Viaene P, Brisson E., van Noije T., Strunk A., Van Looy S., Maiheu B., Veldeman N., Blyth L., De Ridder K., Janssen S., 2014. The effect of climate change and emission scenarios on ozone concentrations over Belgium: a high resolution model study for policy support. *Atmospheric Chemistry and Physics* 14, 5894-5904.

Maes J., Vliegen J., Van de Vel K., Janssen S., Deutsch F., De Ridder K. & Mensink C., 2009: Spatial surrogates for the disaggregation of CORINAIR emission inventories, *Atmos. Environ.* 43, 1246-1254.

Bino Maiheu, Nele Veldeman, Peter Viaene, Koen De Ridder, Dirk Lauwaet, Felix Deutsch, Stijn Janssen (2013), Bepaling van de best beschikbare grootschalige concentratiekaarten luchtkwaliteit voor België, studie uitgevoerd in opdracht van de Vlaamse Milieumaatschappij, MIRA, MIRA/2013/01, Vlaamse Instelling voor Technologisch Onderzoek (VITO).

Mol, W.J.A., van Hooydonk, P.R. and de Leeuw, F.A.A.M. 2011. The state of the air quality in 2009 and the European exchange of monitoring information in 2010. ETC/ATM Technical paper 2011/1. European Topic Centre of Air Pollution and Climate Change Mitigation, Bilthoven (The Netherlands).

Mensink, C., De Ridder, K., Lewyckij, N., Delobbe, L., Janssen, L., Van Haver, P., 2001. Computational aspects of Air quality modelling in Urban Regions using an Optimal Resolution Approach. *Large-Scale Scientific Computing, Lecture Notes in Computer Science* 2179, 299–308.

Trusilova, K., Schubert, S. Wouters, H., Früh, B., Demuzere, M., Großmann-Clarke, S., Becker, P. (in pres). The urban land use in the COSMO-CLM model: a comparison of three parameterizations for Berlin.

Van de Vel, K., Mensink, C., De Ridder, K., Deutsch, F., Maes, J., Vliegen, J., Aloyan, A., Yermakov, A., Arutyunyan, V., Khodzher, T., and Mijling, B. 2009. Air-quality modelling in the Lake Baikal region. *Environmental Monitoring and Assessment*, 165, 665-674.

Van Vuuren, D.P., Edmonds, J., Kainuma, M., Riahi, K., Thomson, A., Hibbard, K., Hurtt, G. C., Kram, T., Krey, V., Lamarque, J.-F., Masui, T., Meinshausen, M., Nakicenovic, N., Smith, S. J., and Rose, S. K. 2011. The representative concentration pathways: an overview. *Climatic Change*, 109, 5-31.

Van Weverberg, K., Goudenhoofdt, E., Blahak, U., Brisson, E., Demuzere, M., Marbaix, P., & van Ypersele, J. P. (2014). Comparison of one-moment and two-moment bulk microphysics for high-resolution climate simulations of intense precipitation. *Atmospheric Research*, 147, 145-161

Waldvogel, A., B. Federer, and P. Grimm: 1979, Criteria for the detection of hail cells. *J. Appl. Meteor.*, 18, 1521–1525.

Witt, A., M. D. Eilts, G. J. Stumpf, J. T. Johnson, E. D. Mitchell, and K. W. Thomas: 1998, An enhanced hail detection algorithm for the WSR-88D. *Wea. and. Forecasting*, 13, 286–303.

Wouters, H., De Ridder, K., Lipzig, N.P.M., 2012. Comprehensive parametrization of surface-layer transfer coefficients for use in atmospheric numerical models. *Bound.-Layer Meteorol.* 145 (3), 539–550. doi:10.1007/s10546-012-9744-3.

Wouters, H., De Ridder, K., Demuzere, M., Lauwaet, D., van Lipzig, N. P. M., 2013. The diurnal evolution of the urban heat island of Paris: a model-based case study during Summer 2006. *Atmospheric Chemistry and Physics* 13 (17), 8525–8541.

Wouters, H., M. Demuzere, K. De Ridder, N. P. M. van Lipzig, 2015. The impact of impervious water-storage parametrization on urban-climate modelling. *Urban Climate* 11 (1), 24–50, doi:10.1016/j.uclim.2014.11.005.

Wouters, H., M. Demuzere, K. De Ridder, U. Blahak, N. P. M. van Lipzig (in prep.). Modelling the seasonal dependency of the contributions to urban heat islands in Belgium.

Wouters, H., Van Lipzig, N. (sup.), Demuzere, M. (cosup.), De Ridder, K. (cosup.) (2014). Improving urban land-cover parametrization in regional climate models: The role of urban aerodynamic, thermal and radiative properties, anthropogenic heat and water retention, 140 pp.